Recent advances in lithium containing ceramics based sorbents for high-temperature CO_2 capture

Yu Zhang[1], Yanshan Gao[1], Heriberto Pfeiffer[2], Benoit Louis[3], Luyi Sun[4], Dermot O'Hare[5], Qiang Wang[1,*]

[1]College of Environmental Science and Engineering, Beijing Forestry University, 35 Qinghua East Road, Haidian District, Beijing 100083, P. R. China

[2]Laboratorio de Fisicoquímica y Reactividad de Superficies (LaFReS), Instituto de Investigaciones en Materiales, Universidad Nacional Autónoma de México, Circuito exterior s/n, Cd. Universitaria, Del. Coyoacan C.P. 04510, Ciudad de México, Mexico

[3]ICPEES - Institut de Chimie et Procédés pour l'Énergie, l'Environnement et la Santé, UMR 7515 CNRS - Université de Strasbourg, 25 rue Becquerel, 67087 Strasbourg cedex 2, France

[4] Institute of Materials Science, Department of Chemical & Biomolecular Engineering, University of Connecticut, Storrs, Connecticut 06269, United States

[5]Chemistry Research Laboratory, Department of Chemistry, University of Oxford, Mansfield Road, Oxford OX1 3TA, United Kingdom

Corresponding author:

College of Environmental Science and Engineering, Beijing Forestry University, 35 Qinghua East Road, Haidian District, Beijing 100083, P. R. China

E-mail: qiang.wang.ox@gmail.com; qiangwang@bjfu.edu.cn

Tel: +86 13699130626

Abstract

Recently, lithium containing ceramics based high-temperature CO_2 sorbents have received tremendous attention due to their high CO_2 capture capacity, low regeneration temperatures, and relatively high stability. With the rapid development of these promising CO_2 capturing materials, a timely review is highly demanded. In this contribution, we critically summarized the performance of all types of lithium containing ceramics including lithium silicates, zirconates, titanates, aluminates, ferrites, cuprate, bismuthates and borates for capturing CO_2 at high-temperatures. For these CO_2 sorbents, all possible schemes for improving their CO_2 capture capacity, kinetics, and cycling stability have been comprehensively reviewed. Their potential applications in high-temperature post-combustion CO_2 capture from stationary flue gases, sorption enhanced methane steaming reforming, sorption enhanced alcohol reforming, and the CO oxidation coupled with subsequent CO_2 capture processes were compared and discussed. We hope this work can inspire and guide researchers from a wide range of backgrounds and help to pave the way for major breakthroughs in both fundamental studies and industrial applications in this field.

Keywords: CO_2 sorbent; alkaline ceramics; pre-combustion CO_2 capture; post-combustion CO_2 capture; greenhouse gas control

CONTENTS

1. Introduction and scope of the review

2. Lithium silicates

2.1. CO_2 sorption/desorption models for Li_4SiO_4

2.2. Influence of synthesis methods for pure Li_4SiO_4

2.2.1. Solid-state method

2.2.2. Sol-gel method

2.2.3. Impregnation precipitation method

2.2.4. Other synthesis methods

2.2.5. Synthesis of Li_4SiO_4 from MOFs or zeolites

2.3. Element substitution of Li_4SiO_4

2.3.1. Li substitution

2.3.2. Si substitution

2.4. Incorporation of a second phase

2.4.1. Incorporation of molten salt components

2.4.2. Incorporation of metal oxide components

2.4.3. Incorporation of porous components

2.5. Synthesis of Li_4SiO_4 from solid wastes or cheap silicon sources

2.5.1. Synthesis of Li_4SiO_4 from industrial fly ash

2.5.2. Synthesis of Li_4SiO_4 from biomass ashes

2.5.3. Synthesis of Li_4SiO_4 from natural minerals

2.6. High lithium content silicate (Li_8SiO_6)

2.7. Low lithium content silicate (Li_2SiO_3)

3. Lithium zirconates

3.1. Mechanism of CO_2 capture on Li_2ZrO_3

3.2. Influence of synthesis methods for pure Li_2ZrO_3

3.3. Formation of metazirconate solid solutions

3.3.1. $Li_{2-x}Na_xZrO_3$

3.3.2. $Li_{2-x}K_xZrO_3$

3.4. Incorporation of molten salt components in Li_2ZrO_3

3.4.1. Li_2CO_3/K_2CO_3

3.4.2. Multiple-eutectic salt
3.5. High lithium content zirconates ($Li_6Zr_2O_7$ and Li_8ZrO_6)
3.5.1. $Li_6Zr_2O_7$
3.5.2. Li_8ZrO_6
4. Other lithium containing ceramics based CO_2 sorbents
4.1. Lithium titanates
4.2. Lithium aluminates
4.3. Lithium ferrites and gallates
4.4. Lithium cuprates
4.5. Lithium bismuthates and borates
5. Thermodynamic analysis
6. Applications of lithium containing ceramics based CO_2 sorbents
6.1. High-temperature post-combustion CO_2 capture from stationary flue gases
6.2. Sorption enhanced methane steam reforming
6.3. Sorption enhanced alcohol reforming
6.4. CO oxidation coupled with subsequent CO_2 chemisorption process
7. Current challenges and future prospects
8. Conclusion

1. Introduction and scope of the review

CO_2 is one of the most important greenhouse gases that contribute to global warming, catastrophic weather, and drought problems. In 2012 it was reported that the ocean surface temperature has increased by 0.65–1.06 °C over the past 133 years.[1] The significant rise in CO_2 concentration in the earth's atmosphere is strongly related to the industrialization and the wide-ranging increase in global energy consumption patterns. Presently, global warming is a worldwide concern.[2-4] Fossil fuels are the most frequently used energy source, releasing large amounts of CO_2, historically accounting for about two thirds of cumulative CO_2 emission.[5] If fossils fuels are to be in continued widespread use, in order to reduce CO_2 emission, the adsorption/sorption and separation of CO_2 from large stationary sources like fossil fuels fired power stations, hydrogen production processes, and the related industries become crucial.[6, 7]

To capture CO_2, many methods have been developed, including solution absorption, membrane separation, and solid materials adsorption/sorption.[8-10] Solution absorbers are generally used to capture CO_2 using physical or chemical methods at room temperature.[8] Typical physical adsorption methods include pressurized water washing method, pyrrolidone, selexol, flour, and rectisol. Chemical sorption methods have two categories: hot potash and alcohol amine methods.[11] However, all these solution-based methods are subject to temperature constraints. Membrane separation technology is promising but its stability and selectivity need to be further improved.[12-14] CO_2 capture using solid materials has many advantages such as low cost and stability over a wide temperature operation range.[15-17] These solid materials based processes also create less waste during cycles, and the spent solid CO_2 adsorbents/sorbents can be disposed without undue environmental strain.

Based on the operation temperatures, the solid CO_2 capturing materials can be divided into low-temperature adsorbents (zeolite, activated carbon, metal organic framework, etc), intermediate-temperature adsorbents (MgO, and layered double hydroxides (LDHs), etc), and high-temperature sorbents (CaO, and alkaline containing materials, mainly lithium ceramics, etc).[18-24] The low-temperature CO_2 adsorbents are mainly used in the post-combustion CO_2 capturing processes, while the intermediate adsorbents and high-temperature CO_2 sorbents are specifically designed for pre-combustion CO_2 capturing processes. Among solid CO_2 adsorbents/sorbents based techniques, sorption enhanced hydrogen production (SEHP) processes have attracted considerable attention. The use of solid CO_2 adsorbents/sorbents can increase hydrocarbon conversion, and in the meantime produce high-purity hydrogen and highly concentrated CO_2.[25-30] For the sorption enhanced steam reforming (SESR) technique, one of the present key challenges is the selection of a suitable high-temperature sorbent. In addition, post-combustion CO_2 capture at high temperatures based on regenerable sorbent materials has also received increasing attention as an alternative to low-temperature CO_2 capture adsorption and conventional chemical absorption solvent systems.

Currently, two types of high-temperature CO_2 sorbents have been developed, CaO[22] and alkali containing ceramics (Li_4SiO_4,[31] Li_2ZrO_3,[32] Li_5AlO_4.[33] Li_2CuO_2,[34] and $K_2Ti_2O_5$[20]). CaO has been widely investigated as a high-temperature CO_2 sorbent because it is highly available, inexpensive, and shows a high CO_2 sorption capacity. However, CaO requires excessively high temperatures for the desorption of CO_2. Such high regeneration temperatures cause sintering of CaO sorbents, reducing its effectiveness in later cycles. Li_4SiO_4, Li_2ZrO_3 and many other lithium containing

ceramics have attracted great attention thanks for their relatively high sorption capacity, fast sorption rate, good cycling stability, and reasonable material costs. In a certain rang Li_4SiO_4 sorbent captures CO_2 at temperatures between 450 and 700 °C, with a theoretical maximum CO_2 capacity of 36.7 wt%. In addition, Li_2ZrO_3 can chemically capture CO_2 at 400–650 °C, with a stoichiometric CO_2 sorption capacity of 28.7 wt%. Li_4SiO_4 and Li_2ZrO_3 samples have been reported to be a promising candidate for CO_2 capture at high temperatures, based on the following reactions (1-2).

$$Li_4SiO_4\ (s) + CO_2\ (g) \leftrightarrow Li_2SiO_3\ (s) + Li_2CO_3\ (s) \quad (1)$$

$$Li_2ZrO_3\ (s) + CO_2\ (g) \leftrightarrow Li_2CO_3\ (s) + ZrO_2\ (s) \quad (2)$$

Although, lithium containing ceramics have excellent CO_2 sorption performances at high temperatures, many limitations still exist.[35-38] The particle size affects the CO_2 sorption capacity and kinetics obviously. According to literature reports, in a certain range (70 nm–3 μm), the smaller the particles are, the more effective the sorption of CO_2 is. Too low particle size (72 nm) will cause the sorbent to be severely sintered in the use. However, samples with large particle size were normally obtained from traditional synthesis method (solid-state method). According to the double shell sorption mechanism, an external shield of alkaline carbonate will form during CO_2 sorption process. Once the shield was formed, the lithium and oxygen elements have to diffuse throughout the external layer and continue to react with CO_2. Regeneration performance is an important evaluation standard for sorbents. Moreover, high production cost represents another limitation of sorbents in practical applications. Noted that lithium containing ceramics show excellent CO_2 sorption at high temperatures with pure CO_2 atmosphere. The CO_2 capture capacity diminishes with the decrease in CO_2 concentration, which is due to the kinetic limitations of CO_2

sorption. In addition, different processes such as high-temperature post-combustion CO_2 capture from stationary flue gases, sorption enhanced methane steaming reforming, sorption enhanced alcohol reforming, and the CO oxidation coupled with subsequent CO_2 capture processes possess different operating conditions, and thus require different types of high-temperature CO_2 capturing materials.

To improve the CO_2 sorption performance of lithium containing ceramics, cut costs, and find more alternative sorbents, great efforts have been made during the past few years. Now we feel that a timely review on the recent advances of lithium containing ceramics based high-temperature CO_2 sorbents is highly desired. In this contribution, different lithium containing ceramics including lithium silicates, lithium zirconates, lithium titanates, lithium aluminates, lithium ferrites, lithium cuprates, lithium bismuthates and borates as promising high-temperature CO_2 capturing materials are thoroughly reviewed. The corresponding mechanisms and schemes for improving the sorption capacity, kinetics, and cycling stability are summarized. The applications of lithium containing ceramics in high-temperature post-combustion CO_2 capture from stationary flue gases, sorption enhanced methane steaming reforming, sorption enhanced alcohol reforming, and CO oxidation coupled with subsequent CO_2 chemisorption processes will be presented. We expect that this review will not only summarize the main research activities in this area, but also shed light on its fundamental studies and practical applications.

2. Lithium silicates

2.1. CO_2 sorption/desorption models for Li_4SiO_4

Li_4SiO_4 has excellent CO_2 sorption capacity at the temperature range of 450–700 °C,

with a theoretical value of 36.7 wt%.[39-42] The CO_2 sorption performance of Li_4SiO_4 is controlled by several factors. So far, several models have been proposed for the CO_2 sorption and desorption processes over Li_4SiO_4, which include double shell model, Avrami-Erofeev model, shrinking core model, and unreacted-core model.[36, 43]

According to the double shell model, it is generally accepted that the CO_2 sorption on Li_4SiO_4 is a two-step process.[44] Initially, Li_4SiO_4 reacts with CO_2 at the particle surface and forms an external shell that consists Li_2CO_3 and Li_2SiO_3. Then, the reactants have to diffuse through the external shell to react with each other.[45] This reaction process that corresponds to the double-shell model is shown in Figure 1(a).[46] Double-shell model shows that at the beginning of the reaction, CO_2 sorption reaction rate is controlled by the CO_2 capture rate of Li_4SiO_4. But, once the carbonate-oxide external shell has been formed, the CO_2 sorption reaction rate will depend on the diffusion processes of CO_2, lithium, and oxygen.[36, 38, 44, 47]

The Avrami-Erofeev model describes the kinetics of crystallization of solids and was applied to the experimental data of decarbonation.[48, 49] According to this model, the CO_2 desorption process can be summarized as follows: (1) Li_2CO_3 reacts with Li_2SiO_3 at the interface to form Li_4SiO_4, (2) CO_2 diffuses out of Li_2CO_3, and the Li_4SiO_4 nuclei grow to form a dense shell in the middle, covering the unreacted Li_2SiO_3, (3) the CO_2 desorption process proceeds with the diffusion of Li^+ and O^{2-} throughout the Li_4SiO_4 solid shell and CO_2 through Li_2CO_3 shell.[36]

Shrinking core model assumes that the particles are uniform non-porous grains, as shown in Figure 1(b). The reaction first takes place at the surface of grains and then moves into the bulk, with a product layer was formed behind. The total particle radius remains unchanged, but the unreacted core and product layer change with time.

Amorim et al.[48] demonstrated that the CO_2 sorption (carbonation) and desorption (decarbonation) cycling process over Li_4SiO_4 can be fitted well with this model. Takasu et al.[50] investigated the reaction mechanism and the activation energy of CO_2 capture on Li_4SiO_4 by kinetic analysis using the shrinking core model, which suggested the shell diffusion is the rate controlling step for the entire reaction at low temperatures. However, the rate controlling step at high temperatures changed from chemical reaction process to the shell diffusion process with the progress of reaction. According to the Arrhenius plots, the activation energy for diffusion E_d was calculated as 22.3 kJ mol^{-1} at 500–600 °C. While the E_d became negative at 700–730 °C, which suggested that an exothermic pre-equilibrium reaction, the dissolution of CO_2 in liquid Li_2CO_3 exists, which may offer a path for CO_2 transportation and an enhanced carbonation over Li_4SiO_4 at high temperatures.

In addition, the CO_2 sorption reactors packed with spherical Li_4SiO_4 pellets showed non-regular temperature distribution and capture performance, which may be due to the unsteady CO_2 sorption rate and highly exothermic process. Tanaka et al.[51] simulated the unsteady-state behavior of Li_4SiO_4 sorbent using an unreacted-core model, which comprised a gas film layer, a product layer, and an unreacted core. In this model, CO_2 only reacts with the surface of unreacted core and the CO_2 transportation through the gas film and product layers is governed by the one-dimensional convection and the diffusion mechanism in a spherical coordinate system. Both layers are responsible for the mass transport resistance, which increases as CO_2 accumulates. But, the resistance caused by the gas film layer will not change with a steady flow field. In addition, with the increase of CO_2 accumulation, the shrinkage of the surface of unreacted core may also hinder the CO_2 sorption process. The decrease

of CO_2 sorption rate is mainly because of these two reasons.

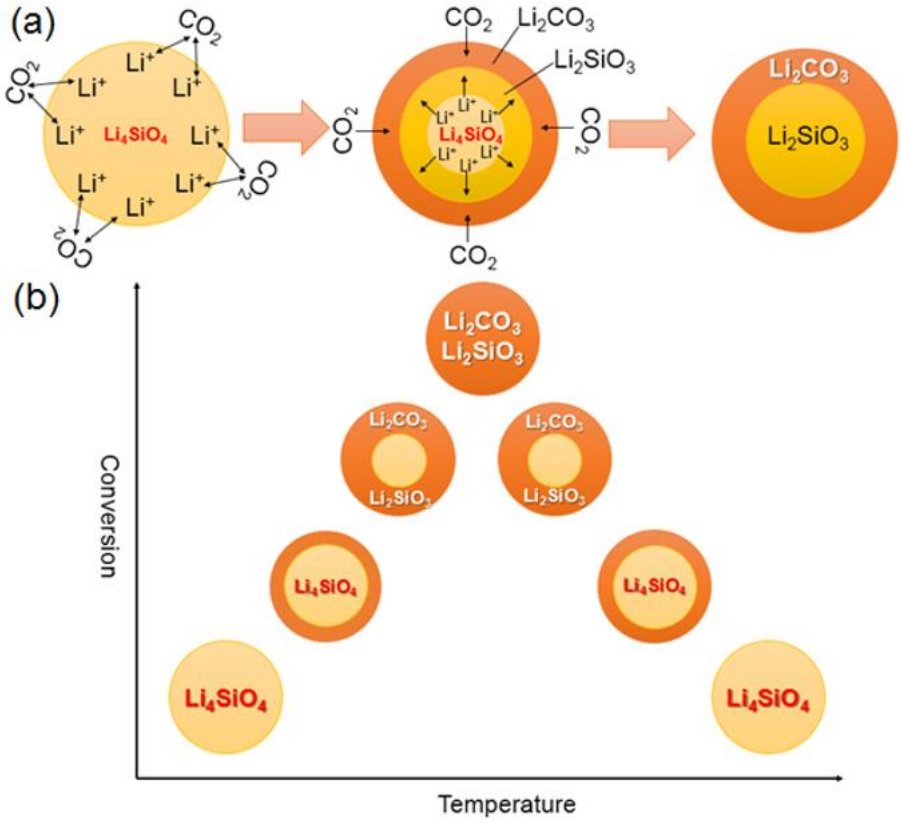


Figure 1. (a) The double-shell model for CO_2 sorption process of Li_4SiO_4.[35] Reprinted with permission from ref 35. Copyright 2015 Elsevier B.V., (b) Shrinking core model for CO_2 sorption/desorption process of Li_4SiO_4.[48] Reprinted with permission from ref 48. Copyright 2015 Elsevier B.V.

2.2. Influence of synthesis methods for pure Li_4SiO_4

It is well documented that pure Li_4SiO_4 has a good CO_2 capture capacity at high temperatures (450–700 °C). However, due to the dense structure and large particle size, the interior of Li_4SiO_4 cannot completely react with CO_2. Hence, Li_4SiO_4 usually cannot reach its maximum theoretical sorption capacity. At the same time, the carbonate shell formed at the surface of Li_4SiO_4 particles by reacting with CO_2 will reduce the sorption rate. In addition, due to particle sintering, the regeneration

capacity will decline after multiple sorption/desorption cycles. To better face the aforementioned issues, great effort has been devoted to improve the Li_4SiO_4 sorbent. So far, several Li_4SiO_4 synthesis methods have been studied, including solid-state reaction, sol-gel, impregnation precipitation, solvo-plasma, spraying drying, and combustion.[31, 52-58] In addition, new reports on the synthesis of Li_4SiO_4 from highly porous precursors such as metal organic frameworks (MOFs) and zeolites for CO_2 capture were also reviewed.[59]

2.2.1. Solid-state method

Solid-state reaction process is a conventional method, with the advantages of high yield, low cost and simple operation process. Recently, many studies have been performed on the synthesis of Li_4SiO_4 using solid state method, including (1) the influence of the particle size of SiO_2, (2) the influence of lithium source, and (3) the effects of synthesis temperature. Xu et al.[6] synthesized four Li_4SiO_4 samples via solid state method by using quartz powders with different particle sizes (75–180, 45–75, 38–45, and < 38 μm) as silicon source. The results indicated that the solid-state reaction led to a larger decrease in the particle size of quartz powders, thus inducing an increase in Li_4SiO_4 phase in all samples. In the meantime, the size of the Li_4SiO_4 grain agglomerated gradually diminished while reducing the quartz particles, providing more active sites for CO_2 capture. With the decrease in quartz particle size, the maximum CO_2 sorption capacity gradually increased from 19.2 (668 ^oC) to 23.6, (669 ^oC) 25.6 (696 ^oC), and 30.5 wt% (715 ^oC), respectively. The maximum CO_2 sorption capacity is only 6.7 wt% lower than the theoretical sorption value of Li_4SiO_4. This research proved that the particle size of SiO_2 precursor has a great effect on the CO_2 sorption performance of Li_4SiO_4, and smaller particles are warranted for enhancing

CO_2 capture rate and capacity.

In addition to SiO_2 precursor, it has been demonstrated that the lithium source also greatly affects the performance of Li_4SiO_4 sorbents. Kim et al.[35] proved that LiOH as lithium source can decrease the synthesis temperature for Li_4SiO_4. With $LiNO_3$ or Li_2CO_3 as the lithium source, pure Li_4SiO_4 can only be obtained at temperatures higher than 700 °C, and as-prepared Li_4SiO_4 showed significant sintering, with very low surface area of 4 $m^2 g^{-1}$. However, when using LiOH as the lithium source, pure Li_4SiO_4 can be obtained at much lower temperatures (e.g. 600 °C). Furthermore, the obtained Li_4SiO_4 showed a three-dimensionally interconnected framework (75–125 nm in thickness), with wormhole like macropores within the framework. The specific surface area was also much higher (15 $m^2 g^{-1}$), which can greatly improve the CO_2 sorption performance at moderate temperatures (e.g. 550 °C). For the Li_4SiO_4 samples synthesized from $LiNO_3$ and Li_2CO_3, their CO_2 sorption capacities remained as low as around 8.0 wt%. However, for the Li_4SiO_4 synthesized from LiOH, a maximum sorption capacity of 29.8 wt% was achieved at 550 °C using 1 atm pure CO_2 gas. Meanwhile, the CO_2 sorption rate of Li_4SiO_4 synthesized from LiOH was 56.1 mg g^{-1} min^{-1}, one order of magnitude higher than that of the non-porous samples. After 10 cycles, the sorption capacity only slightly decreased (< 3%), suggesting an excellent stability.

Oh-ishi et al.[60] systematically studied the effect of calcination temperature (700, 800, 900, and 1000 °C) on the particle size of Li_4SiO_4 samples by solid state method. The results indicated that calcination temperature greatly impacts the particle size of Li_4SiO_4. As shown in Figure 2, the average particle size was about 26, 34, 53, and 70 μm when the calcined temperature was 700, 800, 900, and 1000 ^oC respectively. The CO_2 sorption curve proved that small particles led to faster sorption rates. This study

suggests that reducing the synthesis temperature can improve the CO_2 sorption performance of Li_4SiO_4 to a certain extent. In another work, Izquierdo et al.[61] optimized the solid-state synthesis condition for Li_4SiO_4 to maximize the CO_2 uptake. The unreacted Li_2CO_3 was observed at low synthesis temperatures, and the content decreased with the increase of temperature. The complete conversion of Li_2CO_3 to Li_4SiO_4 was achieved at 900 ^oC. However, the holding time can not be too long at such high temperature to prevent sintering. By increasing calcination time from 2 to 4 h, the CO_2 uptake decreased from 30.5 to 20 wt% (carbonation temperature of 600 ^oC, isothermal period of 120 min). The optimal heating rate was optimized to be 5 $^oC\ min^{-1}$. The crystal size had big effect on CO_2 capture performance, and smaller crystal size led to higher CO_2 uptake.

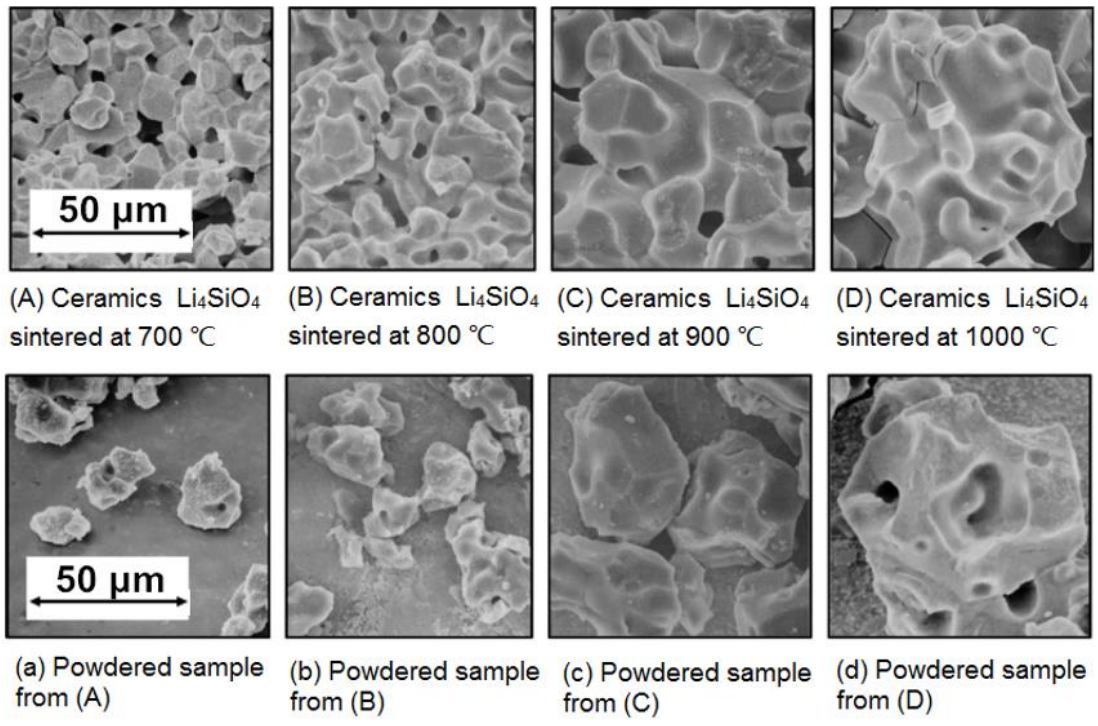


Figure 2. SEM images of Li_4SiO_4 ceramics samples and powdered samples, (A) sample sintered at 700 °C, (B) sample sintered at 800 °C, (C) sample sintered at 900 °C, (D) sample sintered at 1000 °C, and (a) powdered sample from the Li_4SiO_4 sintered at

700 °C, (b) powdered sample from the Li_4SiO_4 sintered at 800 °C, (c) powdered sample from the Li_4SiO_4 sintered at 900 °C, (d) powdered sample from the Li_4SiO_4 sintered at 1000 °C.[60] Reprinted with permission from ref 60. Copyright 2008 American Chemical Society.

Kato et al.[31] synthesized Li_4SiO_4 sorbent using solid state method with Li_2CO_3 and SiO_2 precursors and compared its CO_2 sorption capacity with Li_2ZrO_3 (this lithium ceramic will be reviewed in section 3). In pure CO_2, The CO_2 sorption capacity of Li_4SiO_4 sample reached 35 wt% at 700 °C in dry pure CO_2 gas, which was 50% larger than that for Li_2ZrO_3. Even at lower temperature (550 °C) and lower CO_2 concentration (50 vol% CO_2) conditions, the weight increase of Li_4SiO_4 was also about 50% greater than that of Li_2ZrO_3. Likewise, the CO_2 sorption rate over Li_4SiO_4 was ca. 30 times superior to those achieved over Li_2ZrO_3 material.

However, compared with other synthesis methods, solid-state method also has its limitations. For instance, the Li_4SiO_4 samples synthesized via solid-state method always have a large, dense and non-porous particles. According to the double-shell model sorption theory, this kind of structure will lead to a low sorption rate in the late stage of sorption reaction.[55, 62] Venegas et al.[37] studied the influence of synthesis method on the particle size and CO_2 sorption capacity of Li_4SiO_4. In the latter work, three preparation methods including solid-state, precipitation, and microwave calcined sol-gel methods were compared. The solid-state samples showed very dense particles with an average particle size of 36 μm. However, the Li_4SiO_4 particle prepared via precipitation method was spherical and the particle sized decreased to 3 μm. Although pure Li_4SiO_4 cannot be obtained through the sol-gel method, the particle size

of such sample was even smaller, in the range of 0.5–3 μm. These results clearly indicated that the particle size has a large impact on the CO_2 sorption performance of Li_4SiO_4. For the two samples with particle size of 36 and 3 μm, the maximum CO_2 sorption capacities were 30 wt% and 37.4 wt%, respectively, at 600 °C after 5 h. The higher reactivity of small particles was attributed to the presence of more surface Li atoms, the generated steam pressures on grain boundaries, and the produced triple points among particles.[37]

Kinetic studies indicated that diffusion is the limiting step for CO_2 capture on Li_4SiO_4.[36, 44, 47, 51] Thus, reducing the particle size and increasing the porosity of synthesized Li_4SiO_4 is crucial for improving the CO_2 capture capacity and sorption rate. For this purpose, some modifications were performed following solid state synthesis, for instance, hydration-calcination, ball milling, and carbon coating. Yin et al.[63] used hydration-calcination route to modify the Li_4SiO_4 sample synthesized via solid-state method. They proved that the impurity phases such as Li_2SiO_3 can be prevented by using the hydration-calcination modified method, leading to relatively pure Li_4SiO_4 formation. In addition, such obtained sample possessed smaller grain size and higher specific surface area, which resulted in improved CO_2 sorption capacity.[63] Furthermore, Wang et al.[64] added NaCl during the hydration process. By coupling hydration and NaCl doping, smaller sorbents with larger specific surface area could be synthesized. At the same time, the co-doping with sodium and chlorine on Li_4SiO_4 sample induced a molten phase during CO_2 sorption. These results decreased CO_2 diffusion resistance and facilitated chemisorption process. The CO_2 sorption capacity of SS-Li_4SiO_4 (solid-state method), W-Li_4SiO_4 (water hydration method) and 3 wt% NaCl-W-Li_4SiO_4 samples were 6.1, 13.7, and 34.2 wt%, respectively, at 575 °C and 15 vol% CO_2. In

addition, the 3 wt% NaCl-W-Li_4SiO_4 sorbent showed excellent regeneration properties. The maximum CO_2 sorption capacity was still as high as 32.0 wt% after 10 cycles.[64] Romero-Ibarra et al.[65] examined the influence of ball milling on the Li_4SiO_4 prepared by solid state method. Pristine Li_4SiO_4 sample showed a BET specific surface area of 0.4 $m^2\ g^{-1}$, with a CO_2 sorption capacity reached 13.0 wt% at 600 ^oC after 250 min. However, after ball milling, the modified Li_4SiO_4 showed a 10 times larger specific surface area (4.9 $m^2\ g^{-1}$) after only 60 min of milling. At the same sorption temperature (600 °C), modified Li_4SiO_4 sample showed a greatly improved CO_2 capture capacity of 21.1 wt%, which was attributed to the enhancement of microstructural properties of Li_4SiO_4. In addition, the CO_2 sorption/desorption cycling capacity was more than tripled when compared to that of unmodified samples. This proves that ball milling is a viable method for modifying Li_4SiO_4 sorbents.

Zhao et al.[66] synthesized Li_4SiO_4 sample via solid-state method and modified with gluconic acid ($C_6H_{12}O_7$)-based carbon coating. During this synthesis, gluconic acid was dropped to the solid state-Li_4SiO_4 suspension, which was then stirred and dried. The dried gel was carbonized first under N_2, and then calcined at 700 °C in air for 4 h, obtaining the GAC-Li_4SiO_4 sample. For comparison purpose, GA-Li_4SiO_4 sample was prepared by directly calcining the above dry gel in air. The microstructural studies showed that the Li_4SiO_4 synthesized via solid-state method (SS-Li_4SiO_4) consisted of dense particles. The GA-Li_4SiO_4 sample showed a relatively looser structure. While the GAC-Li_4SiO_4 sample exhibited a big change in morphology, forming hollow polyhedrons with smaller particles. The specific surface area of SS-Li_4SiO_4 (1.20 $m^2\ g^{-1}$), GA-Li_4SiO_4 (3.13 $m^2\ g^{-1}$), and GAC-Li_4SiO_4 (11.95 $m^2\ g^{-1}$) gradually increased. The sorption properties of these three samples were compared. GAC-Li_4SiO_4 led to higher

CO_2 sorption capacity than SS-Li_4SiO_4 and GA-Li_4SiO_4, achieving a high capacity of 34.7 wt% recorded at 665 °C for 10 min. Furthermore, GAC-Li_4SiO_4 sorbent show an encouraging performance at low CO_2 concentrations, the total sorption capacity could reach 23.9% in 15 vol% CO_2, which can be attributed to its unique particle structure. At the same time, the cycling tests suggested that GAC-Li_4SiO_4 maintained high CO_2 uptake even after 10 CO_2 sorption/desorption cycles, with a final CO_2 sorption capacity of 33.5 wt%.

Recently two different research groups synthetized Li_4SiO_4 by solid-state reactions and they analyzed the effect of CO_2 partial pressure during carbonation process. In one hand, Zhang et al.[67] analyzed the kinetics of CO_2 capture using different partial pressures with or without water steam. Li_4SiO_4 showed poor CO_2 capture performance at high temperature and low CO_2 partial pressure, as CO_2 capture was restricted by the thermodynamic equilibrium. Additionally, authors tried to fit the kinetic results to Jander and Ginstling-Brounshtein models, without success. Thus, the double-shell structure and a simplified CO_2 concentration profile in the Li_2CO_3 product layer were introduced to modify Jander model. In this case, data was successfully fitted to the so-called modified Jander-Zhang model. Based on that, modified Jander-Zhang model was applied to describe the CO_2 capture under different CO_2 concentrations with/without water vapor. The model was highly useful, as all data fitted well. In such a case, the activation energy was determined, and it was found that water steam reduced the energy required for the Li_4SiO_4 carbonation process. At the same time, Kaniwa et al.[68] analyzed the effect of CO_2 concentration on the solid-state prepared Li_4SiO_4 using thermogravimetric analysis. Authors observed that if CO_2 partial pressure was decreased, the sorption-desorption equilibrium shifted to lower temperatures. In

fact, thermodynamic calculations and experimental data of approximate equilibrium temperature on CO_2 partial pressure were represented using an Ellingham diagram.

2.2.2. Sol-gel method

The sol–gel process has advantages of low synthesis temperature, small particle size, and controllable morphology and microstructure.[37, 56] The Li_4SiO_4 samples could be synthesized via either water acid-based or ammonium hydroxide-based sol–gel approaches. For better CO_2 capture performance, as-prepared Li_4SiO_4 could be further modified by (1) ball milling into smaller particles, (2) coating onto porous carbon supports, or (3) coating with a carbon shell.

For the water acid-based sol-gel synthesis, citric acid ($C_6H_8O_7$) was generally used as the chelating agent. Wen et al.[62] synthesized nano-sized Li_4SiO_4 (ca. 100 nm) via a water-based sol–gel approach, which was much smaller than the samples obtained by solid-state reaction (10 to 20 μm). Thanks for its small particle size and high specific surface area, such prepared Li_4SiO_4 sample showed a high CO_2 uptake of 32.3 wt% at 680 °C. Smaller particle size can result in a thinner Li_2CO_3-Li_2SiO_3 layer, improving the ion diffusion rate. Meanwhile, the porous structure facilitates CO_2 access to active sites, thereby enhancing CO_2 sorption and diffusion rates.

Subha et al.[55] obtained platelet Li_4SiO_4 particles using an ammonium hydroxide-based sol–gel route. The obtained Li_4SiO_4 showed a higher CO_2 sorption capacity and kinetics than the samples synthesized by solid-state method. At 700 ^oC in pure CO_2 gas, the maximum CO_2 sorption rate was 22.5 mg g^{-1} min^{-1} and the maximum capacity was 35 wt% after 100 min. However, under the same sorption condition, the sorption rate of Li_4SiO_4 synthesized by solid-state method only reached 13.2 mg g^{-1} min^{-1}. This excellent CO_2 sorption performance is attributed to the unique platelet morphology of

the particles. Additionally, to obtain pellet-type sorbents that can be applied in large-scale, the sol-gel based Li_4SiO_4 was coated on porous carbon sheets. At 700 °C, the sorption capacity was 15 wt% for the coated sample, and the first 60% of sorption was completed at a rate of 37.5 mg g^{-1} min^{-1}, which was higher than the powdered samples (22.5 mg g^{-1} min^{-1}). This superior sorption rate can be attributed to the high dispersion of coated Li_4SiO_4 particles.[55]

Lu et al.[56] studied the effect of ball milling on the structure of Li_4SiO_4 synthesized by sol-gel method. The results showed that average sizes of powders without ball-milling was 3.3 μm. In contrast, after ball-milling, the agglomerated large particles were broken down, from 3.3 μm to 102 nm, and the BET specific surface area was significantly increased from 0.4 to 4.9 m^2 g^{-1}.[56, 69]

Carbon coating method has been applied to the modification of solid-state method. Zhao et al.[70] showed that this method can also be applied to the Li_4SiO_4 synthesized by sol-gel method. Different from the ordinary water acid-based sol-gel approach, during this synthesis process, the obtained dry gel was firstly pyrolyzed at 700 °C in flowing N_2 and then calcined at 700 °C in air for 4 h. The main synthesis steps to produce Li_4SiO_4 are shown in Figure 3. During synthesis, citric acid not only served as a complexing agent for mixing precursors homogeneously, but also worked as the carbon source, which effectively prevent the growing of Li_4SiO_4 crystallites. The produced carbon-coated Li_4SiO_4 exhibited a larger specific surface area (12.9 m^2 g^{-1}) and a shell-connected cross-linking structure, which was conducive to a more rapid sorption-desorption process and a higher sorption capacity. At 680 ^oC, the CO_2 sorption capacity of Li_4SiO_4 synthesized by carbon coating method reached 34.2 wt%, and achieved sorption equilibrium in 1 h. However, samples synthesized via sol–gel

route and solid-state method only reached about 32 wt% and 25 wt%, respectively. Furthermore, after 20 cycles, the sample retained its high sorption performance.

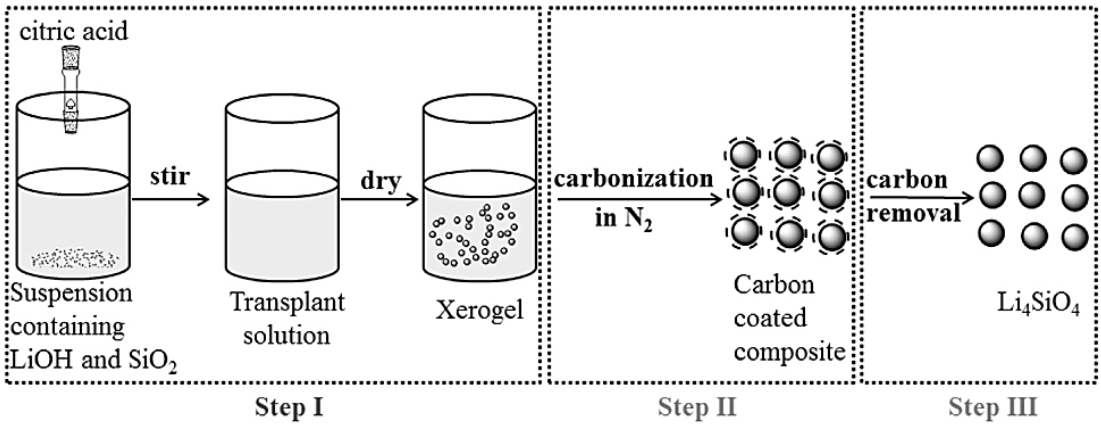


Figure 3. Synthesis steps to produce Li_4SiO_4 via citric acid-based sol-gel route combined with carbon coating.[70] Reprinted with permission from ref 70. Copyright 2015 Elsevier Ltd and Techna Group S.r.l.

2.2.3. Impregnation precipitation method

The impregnation precipitation method consists of suspending one solid precursor in a liquid medium, followed by incorporating an aqueous solution containing other precursors. After well stirring and heating, the mixed precursor powder was then obtained after complete evaporation. Then, the precursor powder was calcined in a muffle furnace.[71] Due to the homogeneous mixing of the precursors during impregnation precipitation, Li_4SiO_4 can be synthesized at relatively low temperatures compared to the solid-state method. The particle size of obtained spherical Li_4SiO_4 can be decreased to 3 μm, which is 10 times smaller than that obtained through the solid-state method.[37] This is the reason why the Li_4SiO_4 particles synthesized by impregnation precipitation method generally exhibit higher sorption capacities and faster sorption rates.[71]

Shan et al.[71] synthesized Li_4SiO_4-based sorbent via impregnation precipitation method by using diatomite as the silicon precursor, and compared the CO_2 sorption performance with Li_4SiO_4 samples synthesized from diatomite and SiO_2 using solid-state method. At 700 ^oC within 100 min, the maximum CO_2 sorption capacity for the Li_4SiO_4 synthesized by impregnation precipitation method reached 29.89 wt%, which was higher than that for the Li_4SiO_4 samples synthesized from SiO_2 (11.34 wt%) and diatomite (24.23 wt%) by solid state method. It also has a faster sorption rate, which reached its maximum capacity of 96% within 15 min. However, the other two samples only reached 45–75 wt% of their maximum capacity after 15 min. Figure 4(a) shows the CO_2 sorption/desorption cycling performance of Li_4SiO_4 synthesized via impregnation precipitation method. After 15 cycles, the CO_2 uptake only decreased by 1.05 wt%, from 34.14 wt% to 33.09 wt%.

Xu et al.[72] prepared Li_4SiO_4 using SiO_2 sol and two different organic lithium precursors (lithium acetate dehydrate and lithium lactate) via impregnation precipitation method. The synthesis procedure and sorption properties of obtained Li_4SiO_4 samples are shown in Figure 4(b). This novel Li_4SiO_4 sample showed a bulgy surface morphology with significantly higher specific surface area, which contributes to a higher sorption capacity. As a result, the reversible CO_2 uptake of this Li_4SiO_4 with 15 vol% CO_2 was about 8 times higher than that of the solid-state prepared Li_4SiO_4. The CO_2 uptake kept increasing during the tested 40 cycles, and this observed trend was not seen to stop within tested cycles. The progressively increasing sorption capacity can be attributed to the increased contacting surface due to the formed massive micro-sized pores over multicycles.

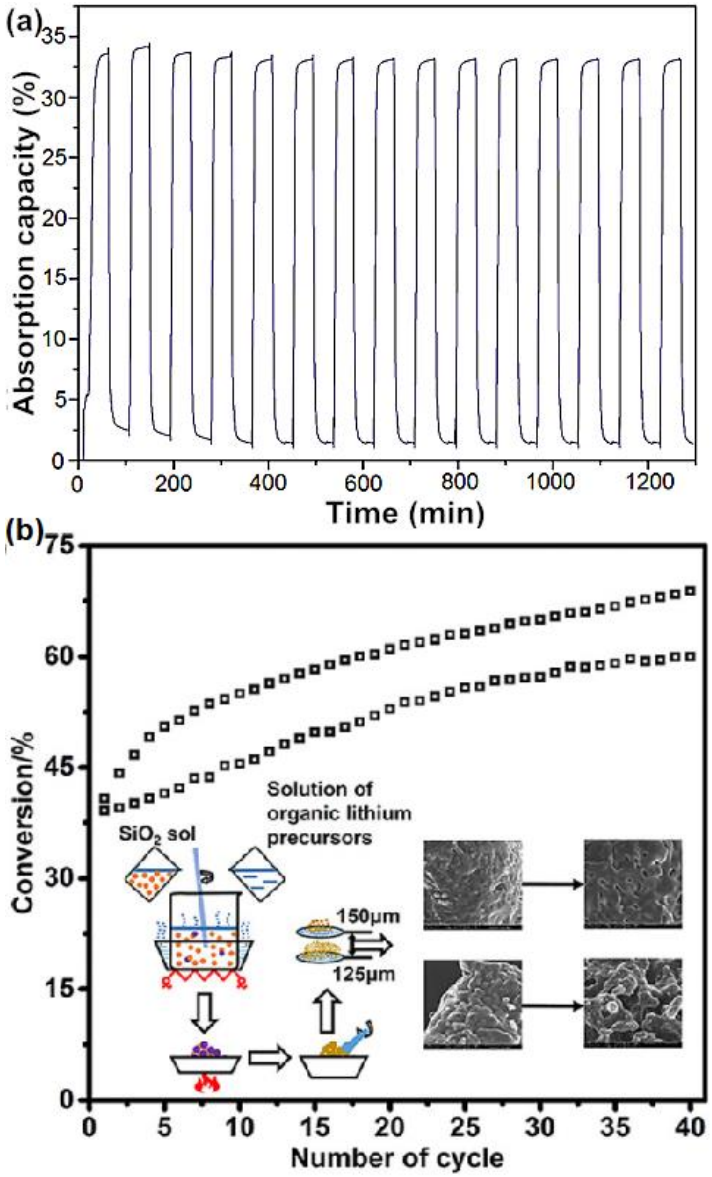


Figure 4. (a) CO_2 sorption/desorption performance of Li_4SiO_4 synthesized via impregnation precipitation method using diatomite as silicon source. Reprinted with permission from ref [73]. Reprinted with permission from ref 73. Copyright 2013 American Chemical Society, (b) The synthesis procedure and sorption properties of Li_4SiO_4 synthesized using two different organic lithium precursors (lithium acetate dehydrate and lithium lactate) via impregnation precipitation method.[72] Reprinted with permission from ref 72. Copyright 2016 Wiley-VCH Verlag GmbH&Co. KGaA, Weinheim.

2.2.4. Other synthesis methods

Recently, several new synthesis methods including solvo-plasma method, spray-drying method, and combustion method have been reported for the synthesis of Li_4SiO_4 for high-temperature CO_2 capture. For instance, Nambo et al.[74] successfully synthesized Li_4SiO_4 nanowires using a so-called "solvo-plasma" technique which contains plasma oxidation of Si precursors mixed with LiOH (Figure 5). The specific surface area of these Li_4SiO_4 nanowires sorbent reached 10.2 $m^2 g^{-1}$ and the average pore size was 11.5 nm. The sorption capacity of Li_4SiO_4 nanowires reached 25 wt% within only 3 min, demonstrating the nanowire morphology can lead to ultra-fast CO_2 sorption. It also exhibited a very high CO_2 sorption capacity of ca. 35 wt%, close to the theoretical value (36.7 wt%).[35] However, one drawback of this Li_4SiO_4 nanowire sorbent is the relatively poor regeneration performance during CO_2 sorption/desorption cycles. The CO_2 capture capacity diminished dramatically from 33 to 25 wt% from the first to the second cycle.[74]

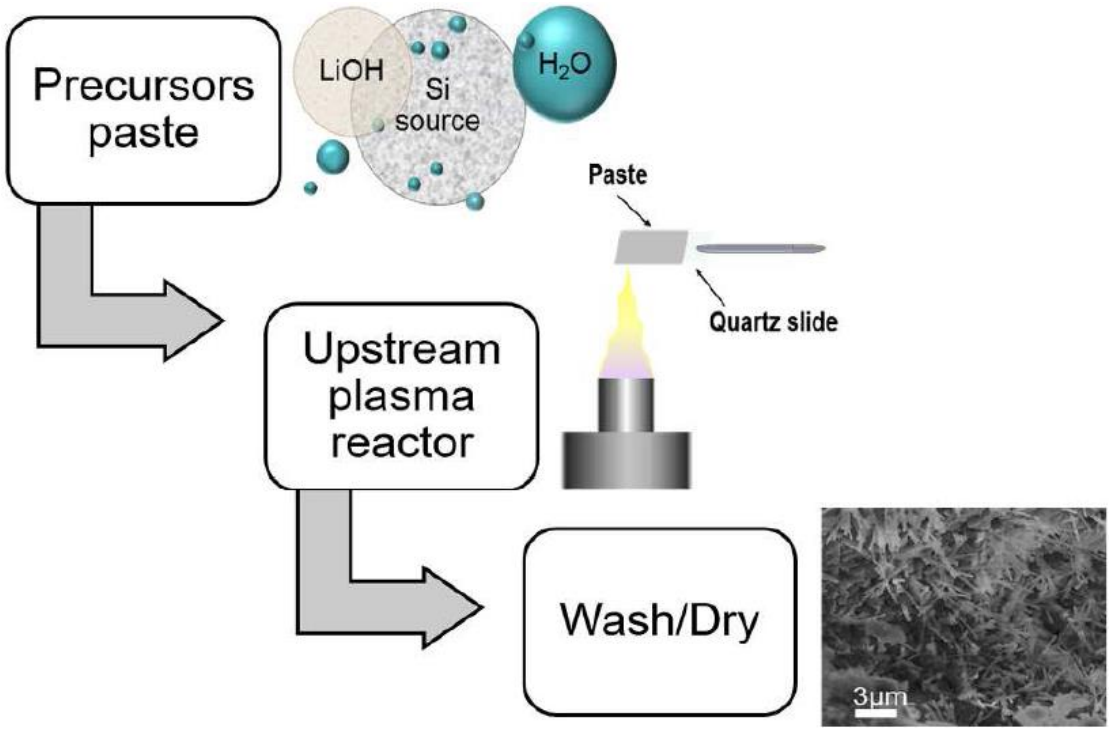


Figure 5. The schematic illustration of the solvo-plasma synthesis method.[74] Reprinted with permission from ref 74. Copyright 2017 American Chemical Society.

For most Li_4SiO_4 synthesis methods, the drying step is generally performed in oven, or water/oil bath, which are somehow energy-consuming and slow processes. Hu et al.[75] prepared Li_4SiO_4 sorbents using a spray drying technique, which resulted in highly efficient Li_4SiO_4 samples with high CO_2 uptake and excellent cycling stability. After 50 cycles in 15 vol% CO_2, the CO_2 uptake only slightly decreased from 27.5 to 24.8 wt%. The superior performance of such prepared Li_4SiO_4 samples was ascribed to the fine crystallites and high specific surface area of Li_4SiO_4.[75]

In a recent publication, Rao et al.[76] synthetized Li_4SiO_4 nanoparticles by a solution combustion method, where glycine was used as fuel, while silicic acid and lithium nitrate were the lithium silicate precursors. Authors determined that fuel-oxidizer ratio highly influenced the combustion process and synthesis evolution. In fact, using

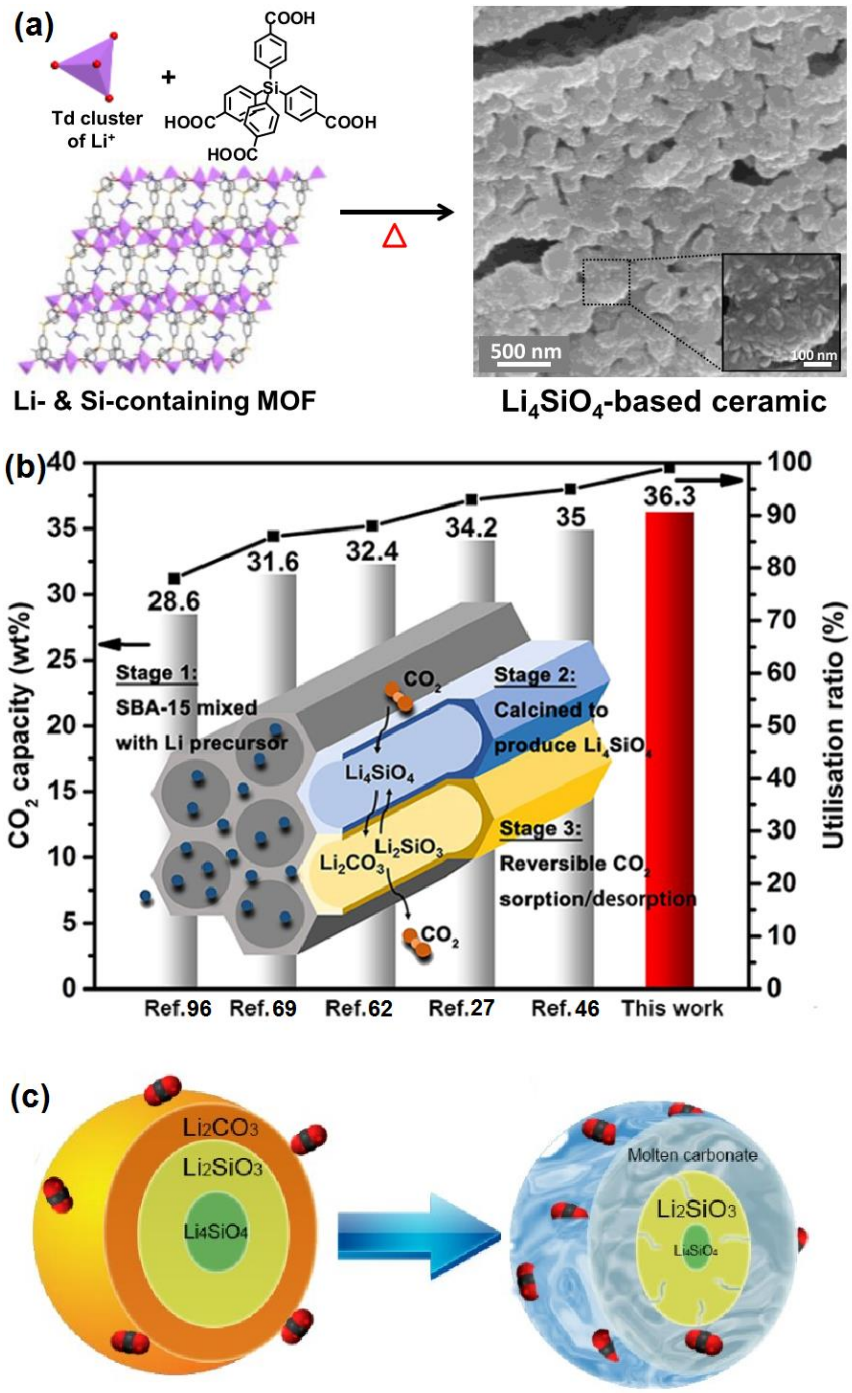
this kind of control, authors were able to obtain pure Li_4SiO_4 at 700 °C. The Li_4SiO_4 showed an average particle size of 72 nm, and a high specific surface area of 26.7 m^2 g^{-1}. Moreover, this sample presented a high sinterability capacity (around 11%) in comparison to solid state samples, which may be beneficial for pelletizing processes. Li_4SiO_4 synthesized via the combustion method showed a good CO_2 uptake of 30.7 wt% at 700 °C.[76]

2.2.5. Synthesis of Li_4SiO_4 from MOFs or zeolites

Recently, using a conversion reaction of MOFs or zeolites as precursors has been recognized as a novel synthesis scheme, which imparts the materials with unprecedented physiochemical properties. This is a result of MOF and zeolite's possession of highly ordered nano- or meso-pores and channels.[59, 77] Recently, Moon et al.[77] demonstrated that coral-like Li_4SiO_4 samples can be synthesized from a MOF precursor (Figure 6(a)). The coarse integration of the secondary particles creates macro-porous voids. With 15 vol% CO_2, the CO_2 uptake of this sample has a relatively slow saturation to 29.4 wt% at 500 °C for 6 h, and the ultimate CO_2 uptakes at 550 and 600 °C similarly approached 32.4 wt%. This good performance can be attributed to the material's macropores, which favor the mass transport during CO_2 capture. However, the regeneration stability (sorption: 550 ^oC in 15 vol% CO_2; desorption: 650 ^oC in N_2) of this MOF-Li_4SiO_4 sample was relatively poor. A severe decay of sorption capacity from 22.4 to 11.4 wt% was observed during the first four cycles, which continuously decreased to 7.7 wt% after 25 cycles. SEM analyses indicated that the porous coral-like morphology had mostly collapsed after cycling tests, explaining the decrease of CO_2 capture performance.

Zeolite-related materials exhibit very high specific surface area and regular porous structure. Wang et al.[78] revealed SBA-15 is excellent Si precursor for the preparation of Li_4SiO_4 with enhanced performance for CO_2 capture. The best sample Li-SBA15-4, which was obtained with the Si/Al ratio of 4, showed a record CO_2 uptake of 36.3 wt%, as compared in Figure 6(b). The results revealed that using SBA-15 as precursor can lead to a sorbent with higher content of Li_4SiO_4 phase (98 wt%), which is higher than the sample obtained from SiO_2 precursor (80 wt%) at 650 ^oC in pure CO_2 gas. After 15 cycles, the CO_2 uptake of Li-SBA15-4 only slightly decreased by 1.0 wt%, suggesting a very excellent cycling stability.

In addition, Wang et al. [79] compared the CO_2 capture performance of different Li_4SiO_4 sorbents synthesized from different zeolites (MCM-41, MCM-48, ZSM-5, TS-1). Among of sorbents, Li_4SiO_4 synthesized from MCM-41 (MCM-41-Li_4SiO_4) showed excellent cycling stability at 650 °C under 100 vol%, with a stable reversible CO_2 uptake of 29.1 wt% during 20 cycles. The sorption capacity of metal modified MCM-41-Li_4SiO_4 can be further improved. The Na-MCM-41-Li_4SiO_4 sorbent showed the highest sorption rate, and reached the equilibrium sorption capacity close to the theoretical value of 36.7 wt% within 20 min. In order to further improve the sorption performance of MCM-41-Li_4SiO_4 at low CO_2 concentration, the sample was further coated with K_2CO_3 and Na_2CO_3. At 550 °C and under 20 vol% CO_2, 15 wt% K_2CO_3-MCM-41-Li_4SiO_4 and 10 wt% Na_2CO_3-MCM-41-Li_4SiO_4 sorbents resulted in a CO_2 uptake of 32.2 wt% and 34.7 wt%, respectively, which are much higher than that of MCM-41-Li_4SiO_4 (11.8 wt%). The promoting mechanism by doping alkali carbonates onto Li_4SiO_4 was explained by a double-shell model, as illustrated in Figure 6 (c).



1

2 **Figure 6.** (a) The scheme for the synthesis of Li_4SiO_4 from MOFs that contain Li and Si.[77]

3 Reprinted with permission from ref 77. Copyright 2012 The Royal Society of Chemistry,

4 (b) Comparison of the CO_2 uptake of Li-SBA15-4 (Li_4SiO_4) with literature reports.[78]

5 Reprinted with permission from ref 78. Copyright 2017 American Chemical Society. (c)

6 Illustration of the sorption processes over unmodified MCM-41-Li_4SiO_4 and alkali

carbonates-coated MCM-41-Li_4SiO_4.[79] Reprinted with permission from ref 79. Copyright 2018 Elsevier B.V.

Later on, Zhao et al.[80] synthesized a series of Li_4SiO_4 from six different silicon precursors including SBA-15, MCM-41, ZSM-5, fumed silica, precipitated silica, and waste-derived silica. CO_2 sorption/desorption cycling tests (Figure 7) indicated that the total CO_2 uptake over 30 cycles followed the order of Li_4SiO_4 (Fumed) > Li_4SiO_4 (ZSM-5) > Li_4SiO_4 (SBA-15) > Li_4SiO_4 (MCM-41) > Li_4SiO_4 (Waste) > Li_4SiO_4 (Precipitated). The results revealed that the CO_2 uptake at the last cycle is much more important than the initial CO_2 uptake. For instance, although the sorbent prepared from precipitated silica had very high initial CO_2 uptake, its long-term cycling performance was very disappointing. However, an opposite trend was observed with the sample prepared from fumed silica, which showed the second lowest CO_2 capacity in the 1st cycle (19.90 wt%), but gradually grew to a stable capacity of 34.23 wt%.

It was also proved that the pore size has a great effect on the performance of Li_4SiO_4 samples, and the optimal pore size was determined to be ~4 nm, as illustrated in Figure 8. Comparing to large pores, smaller pores are preferred as they provide more specific surface area for nucleation. However, the sorbents normally swell after being converted from Li_4SiO_4 to Li_2SiO_3 and Li_2CO_3, because the molar volume of resulting Li_2SiO_3 (35.542 cm^3 mol^{-1}) and Li_2CO_3 (35.019 cm^3 mol^{-1}) is higher than that of Li_4SiO_4 (50.146 cm^3 mol^{-1}). Thus, the small pores are easier to be blocked due to the volumetric expansion, due to which nucleation may only take place on the external part of sorbents. The results suggested ~4 nm is the optimal size for Li_4SiO_4 sorbents, which allows CO_2 diffuse rapidly into the interior part of sorbent without being

blocked.[80]

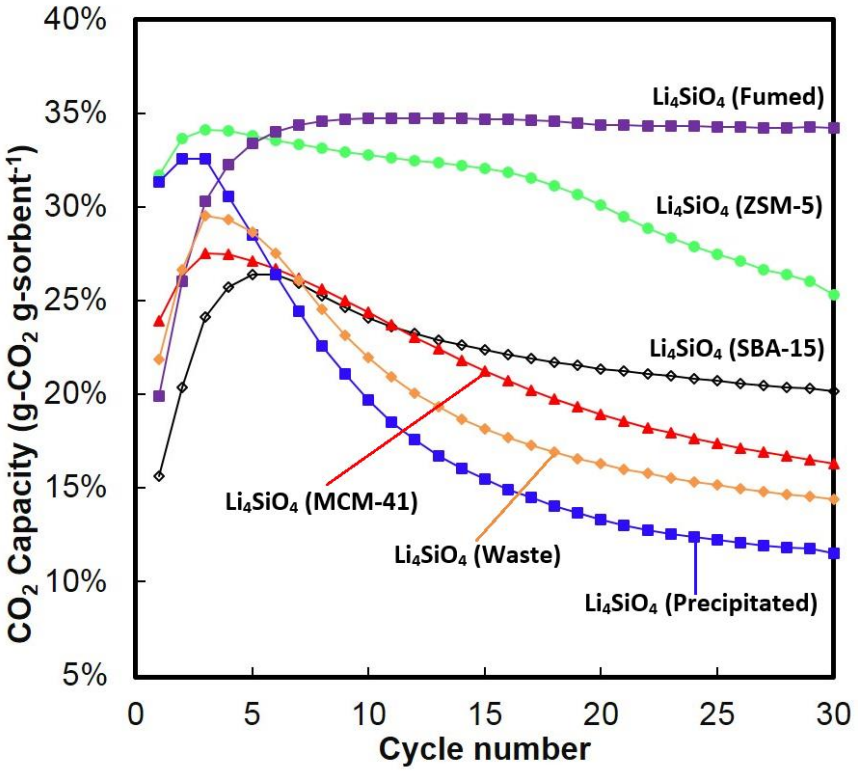


Figure 7. The cyclic CO_2 capture capacity of Li_4SiO_4 (Fumed), Li_4SiO_4 (ZSM-5), Li_4SiO_4 (SBA-15), Li_4SiO_4 (MCM-41), Li_4SiO_4 (Waste), and Li_4SiO_4 (Precipitated) over 30 cycles.[80] Reprinted with permission from ref 80. Copyright 2018 Royal Society of Chemistry.

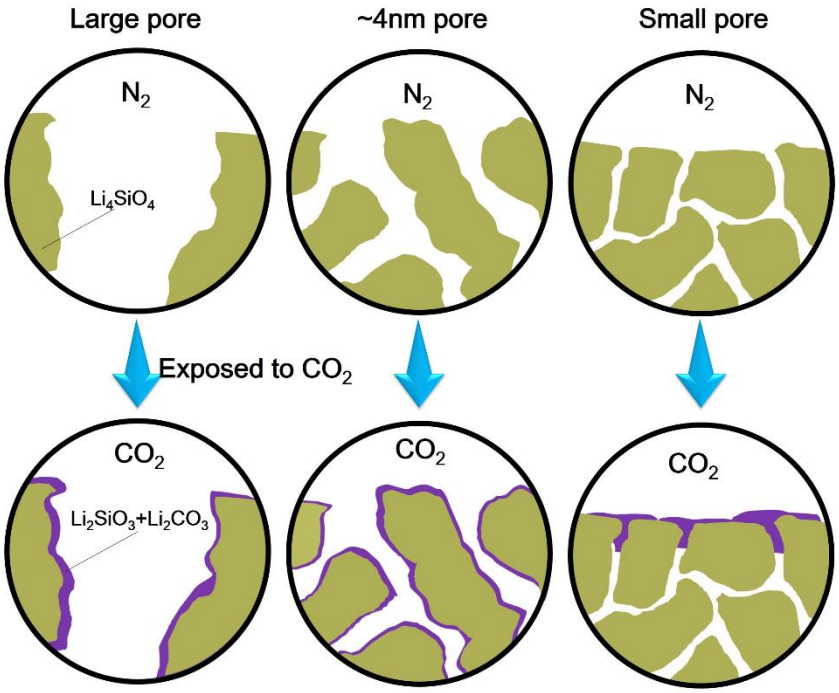


Figure 8. The schematic of nucleation of Li_4SiO_4 samples with different pore sizes.[80] Reprinted with permission from ref 80. Copyright 2018 Royal Society of Chemistry.

In all, for comparison purpose, we summarized the advantages and disadvantages of different methods for the synthesis of Li_4SiO_4 in Table 1. For the solid state method, although it possesses high yield and low cost due to its simple operation process, the obtained products are generally large, dense and non-porous particles. With sol-gel method, the synthesis of Li_4SiO_4 can be achieved at relatively lower temperatures, and the final products are of small particle size and controllable morphology and microstructure. While the drawbacks of sol-gel method are complex operation process, use of chemicals, and high cost. Impregnation precipitation method enables the synthesis of Li_4SiO_4 from various solid Si precursors such as solid wastes and minerals, etc. But in the meantime, the properties of products are limited by the nature of solid Si precursors. The solvo-plasma method, spray-drying method, and

combustion method are emerging processes for the synthesis of fine Li_4SiO_4 nanoparticles. All these methods are relatively fast processes and can obtain high surface area Li_4SiO_4, but the overall cost and more evaluations are needed. Synthesis of Li_4SiO_4 from MOFs or zeolites has attracted some interests as the products showed high sorption capacity, and fast sorption kinetics, and good cycling stability, but the price of the MOFs and zeolites should be concerned.

Table 1. Summary of the advantages and disadvantages of different methods for the synthesis of Li_4SiO_4.

Synthesis method	Advantages	Disadvantages	Refs
Solid state method	High yield, low cost and simple operation process	Large, dense and non-porous particles	6, 31, 35, 55, 56, 60, 62-68
Sol-gel method	Low synthesis temperature, small particle size, and controllable morphology and microstructure	Complex operation process, use of chemicals, and high cost	
Impregnation precipitation method	Relatively lower synthesis temperature and smaller particle size comparing to solid state method, possible to use various solid Si precursors (solid wastes and minerals, etc)	The properties of products are limited by the nature of the solid Si precursors	71, 72, 81
Solvo-plasma method	Fast process, small particle size with nanowire morphologies	High cost, use of solvents, energy consumption needs to be evaluated	74
Spray-drying method	Industrial-scale mature, fast process,	CO_2 sorption capacity needs to be improved, more evaluations are needed for this new method	75
Combustion method	Fast process, high surface area of product	Energy consumption needs to be clarified, more evaluations are needed for this new method	76

Synthesis of Li_4SiO_4 from MOFs or zeolites	High sorption capacity and sorption kinetics, good cycling stability	Precursors are expensive	[77, 78, 80]

2.3. Element substitution of Li_4SiO_4

For CO_2 capture on Li_4SiO_4, it is believed that the ion diffusion of Li^+ and O^{2-} is very important, and doping of foreign elements can improve its reactivity.[82] Recently, it has been proven that doping hetero-elements such as Al^{3+}, Fe^{3+}, Na^+, V^{5+}, Ti^{4+} into Li_4SiO_4 can reduce diffusion resistance by forming defects or secondary phases in Li_4SiO_4, which consequently improved its CO_2 sorption rate and capacity. Hence in this section, we will discuss the effect of doping hetero elements in Li_4SiO_4 at lithium (Na^+) or silicon (Al^{3+}, Fe^{3+}, V^{5+} or Ti^{4+}) crystal structural sites on CO_2 sorption performance in detail. All the hetero heteroelements substituted Li_4SiO_4 samples and their CO_2 sorption capacities are summarized in Table 2.

Table 2. The CO_2 sorption capacities of various elements doped Li_4SiO_4.

Samples	CO_2 uptake	Reference
$Li_{3.85}Na_{0.15}SiO_4$	19.3 wt% at 500 °C	[83]
$Li_{3.9}Na_{0.1}Si_{0.96}Ti_{0.04}O_4$	31.6 wt% at 650 °C	[84]
$Li_4SiO_{0.96}Ti_{0.04}O_4$	30.4 wt% at 650 °C	[84]
$Li_{3.5}Si_{0.5}Al_{0.5}O_4$	17.1 wt% at 750 °C	[85]
$Li_{3.8}Si_{0.8}V_{0.2}O_4$	4.3 wt% at 525 °C	[85]
$Li_{3.7}Fe_{0.1}SiO_4$	28.8 wt% at 540 °C	[82]
$Li_{3.7}Al_{0.1}SiO_4$	33.0 wt% at 550 °C	[82]
$Li_{4.1}Al_{0.1}SiO_{0.9}O_4$	35.5 wt% at 685 °C	[82]

2.3.1. Li substitution

Many studies have shown that doping some hetero elements in lithium silicate can lead to better CO_2 sorption performances than pure Li_4SiO_4. The influence of Li^+ substitution by Na^+ on the CO_2 performance of Li_4SiO_4 was studied by Pfeiffer et al.[83] where a series of $Li_{4-x}Na_xSiO_4$ were synthesized via a co-precipitation method. In this type of solid solution, they revealed that the maximum Na solubility in Li_4SiO_4 is only 0.1 ($Li_{3.9}Na_{0.1}SiO_4$), which means that Na atoms could not diffuse into Li_4SiO_4, but rather located on particle surface. SEM analyses also proved that Na inhibited the growth of particles. The particle size of pure Li_4SiO_4 was roughly 96 μm. However, with the increase in Na content, the particles became smaller, down to 25 μm for $Li_{3.7}Na_{0.3}SiO_4$. Meanwhile, the specific surface area was doubled, from about 3 $m^2\ g^{-1}$ for Li_4SiO_4 to 6 $m^2\ g^{-1}$ for $Li_{3.7}Na_{0.3}SiO_4$. In addition, the surface located Na atoms are the active sites for capturing CO_2 as well. Figure 9 shows the CO_2 sorption capacities of $Li_{3.85}Na_{0.15}SiO_4$, and $Li_{3.8}Na_{0.2}SiO_4$ are higher than that of pure Li_4SiO_4 at 500 °C. In fact, Li_4SiO_4 sorbed CO_2 at a slower rate, as the slope (at short times, 0–10 min) for Li_4SiO_4, $Li_{3.85}Na_{0.15}SiO_4$, and $Li_{3.8}Na_{0.2}SiO_4$ was 0.9, 4.3, and 5.2 mg g^{-1} min^{-1}, respectively. These results confirmed Na addition can enhance CO_2 capture capacity up to 5 times higher. For $Li_{3.85}Na_{0.15}SiO_4$, the kinetic constant parameters were higher than those of Li_4SiO_4. While, the sorption process of $Li_{3.85}Na_{0.15}SiO_4$ was improved by one order of magnitude, and the diffusion process was enhanced by four times. In the meantime, desorption constant value was improved by two orders of magnitude. Therefore, it can be concluded that the CO_2 sorption kinetics and lithium diffusion could be significantly enhanced by Na addition.[83, 86]

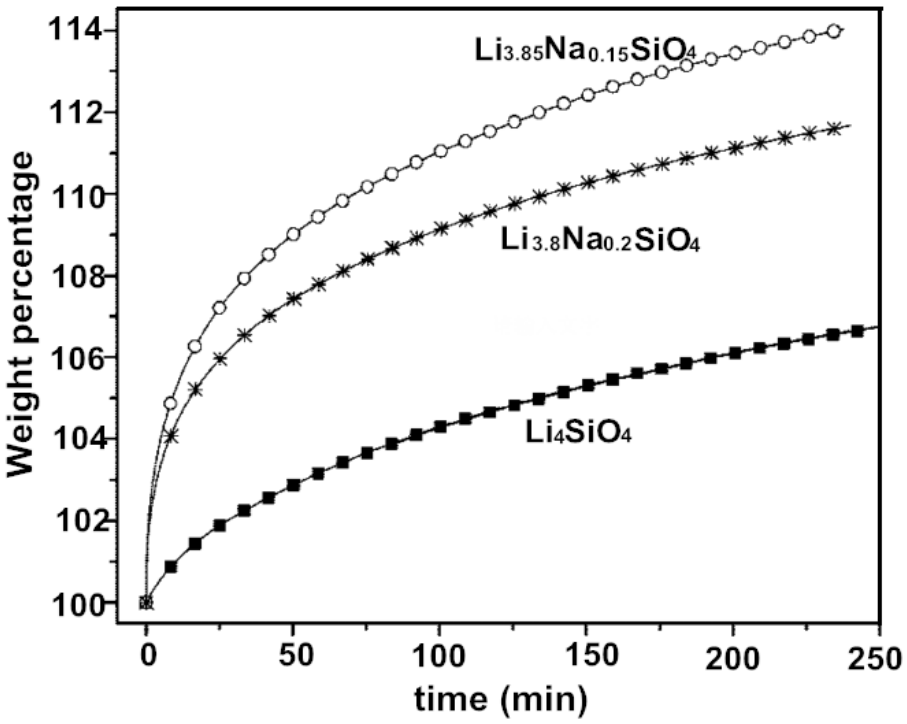


Figure 9. Isothermal CO_2 uptakes of $Li_{4-x}Na_xSiO_4$ samples at 500 °C with a flux of CO_2.[83] Reprinted with permission from ref 83. Copyright 2008 American Chemical Society.

2.3.2. Si substitution

In addition to the Li substitution by Na, the substitution of Si by Ti^{4+}, Al^{3+}, Fe^{3+}, V^{5+}, and Ge^{4+} on the CO_2 sorption capacity of Li_4SiO_4 was also studied. Xiang et al.[84] studied the CO_2 sorption performance of $Li_4Si_{1-x}Ti_xO_4$ (x = 0, 0.005, 0.01, 0.02, 0.04, 0.06) and $Li_{3.9}Na_{0.1}Si_{0.96}Ti_{0.04}O_4$. These solid solutions were synthesized via a sol-gel process, and the specific steps are shown in the Figure 10(a). The results indicated that the crystallization of Li_4SiO_4 could be inhibited by Ti doping. The average grain size decreased from 3 μm (Li_4SiO_4) to 0.23 μm ($Li_4Si_{0.96}Ti_{0.04}O_4$). With the increase in x value, the specific surface area and total pore volume increased while the pore size decreased to certain extent. For instance, the specific surface area increased from 8.43 to 13.04 $m^2\ g^{-1}$ when the value of x increased from 0 to 0.06. The CO_2 sorption

performance of Ti-doped Li_4SiO_4 is shown in Figure 10(b). $Li_4Si_{0.96}Ti_{0.04}O_4$ showed a significant improvement in sorption capacity (30.4 wt%), which is much higher than that of Li_4SiO_4 (20.1 wt%) at 650 ^oC. The raise in $Li_{4-x}(Si_{1-x}Ti_x)O_4$ series can be attributed to the enhancement in Li^+ diffusion and the decrease in grain size by Ti doping. In addition, sorption isotherm also showed that when Ti and Na elements were co-doped into Li_4SiO_4, the sorption properties were enhanced. Compared to other samples, $Li_{3.9}Na_{0.1}Si_{0.96}Ti_{0.04}O_4$ demonstrated the highest CO_2 sorption capacity of 31.6 wt%. Furthermore, $Na_{0.1}Si_{0.96}Ti_{0.04}O_4$ were exposed to CO_2 (160 mL/min) for 1 h and then to N_2 (200 mL/min) for 40 min at 650 ^oC. The chemisorption capacity of $Li_{3.9}Na_{0.1}Si_{0.96}Ti_{0.04}O_4$ reached 32.5 wt% for the first cycle, and after 10 cycles it stabilized at 33.1 wt%. However, after 10 cycles, the stabilized chemisorption capacity of neat Li_4SiO_4 was only 29.2 wt%. The enhanced CO_2 capture performance of $Li_{3.9}Na_{0.1}Si_{0.96}Ti_{0.04}O_4$ can be attributed to the co-doping of Ti and Na into Li_4SiO_4 crystal lattice, which could enhance Li^+ and O^{2-} diffusion by forming lattice distortion, dislocations, interstitial atoms, and vacancies.[84]

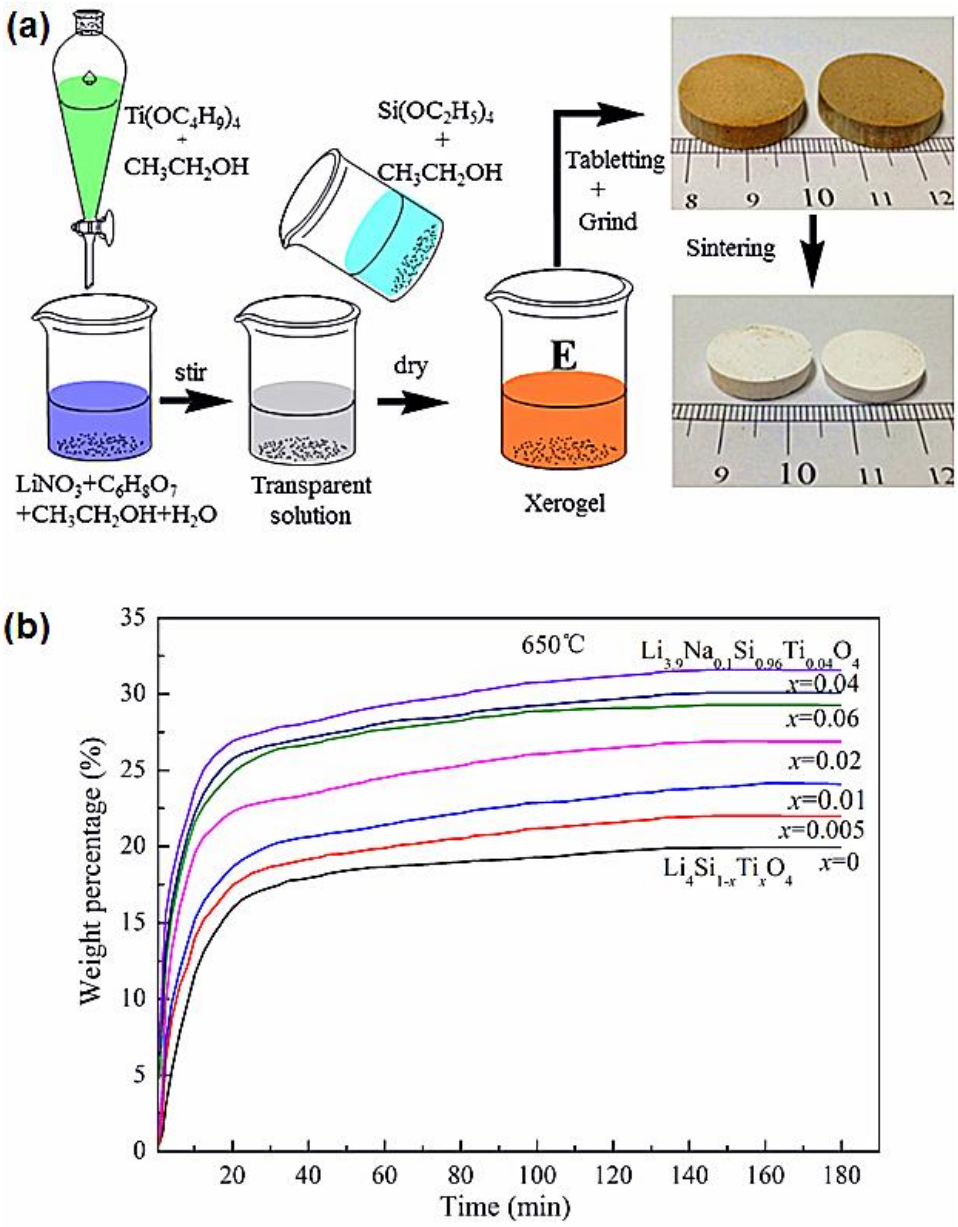


Figure 10. (a) Synthesis procedures for the tablet-like $Li_4Si_{1-x}Ti_xO_4$ ($0 < x < 0.06$) and $Li_{3.9}Na_{0.1}Si_{0.96}Ti_{0.04}O_4$, (b) CO_2 sorption behaviors of $Li_4Si_{1-x}Ti_xO_4$ and $Li_{3.9}Na_{0.1}Si_{0.96}Ti_{0.04}O_4$ at 650 °C under pure CO_2 flow.[84] Reprinted with permission from ref 84. Copyright 2015 Springer Science + Business Media New York.

Except for Ti^{4+}, Pfeiffer et al.[85] synthesized a series of $Li_{4+x}(Si_{1-x}Al_x)O_4$ and $Li_{4-x}(Si_{1-x}V_x)O_4$ by solid state method, in which both Al and V were totally incorporated into Li_4SiO_4, occupying the Si sites. They revealed that adding Al and V modified the

CO_2 capture process in important but different ways. $Li_{4-x}(Si_{1-x}V_x)O_4$ possessed the same CO_2 capture temperature range as Li_4SiO_4, but the uptake decreased. In contrast, $Li_{4+x}(Si_{1-x}Al_x)O_4$ showed improved CO_2 uptakes in a wider temperature range. Particularly the CO_2 capture temperature shifted to a range of 600–770 °C, which is in good agreement with some Li_5AlO_4 reports. For these two types of samples, the produced external shell were all composed of Li_2CO_3 and Li_2SiO_3, with the only difference of Li_3VO_4 or $LiAlO_2$. Because Li_3VO_4 possesses smaller Li diffusion coefficient than Li_2CO_3, Li_2SiO_3, and $LiAlO_4$, it was proposed that the reduced CO_2 uptakes of $Li_{4-x}(Si_{1-x}V_x)O_4$ can be attributed to the decreased Li diffusion in the external shell due to the presence of Li_3VO_4.[31, 87] Kinetic studies suggested that the CO_2 capture process was influenced by not only the modification of structures but also the change of lithium diffusion properties.[33, 77]

Gauer et al.[82] investigated the effects of doping of Li_4SiO_4 with hetero-elements such as aluminum or iron on CO_2 sorption of Li_4SiO_4. Thermogravimetric sorption measurements showed that in 100 vol% CO_2, the sorbent capacity of $Li_{4.1}Al_{0.1}Si_{0.9}O_4$ is similar to that of pure Li_4SiO_4, the maximum capacity of which is about 35.4 wt%. The other modifications exhibited significantly lower maximum capacity at temperature higher than 650 °C, because additional components reduced the active mass and the Li-concentration. Similarly, the performance of $Li_{3.7}Fe_{0.1}SiO_4$ was lower than pure Li_4SiO_4 when the temperature was higher than 650 °C. These results suggested Al^{3+} and Fe^{3+} cannot improve the CO_2 sorption capacity at temperatures higher than 650 °C. However, the CO_2 sorption capacities of Al and Fe doped Li_4SiO_4 were greatly enhanced at temperatures below 650 °C. When the sorption temperatures for $Li_{3.7}Al_{0.1}SiO_4$ and

$Li_{3.7}Fe_{0.1}SiO_4$ were between 540 and 555 °C, their maximum CO_2 sorption capacities were 33.0 wt% and 28.8 wt%, respectively. These CO_2 sorption capacities were higher than that of Li_4SiO_4 at the same temperature. Unfortunately, both $Li_{4.1}Al_{0.1}Si_{0.9}O_4$ and $Li_{3.7}Al_{0.1}SiO_4$ sorbents cannot be completely desorbed, even at temperatures higher than 800 °C. Although hetero-elements doping into the lattice of Li_4SiO_4 can somehow improve CO_2 sorption capacity, such raise remains limited. The thermal stability of these sorbents should be noted. The cyclic capacity of $Li_{3.7}Al_{0.1}SiO_4$ decreased with the increase of cycle number. A reduction of the initial capacity to 85% in the fifth cycle reveals inferior durability of $Li_{3.7}Fe_{0.1}SiO_4$. In a similar way, Gao et al.[88] prepared K and Al co-doped Li_4SiO_4 using kaolin as silica source, and obtained a significant improvement in CO_2 capture efficiency. Authors reported that lithium diffusion was greatly improved by the addition of these two heteroatoms as the rate constant values were two times higher than that of pure Li_4SiO_4 between 575–650 °C. The sorption/desorption test showed that the CO_2 sorption capacity of 8K15Al-Li_4SiO_4 reached 24.6 wt% in the first cycle. Then, the CO_2 sorption capacity gradually decreased, and finally maintained at 22.0 wt% after 3 cycles.

Because germanium (Ge) exhibits similar physical and chemical properties to Si, the substitution of Si by Ge is possible and Li_4GeO_4 is iso-structural to Li_4SiO_4. It was also found that the Ge compounds possess higher lithium ion diffusivity. At 360 ^oC for instance, the lithium ion diffusivity in Ge matrices is approximately 15 times higher than that in Si matrices.[89] Therefore, the incorporation of Ge in Li_4SiO_4 was considered as an option to enhance the kinetics and sorption capacity of Li_4SiO_4 sorbents. Subha et al.[90] reported a facile synthesis strategy for Ge-incorporated Li_4SiO_4, and the as-synthesized samples exhibited enhanced CO_2 uptake and kinetics at 150–680 ^oC. For

the sample with a Si : Ge molar ratio of 1 : 0.183, a sorption capacity of 32.4 wt% at the rate of 117 mg g^{-1} min^{-1} and a sorption capacity of 4.9 wt% at the rate of 36 mg g^{-1} min^{-1} were obtained at 680 and 300 °C (100 vol% CO_2), respectively. This study demonstrated the possibility of employing Ge-incorporated Li_4SiO_4 to capture CO_2 from chemical and petrochemical reactions in a wide temperature range, such as the WGS reaction that occurs at low temperature ranges of 150–450 °C, which is not possible with pure Li_4SiO_4.

2.4. Incorporation of a second phase

Although Li_4SiO_4 sorbent has shown good sorption performance for CO_2 capture, the CO_2 uptake becomes low with low CO_2 concentrations and decreases severely due to the agglomeration or sintering of particles during processing or repeated sorption/desorption cycles. In order to solve these problems, a second phase such as molten salt, metal oxide, or porous component can be introduced to the Li_4SiO_4 sorbents.

2.4.1. Incorporation of molten salt components

According to the double-shell model and dynamic investigations, the formed external shell consisting of Li_2CO_3 might limit the CO_2 diffusion into Li_4SiO_4 bulk during the CO_2 sorption process at low CO_2 concentrations. In order to avoid this problem, different single alkali carbonates (Na_2CO_3, K_2CO_3), binary alkali carbonates (K_2CO_3/Li_2CO_3, Na_2CO_3/Li_2CO_3) and ternary alkali carbonates (K_2CO_3/Na_2CO_3/Li_2CO_3) were doped to Li_4SiO_4. A liquid eutectic layer assists in reducing the CO_2 diffusion resistance, and gaining enhanced sorption kinetics.[91-93] The melting points of different alkali metal carbonates were summarized in Table 3.[72, 94]

Table 3. Melting points of different alkali carbonates.

Eutectic composition (mol%)	Melting point (°C)	Reference
Li_2CO_3	723	[95]
Na_2CO_3	858	[96]
K_2CO_3	898	[94]
Li_2CO_3 (42.7%)/K_2CO_3 (57.3%)	498	[92]
Li_2CO_3 (52 %)/Na_2CO_3 (48%)	500	[92]

Seggiani et al.[92] performed a systematic investigation on the influence of different alkali carbonates and their mixtures on the CO_2 capture performance of Li_4SiO_4 at high-temperatures (500–600 °C) and under low CO_2 partial pressure (as low as 0.04 atm). It was found that the temperature, promoter type, and promoter loading can significantly affect the CO_2 capture performance of sorbents. For all doped-sorbents, the optimal sorption temperature was determined to be 580 °C. All doped-Li_4SiO_4 samples showed significantly higher sorption rate than pure Li_4SiO_4. During CO_2 capture, a molten salt shell consisting of Li-K and Li-Na carbonates was formed on the surface of Li_4SiO_4, which can significantly improve the capture performance. This work revealed the CO_2 sorption process is governed by the diffusion of CO_2 within the outer Li_2CO_3 layer. At 580 °C under 100 % CO_2, the Li_4SiO_4 samples loading with 30 wt% K_2CO_3 or Na_2CO_3 exhibited the best CO_2 capture performance, with a CO_2 uptake of 29.3 wt% after 120 min.

Inspired by the aforementioned research, Xu et al.[97] prepared different contents of Na_2CO_3 (5, 10, and 20 wt%) or K_2CO_3 (1, 5, and 10 wt%) doped Li_4SiO_4 samples for

CO_2 capture at low CO_2 concentrations. All doped Li_4SiO_4 samples showed good CO_2 sorption performance. It was also noticed that a greater addition of dopants favors the faster sorption. For instance, both 20 wt%-Na_2CO_3-doped Li_4SiO_4 and 5 wt%-K_2CO_3-doped Li_4SiO_4 samples attained the highest CO_2 uptake within only 15 min. They also confirmed that the formed eutectic melts can reduce the resistance for CO_2 diffusion.

However, when the sorption temperature was lower than eutectic point, CO_2 sorption capacity of doped sample became only slightly higher than that of the pure sample, which may be due the high specific surface area of doped Li_4SiO_4. Compared with the specific surface area of pure Li_4SiO_4 (2.2 m^2 g^{-1}), both 10 wt%-Na_2CO_3-doped Li_4SiO_4 and 5 wt%-K_2CO_3-doped Li_4SiO_4 had higher specific surface area of 8.4 and 8.8 m^2 g^{-1}, respectively. As shown in Figure 11(a), the disordered arrangement of doped sorbents contributed to the increase of specific surface area. It is worth noting that the conversion of 10 wt%-Na_2CO_3-doped Li_4SiO_4 only slightly decreased from 96.5% to 89.8% after 40 cycles, but it is still higher than Li_4SiO_4 by at least 20%. With respect to 5 wt%-K_2CO_3-doped Li_4SiO_4, its conversion remained as high as 90%.

Many studies have revealed that Li_4SiO_4 samples loaded with K_2CO_3 exhibit better cycling stability than those loaded with Na_2CO_3. Therefore, there are several more studies on the performance of K_2CO_3 loaded Li_4SiO_4 samples. Kato et al.[98] compared the performance of 10 mol%-K_2CO_3-doped Li_4SiO_4 and Li_2ZrO_3 at different CO_2 concentrations. At 500 °C in 20 vol% CO_2 flow, the weight increase of 10 mol%-K_2CO_3-doped Li_4SiO_4 was about 50% greater than that of Li_2ZrO_3, and the CO_2 sorption rate of Li_4SiO_4 was more than 30 times faster than that of Li_2ZrO_3. Furthermore, at 500 °C in 2 vol% CO_2 flow, the weight increase of 10 mol%-K_2CO_3-doped Li_4SiO_4 nearly reached 25 wt%, but Li_2ZrO_3 had no clear weight increase. Therefore, K_2CO_3-doped Li_4SiO_4 was

thought to be more suitable than Li_2ZrO_3 for CO_2 capture in lower CO_2 concentration atmospheres.

In addition to the quantity of loading, the doping method, the type of Li_4SiO_4 and the conditions of use also affect the performance of the sorbent. Seggiani et al.[94] explored the CO_2 sorption performance of three kinds of Li_4SiO_4-based sorbents which were synthesized using different silicon precursors (fumed silica, quartz wool, crystalline quartz) and two different doping methods (eutectic-doping and direct addition method) by use of potassium. The isotherms of CO_2 sorption at 580 °C in 4 vol% CO_2 showed that pure Li_4SiO_4 sample had low sorption capacity (5 wt%), which resulted independently of the used above three kinds of silica type. With the eutectic doping, sample showed higher CO_2 sorption capacity of 10–13 wt%. This research proved that the direct loading method is more effective than eutectic-doping one. In addition, the quartz appears more suitable as a silicon source for the synthesis of Li_4SiO_4.[94]

Zhang et al.[99] doped K_2CO_3 molten salt on glacial acetic acid treated Li_4SiO_4 (HAc-Li_4SiO_4) samples and studied their performance for CO_2 capture. The K_2CO_3-doped HAc-Li_4SiO_4 sample showed a much higher reversible CO_2 uptake than other pure Li_4SiO_4 and HAc-Li_4SiO_4 during sorption/desorption cycles. Under a 10 vol% CO_2 atmosphere, the high CO_2 sorption capacity of K_2CO_3-doped HAc-Li_4SiO_4 reached 19.5 wt%, which was five times higher than commercial Li_4SiO_4 and two time higher than HAc-Li_4SiO_4. After 10 cycles, the CO_2 sorption capacity of Li_4SiO_4 and HAc-Li_4SiO_4 sorbents decreased to 40% and 85% of its first capacity, respectively. However, the CO_2 uptake of K_2CO_3-doped HAc-Li_4SiO_4 only decreased by 5% after the 10^{th} cycle.[99]

Zhang et al.[49] further evaluated the influence of water vapor on the CO_2 capture

performance of K_2CO_3-doped Li_4SiO_4 sorbent. The results indicated that steam (15–20 vol%) could promote the CO_2 sorption capacity. While the regeneration performance (sorption process: 100 ml/min CO_2 at 575 ^oC; desorption process: 100 ml/min N_2 at 700 ^oC) decreased slightly after 10 cycles, and the weight gain was reduced to 22.2 wt%, which is approximately 10% lower than the maximum weight gain (24.4 wt%). Zhang et al.[100] observed the structural changes of K_2CO_3-doped Li_4SiO_4 during sorption/desorption process, and discussed the self-activation mechanism in detail by utilizing eutectic mixture theory. Fresh K_2CO_3-doped Li_4SiO_4 sorbent possessed pores in the range of 1–8 nm. Whereas, after 3 and 10 cycle, the pores were enlarged to be 1–56 nm and 1–170 nm, respectively. These results further validated that a significant number of large pores were formed after several cycles. In addition, after the sorption/desorption cycling performance, the CO_2 uptake of K_2CO_3-doped Li_4SiO_4 sorbent was enhanced from 8.8 to 22 wt% at 565 °C in 10 vol % CO_2. These results again confirmed the pore widening process occurred during cycles, which great improved the CO_2 capture performance. The pore-core model, which illustrates the self-activation mechanism of the K_2CO_3-doped Li_4SiO_4 sorbent, is shown in Figure 11(b). Pore widening occurs in the presence of melting eutectic mixture, and the formation of more porous surface can be attributed to CO_2 diffusion. The unreacted Li_4SiO_4 core has a solid skeleton structure, which helps in stabilizing the performance of sorbent.[100]

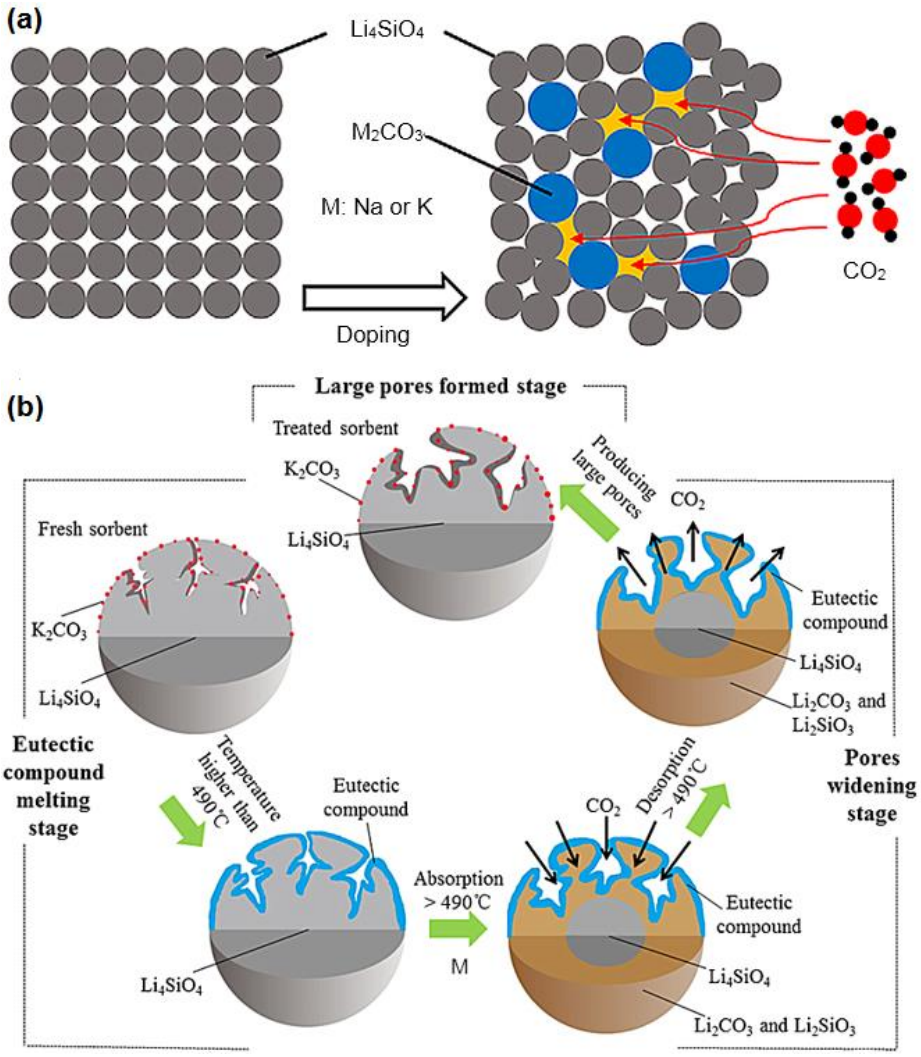


Figure 11. (a) Illustration of the possible mechanism contributing to the increased specific surface area and number of pores during the doping process.[97] Reprinted with permission from ref 97. Copyright 2016 Wiley-VCH Verlag GmbH&Co. KGaA, Weinheim, (b) Schematic illustration of proposed pore−core model for self-activation on K_2CO_3-doped Li_4SiO_4 sorbent.[100] Reprinted with permission from ref 100. Copyright 2015 American Chemical Society.

Wang et al.[101, 102] prepared a different type of molten salt, sodium fluoride (NaF) or lithium fluoride (LiF), doped Li_4SiO_4 for CO_2 capture at low CO_2 partial pressures. Moreover, the Li_4SiO_4 was synthesized using carbon as a sacrificial template. For NaF

doped Li_4SiO_4, all characterizations showed that Na and F substituted Li and O ions, inducing a high concentration of Li–O sites on the molten surface at around 475–575 °C. Therefore, CO_2 capture was highly favored at the surface level. LiF doping resulted in an even higher CO_2 uptake. At a loading of 10 mol%, the smaller crystallites and particles and a species of Li_2O on Li_4SiO_4 surface led to the maximum CO_2 uptake of 36.2 wt% (after 120 min of sorption at 575 °C, under 15 vol% CO_2). It also showed good stability during 8 cycles, indicating the LiF-doped Li_4SiO_4 has great potential for practical applications.

2.4.2. Incorporation of metal oxide components

It is well accepted that the decrease in sorption capacity of Li_4SiO_4 sorbent is mainly due to the sintering of particles during repeated sorption/desorption cycles.[103] In order to improve the stability of Li_4SiO_4 against such high-temperature sintering, the incorporation of a thermally and chemically stable second-phase is one of the possible solutions. In addition, this second-phase materials might also improve the CO_2 sorption performance of Li_4SiO_4 to some extent. Currently, several types of metal oxides including Y_2O_3, Gd_2O_3, CeO_2, and CaO have been studied as the effective separating materials for Li_4SiO_4 sorbents.

Subha et al.[90] added a second phase (Y_2O_3, Gd_2O_3, and $LaPO_4$) to prevent the sintering of Li_4SiO_4 at high temperatures. They demonstrated that the influence by the type of second phase on the CO_2 capture performance was negligible when the composites were rich in sorbent (10:1 and 20:1 in sorbent/second phase), but became obvious when the second phase was higher (2:1). Among them, Y_2O_3 and Gd_2O_3 showed better promoting effect on the CO_2 capture performance of Li_4SiO_4. It was

believed that the non-reactive second-phase components formed a virtual shell that can prevent the segregation of sorbent phase and thus improve its performance (Figure 12(a)).

Except for the aforementioned rare-earth metal oxides, other metal oxides with high thermal stability have also been evaluated. Zhao et al.[104, 105] prepared Li_4SiO_4 doped with different metallic elements (K, Mg, Cr, or Ce). Comparing to other metals, Ce doping can effectively inhibit crystal aggregation and the resulting Ce-Li_4SiO_4 formed a foam-like morphology with smaller particle size. Thanks for the prevention of particle sintering by CeO_2, Ce-Li_4SiO_4 exhibited the best CO_2 capture performance, with a higher sorption capacity. The optimal doping molar content of Ce/Li_4SiO_4 was 0.02, with the highest CO_2 uptake of 34.57 wt%, after 60 min CO_2 sorption process at 690 ^oC. Under the same condition, K-Li_4SiO_4 and Cr-Li_4SiO_4 only achieved 32.85 wt% and 33.57 wt%, respectively. The sorption capacity of all samples were higher than the non-doped Li_4SiO_4 sample. However, because CeO_2 did not participate in CO_2 sorption, too much Ce addition led to a decreased overall sorption capacity. However, CeO_2-Li_4SiO_4 showed good cycling property and maintained its high reversible sorption capacity after 10 cycles.

As an effective and cheap CO_2 sorbent, CaO has attracted much attention in the field of high temperature CO_2 sorption.[22, 106] Recently, Chen et al.[107] studied the CO_2 sorption performance of CaO doped Li_4SiO_4, with the molar ratio of SiO_2:Li_2CO_3:$CaCO_3$ = 1:2.1–*x*:*x* (*x* = 0, 0.02, 0.06, 0.14, or 0.32), and the obtained samples were denoted as LiCa*x*. This work demonstrated that the surface coated Ca species can inhibit the agglomeration of Li_4SiO_4 particles and facilitate the sufficient contact between CO_2 and Li_4SiO_4. LiCa6 sorbent exhibited the highest CO_2 uptake of 35.1 wt% at 700 °C for

1 h as well as excellent CO_2 sorption/desorption cycling performance. After 15 cycles, the CO_2 uptake remained ~26 wt%. The transformation of Ca species from Ca_2SiO_4 to Li_2CaSiO_4 occurred during the cycling tests. While LiCa32 showed much lower initial CO_2 uptake than pure Li_4SiO_4, which was due to lower Li_4SiO_4 content in LiCa32.[107]

The modified double-shell model for the CO_2 sorption/desorption over the Ca-doped Li_4SiO_4 sorbent was proposed in Figure 12(b). According to this model, the transformation of $CaSiO_4$-$CaCO_3$-Li_2CaSiO_4 during the CO_2 sorption process plays a key role in transferring CO_2 to the Li_4SiO_4 core, thus enhancing the CO_2 sorption capacity of Li_4SiO_4.The transformation of Ca species from Ca_2SiO_4 to Li_2CaSiO_4 during the sorption process is also helpful for transferring CO_2 to the Li_4SiO_4 core, and the transformation of Li_2CaSiO_4 to Ca_2SiO_4 in the desorption process favors CO_2 desorption. In addition, during the CO_2 sorption-desorption process, the Ca species covers the surface of Li_4SiO_4 and inhibits the agglomeration of Li_4SiO_4 particles, thus improving the cycling performance of Li_4SiO_4 (Figure 12(b)).[107]

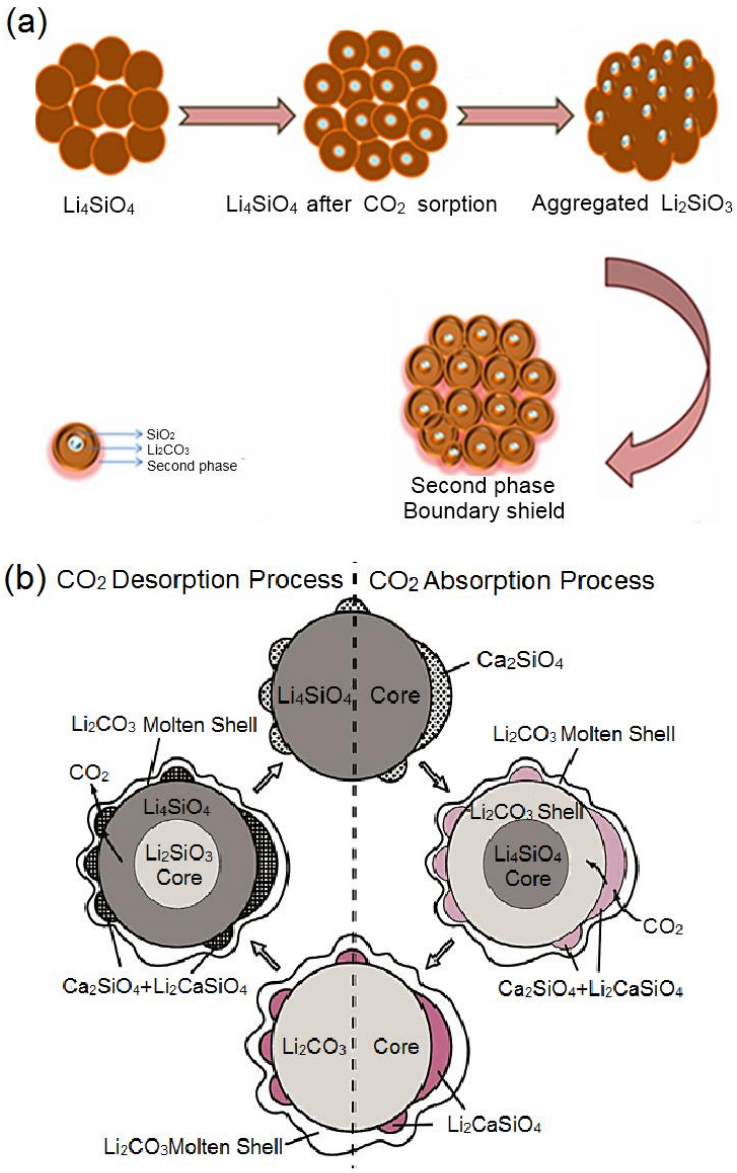


Figure 12. (a) Schematic representation of the boundary pinning by second phases, limiting segregation of molten phase and sintering of sorbent particles.[103] Reprinted with permission from ref 103. Copyright 2015 American Chemical Society, (b) Mechanism of CO_2 sorption/desorption over Ca-doped Li_4SiO_4.[107] Reprinted with permission from ref 107. Copyright 2016 Elsevier Ltd.

2.4.3. Incorporation of porous components

It is well known that the CO_2 sorption capacity and sorption kinetics of Li_4SiO_4 are

somehow limited by its low specific surface area and high resistance to lithium ions and/or CO_2 transfer. In order to deal with these problems, one strategy is to introduce porous materials to Li_4SiO_4. These introduced porous components can not only provide more lithium ions and/or CO_2 diffusion pathways, but also create high specific surface area to Li_4SiO_4 sorbents. The additives chosen for this purpose must be non-reactive with the lithium precursors to avoid undesired production of unnecessary species for CO_2 sorption. So far, two types of porous materials have been studied, TiO_2 nanotubes and porous carbon.

TiO_2 nanotubes with open channel structures have been reported to be able to promote channeling gas flow and reduce diffusion limitation,[108-110] Yavuz et al.[111] reported that the CO_2 sorption and desorption kinetics of Li_4SiO_4 can be significantly increased by adding TiO_2 nanotubes that provided channels for Li^+ to move freely within bulky Li_4SiO_4. The Li_4SiO_4-TiO_2 composite sorbent resulted in a high CO_2 sorption capacity of 34.5 wt% and excellent stability at 700 °C under 100 vol% CO_2. These results indicated that the CO_2 sorption kinetics and cycling stability of Li_4SiO_4 can be greatly improved by the induction of TiO_2 nanotubes.[111]

Different from TiO_2, which mainly provides channels for lithium ions transfer, the porous carbon can provide internal gas pathways and increase the specific surface area, as illustrated in Figure 13(b). Jeoung et al.[112] studied the effects of doping different kinds of porous carbon (CMK-3, multi-walled carbon nanotube (MWCNT)) on CO_2 sorption performance of Li_4SiO_4 sorbents. For Li_4SiO_4@CMK-X% (X% means the amounts of CMK-3), the carbon amount can be controlled in the composites by changing calcination conditions. When the loading of CMK-3 was low (Li_4SiO_4@CMK-0.5%), the additive was mainly observed near the surface of Li_4SiO_4; while the loading

of CMK-3 was high (Li_4SiO_4@CMK-1.8%), CMK-3 was distributed over the whole Li_4SiO_4. CO_2 sorption study showed that the pores of CMK-3 in Li_4SiO_4 help the diffusion of CO_2. In addition, the incorporated CMK-3 could provide additional active sites for capturing CO_2 through the formation of cavities between Li_4SiO_4 and CMK-3. After adding 1.8 wt% of CMK-3, the CO_2 sorption capacity and rate were increased from 16.3 wt% and 5.1 wt% for the first 5 min for pure Li_4SiO_4 to 35.4 wt% and 15.2 wt% for the first 5 min for Li_4SiO_4@CMK-1.8% at 600 °C under 100 vol% CO_2. They also demonstrated that MWCNT could provide the similar promoting effect on the CO_2 sorption properties of Li_4SiO_4.[112]

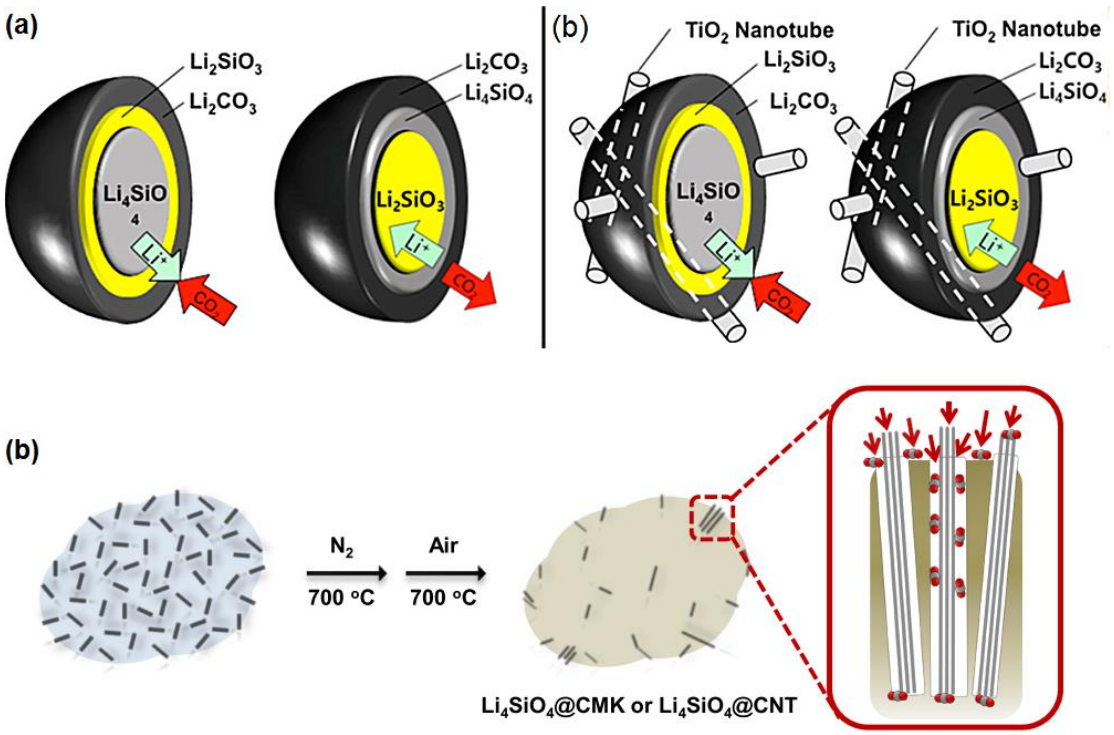


Figure 13. (a) Schematic representation of an ideal CO_2 sorption mechanism of conventional Li_4SiO_4.[111] Reprinted with permission from ref 111. Copyright 2017 American Chemical Society, (b) Preparation scheme of porous carbon containing Li_4SiO_4 sorbents.[112] Reprinted with permission from ref 112. Copyright Elsevier B.V.

2.5. Synthesis of Li_4SiO_4 from solid wastes or cheap silicon sources

In addition to improving the CO_2 sorption performance of Li_4SiO_4 sorbent, it is also important to lower the cost of precursors.[113] Until now, many kinds of cheap silicon sources such as fly ash,[114, 115] rice husk ash,[49, 116, 117] biomass ashes,[118] halloysite,[119] diatomite,[120] and vermiculite[121] have been used for the synthesis Li_4SiO_4-based sorbents. Generally, the Li_4SiO_4-based sorbents synthesized from solid wastes or cheap silicon sources exhibited similar or even higher CO_2 sorption capacity and/or better cycling performance compared to the Li_4SiO_4 synthesized from commercial SiO_2, as summarized in Table 4.

Table 4. CO_2 sorption capacity of Li_4SiO_4 sorbents synthesized from solid wastes or different cheap silicon sources.

Li_4SiO_4 precursors	CO_2 uptake	Reference
Halloysite	34.75 wt% at 700 °C	119
Diatomite	30.32 wt% at 620 °C	71
Vermiculite	34.39 wt% at 650 °C	121
Rice husk ash	32.40 wt% at 650 °C	23
Fly ash	10.7 wt% at 600 °C	114
Rice straw ash	31.6 wt% at 680 °C	118

2.5.1. Synthesis of Li_4SiO_4 from industrial fly ash

Fly ash contains appreciable amounts of silica, which has been used for the manufacture of several ceramic materials. It should be noted that the fly ashes obtained by different factories and collection methods have great difference, which

may influence the performance of Li_4SiO_4. Olivares-Marin et al.[114] synthesized Li_4SiO_4 sorbents using three kinds of fly ashes. Among them, fly ash-1 and fly ash-3 were collected from La Loma-Colombian coal and fly ash-2 was collected from a Russian coal. Fly ash-1 and fly ash-2 were collected from an electrostatic precipitator, while fly ash-3 was collected from a mechanical separator. Li_4SiO_4 sorbents were obtained by calcining these three fly ashes at 950 °C in the presence of Li_2CO_3. For comparison purpose, pure Li_4SiO_4 was also prepared by solid state reaction from SiO_2 and Li_2CO_3. At the same time, certain amount of K_2CO_3 (10, 20, 40 mol%) as an additive was doped into fly ash-Li_4SiO_4. At 500 °C in 100 vol% CO_2, the CO_2 sorption capacity of pure Li_4SiO_4 sorbent can reached 4.7 wt%, while fly ash-1-Li_4SiO_4 without the addition of 10 mol% K_2CO_3 changed little in weight. However, after doping with 10 mol% K_2CO_3, the CO_2 sorption capacity was enhanced for both samples, to 14.1 and 2.3 wt%, respectively. In addition, the effect of temperature on the sorption capacity of fly ash-1-Li_4SiO_4 was studied. At 600 °C, the sorption capacity of fly ash-1-Li_4SiO_4 was increased to 2.6, 5.6, and 10.7 wt% by doping with 10, 20, and 40 mol% K_2CO_3, respectively. The cycling stability of 40 mol% K_2CO_3 doped three fly ash-Li_4SiO_4 sorbents was examined at 600 °C over five CO_2 sorption/desorption cycles. All sorbents showed good regeneration performance. After five cycles, the doped fly ash-1-Li_4SiO_4 presented the highest sorption capacity (10.1 wt%), followed by doped fly ash-2-Li_4SiO_4 (6.4 wt%) and doped fly ash-3-Li_4SiO_4 (4.6 wt%). But, the cycling CO_2 sorption capacity of doped fly ash-Li_4SiO_4 (adding 40 mol% K_2CO_3) was lower than doped pure Li_4SiO_4 (adding 20 mol% K_2CO_3), thus requiring further improvements.

Sanna et al.[115] studied the effect of Na/Li/K carbonate doping on the CO_2 sorption performance of fly ash-Li_4SiO_4 at 500–700 °C in presence of H_2O (2–12 vol%) and

diluted CO_2 (14 vol%). There sorbents were synthesized by changing the Li_2CO_3: Na_2CO_3:SiO_2 molar ratios to be 1:1:1, 0.5:1:1, and 0.5:0.5:1. The results proved that the carbonate:silica molar ratio has a significant effect on CO_2 sorption capacity. The samples synthesized with Na:Li:fly ash molar ratios of 0.5:0.5:1 and 1:1:1 were the best sorbents in terms of combined sorption/desorption rates, CO_2 uptake and regeneration. A maximum CO_2 sorption capacity of 11.2 wt% was achieved at 700 ^oC in the presence of 12% H_2O, 14% CO_2 and 20% with K_2CO_3 as a promoter. Sorption/desorption can be completed within 15 min with reaction kinetics comparable to pure Li_4SiO_4 sorbents.

Izquierdo et al.[122] compared the CO_2 capture performance of Li_4SiO_4 sorbents synthesized from pure SiO_2 and fly ash, with the main goal to assess the role of foreign elements present in the fly ash. At 600 °C after 120 min, for the sorbent synthesized from Li_2CO_3 and SiO_2, the CO_2 uptake was as high as 31.9 wt%, while the sorbents synthesized from FA only resulted in an uptake of 7.3–15.3 wt%, no matter what methods were used. It was revealed that such performance is related to the chemical composition of FA. Despite the high CaO content in some of the FA-derived samples, the carbonation reaction did not proceed via $CaCO_3$ formation because of the presence of Li_2CaSiO_4 and $Ca_5(SiO_4)_2CO_3$ crystal in the carbonated samples, which limited the CO_2 capture on CaO presented in the fly ash.[122]

2.5.2. Synthesis of Li_4SiO_4 from biomass ashes

Synthesis of Li_4SiO_4-based sorbents from biomass ashes is an attractive and cost-effective route. Recently, the biomass ash used for the synthesis of Li_4SiO_4 was mainly rice husk. Additionally, some other biomass ashes such as cotton stalk, wood dust, and

rice straw have also been reported. Rice husk is rich in SiO_2, and the SiO_2 can be directly extracted out for the synthesis of Li_4SiO_4. By using the cost-effective, renewable and nano-sized rice husk ash (CRHA) with citric acid pretreatment as a silicon source, Zhao et al.[49] prepared CRHA-Li_4SiO_4 from rice husk and compared with another two Li_4SiO_4 samples from nano-structured aerosil (aerosil-Li_4SiO_4) and crystalline Quartz powders (Quartz-Li_4SiO_4). Although calcined quartz maintained its micron-particle structure, its reactivity was too low to react completely with Li_2CO_3. Pure Li_4SiO_4 can be obtained from aerosol, but formed large particles with dense morphology. However, the CRHA-Li_4SiO_4 sample formed porous agglomerates of submicron particles due to the high anti-sintering character of calcined CRHA. With such favorable structure, CRHA-Li_4SiO_4 resulted in higher CO_2 sorption capacity, faster kinetic behavior and improved regeneration. The rice husk derived CRHA-Li_4SiO_4 sorbent reached its maximum sorption capacity of 30.5 wt% at 710 °C, which is higher than that of Aerosil-Li_4SiO_4 (28 wt%) and Quartz-Li_4SiO_4 (25 wt%). Its sorption capacity only diminished by 2.1 wt% between the first cycle and the 15th cycle. However, for the acid treatment of rice husk ash, the cost and the secondary pollution should be considered.

Considering that the metal impurities in rice husk might work as separating materials and thus decrease the particle size of obtained Li_4SiO_4 samples, Guo et al.[123] studied the performance of Li_4SiO_4 synthesized directly from rice husk without acid treatment. In this work, husk-1 was washed with distilled water and rice husk-2 was treated with 10 wt% HCl aqueous solution at 100 °C for 2 h. Rice husk-1 contained mainly SiO_2 with some trace elements (K, Na, Ca, Mg, and Al). After acid treatment, the trace elements, especially alkali metals (K_2O and Na_2O), sharply decreased in rice

husk-2 and the amount of SiO_2 increased. Compared with pure Li_4SiO_4 (60 and 100 µm), the particle size of rice husk-1-Li_4SiO_4 (16 µm) and rice husk-2-Li_4SiO_4 (45 µm) were much smaller. This can be attributed to the metal impurities such as Mg and Al that resisted the sintering of particles. At 710 °C, the maximum CO_2 sorption of pure Li_4SiO_4 was 22.1 wt%. Rice husk-2-Li_4SiO_4 only showed slight improvement in comparison with pure Li_4SiO_4. However, rice husk-1-Li_4SiO_4 showed a significantly improved CO_2 sorption, with a total capacity of 32.4 wt%. In addition, the kinetic constant value for rice husk-1-Li_4SiO_4 was also higher than that of pure Li_4SiO_4. Figure 14 shows the cycling performance of pure Li_4SiO_4 and rice husk-1-Li_4SiO_4 sorbents. After 15 cycles, the reversible CO_2 sorption capacity of rice husk-1-Li_4SiO_4 remained almost unchanged, showing that this sorbent possesses excellent cycling stability and may become a new option for CO_2 sorption at high temperatures.

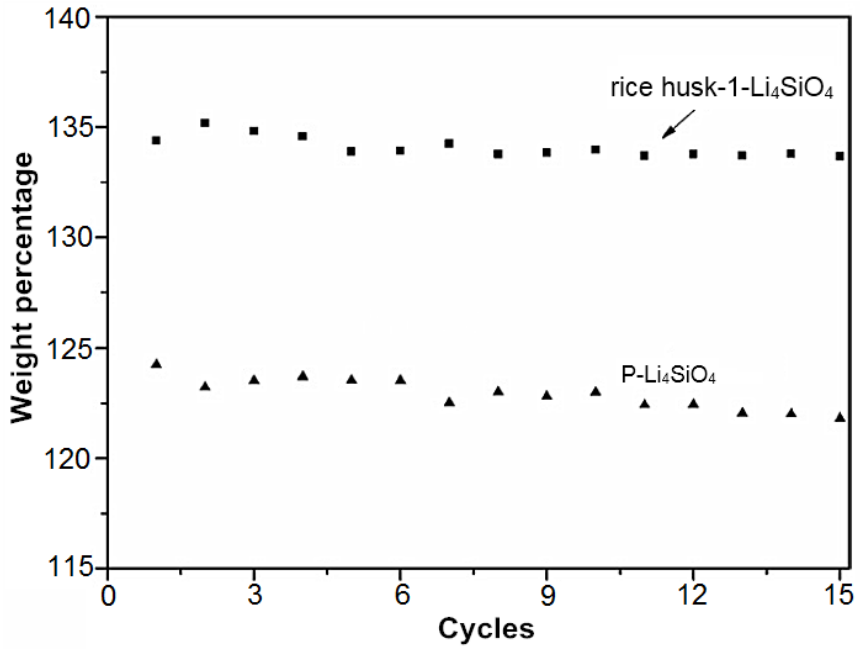


Figure 14. Multiple cycles of CO_2 sorption (15 min) and desorption (10 min) on P-Li_4SiO_4 and rice husk-1-Li_4SiO_4 under the same testing conditions.[23] Reprinted with permission from ref 23. Copyright 2011 Elsevier B.V.

Besides rice husk ash, several other types of biomass ashes such as cotton stalk, wood dust, and rice straw have also been studied for the synthesis of Li_4SiO_4. Zhao et al.[118] prepared highly efficient bio-based Li_4SiO_4 for CO_2 capture at high temperatures. Three typical biomass ashes (cotton stalk, wood dust, and rice straw) and a water pretreated biomass ash (rice straw) were used for preparing bio-based Li_4SiO_4 sorbents. The water pretreated biomass ash derived sorbent was found to possess higher amount of Li_4SiO_4, smaller particle size and larger specific surface area. This special structure further resulted in enhanced CO_2 uptake (31.6 wt%) and sorption kinetics at 680 ^oC in 100 vol.% CO_2, and excellent stability during multiple cycles. It was thus concluded that the synthesis of Li_4SiO_4 sorbent from pretreated biomass ashes is a promising approach for high-temperature CO_2 capture.

2.5.3. Synthesis of Li_4SiO_4 from natural minerals

Natural minerals have low prices and are harmless to the environment. Some of them contain mainly silica with different metal oxides. In addition, natural minerals exhibit unique structures, such as lamellar structure, porous structure, and rod-like structure, etc. These unique structures may be beneficial for the synthesis of Li_4SiO_4 sorbents. So far, three types of natural minerals including diatomite, halloysite, and vermiculite have been studied for the synthesis of Li_4SiO_4 sorbents for high temperature CO_2 capture.

Cheap porous diatomite that contains ca. 75 % SiO_2 is very suitable as a silicon source for the synthesis of Li_4SiO_4. Shan et al.[71] and Peng et al.[120] proved that the diatomite derived Li_4SiO_4 samples not only possessed excellent CO_2 sorption capacity, but also exhibited good sorption/desorption cycling stability. Compared with pure

Li_4SiO_4, diatomite-Li_4SiO_4 had much quicker sorption rate within the first 10 min, and its sorption capacity was almost twice as high as pure Li_4SiO_4. In addition, the sorption reaction reached the equilibrium at 80 min for diatomite-Li_4SiO_4, but pure Li_4SiO_4 did not reach the equilibrium until 200 min. The activation energies for the sorption process and diffusion of pure Li_4SiO_4 were higher than those of diatomite-Li_4SiO_4, indicating that diatomite-Li_4SiO_4 had higher reactivity and better diffusivity. This result may be due to structural differences produced by aluminum and other elements in diatomite-Li_4SiO_4. With increasing cycle number, the sorption capacity decreased by 6.44 wt% from the first cycle (34.14 wt%) to the 16th cycle (27.70 wt%) at a fixed temperature, 700 ^{o}C. It was believed that diatomite-Li_4SiO_4 has specific morphologies, which refrained it from sintering in multi-number cycles. Figure 15(a) shows that diatomite has a rich pore structure and uniform pore distribution with the pore size of 0.5–1.0 mm. As-prepared diatomite-Li_4SiO_4 sorbent did not inherit the morphologies of diatomite. It is noticeable that the morphology of diatomite-Li_4SiO_4 sorbent after 16 cycles remained similar to fresh diatomite-Li_4SiO_4 sorbents (Figure 15(b) and (c)), thus explaining its better cycling stability.

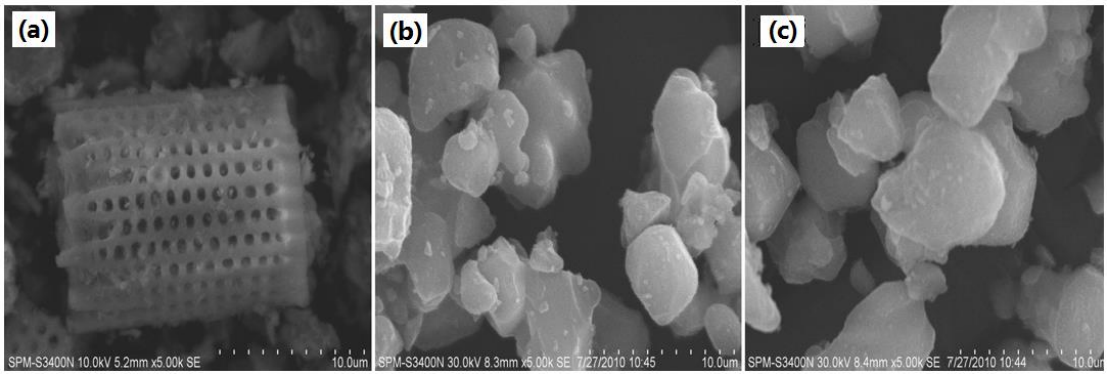


Figure 15. SEM images of (a) diatomite, (b) diatomite derived Li4SiO4 sorbent, and (c) the diatomite derived Li_4SiO_4 sorbent after 16 cycles.[71] Reprinted with permission from ref 71. Copyright 2012 Elsevier Ltd and Techna Group S.r.l.

Natural halloysite clay nanotubes that mainly consisted of silica-like sheet (SiO_2) and diaspore-like sheet (Al_2O_3) have been used as cheap and easy available mineral resource. When natural halloysite clay nanotubes were acid-treated with 6 M HCl solution at 100 °C for 6 h, the silicon content rose to 96.12%, with tiny amount of Al, Zn, Ca, and Mg in the sample. Such acid treated halloysite was believed to be a suitable silica precursor for Li_4SiO_4. Yang et al.[119] synthesized Li_4SiO_4 based sorbents from acid treated halloysite by solid state reaction and studied their high temperature CO_2 capturing performance. At 700 ^oC (uptake conditions in a CO_2 atmosphere for 60 min, desorption conditions in a N_2 atmosphere for 60 min), a very high CO_2 sorption capacity of 34.75 wt% was achieved with acid treated halloysite-Li_4SiO_4, higher than pure Li_4SiO_4 (30.49 wt%). Meanwhile the sorbent exhibited fast kinetics and good stability over 10 CO_2 sorption/desorption cycles. The sorption capacity increased firstly from 28.74 wt% to 31.99 wt% after the 3rd cycle, and then slightly decreased to 28.9 wt% after 10th cycle. Such capacity variation might be due to the microstructure changes during cycles.

Vermiculite is a lamellar hydrated aluminum iron magnesium silicate, and has an unusual property of expanding due to the interlamellar generation of steam at high temperatures. The SiO_2 content of this natural mineral is about 41 %. Zhang et al.[121] reported a new synthesis route for obtaining two CO_2 sorbents, Mg-Al LDH and Li_4SiO_4, from vermiculite. As described in Figure 16, SiO_2 could be first leached out from vermiculite using an acid and then utilized for the synthesis of Li_4SiO_4. In the meantime, the leaching waste water could be utilized as metal (Mg^{2+}, Al^{3+}, etc) precursors for the synthesis of Mg-Al LDH, by which no waste was produced during the whole process.

The influence of Li/Si molar ratio, calcination temperature and time, and sorption temperature on the CO_2 sorption capacities of these two sorbents were comprehensively investigated. Relatively pure Li_4SiO_4 could fabricated at Li/Si = 4–5, The best Li_4SiO_4 and Mg-Al-CO_3 LDH sorbents reached a high CO_2 uptake of 34.39 wt% at 650 °C and 2.08 wt% at 200 °C in pure CO_2 gas, respectively. They also demonstrated that the chemical compositions and the cycling stability of these two sorbents were highly depended on the concentration of leaching acid used for pretreatment. When the concentration of leaching acid was low, although the initial CO_2 uptake was not so high, the obtained sorbent showed very high cycling stability, which can be attributed to separating and supporting effect by the remaining impurity phases. The LDH-derived sorbent also showed good stability during 15 cycles.[121]

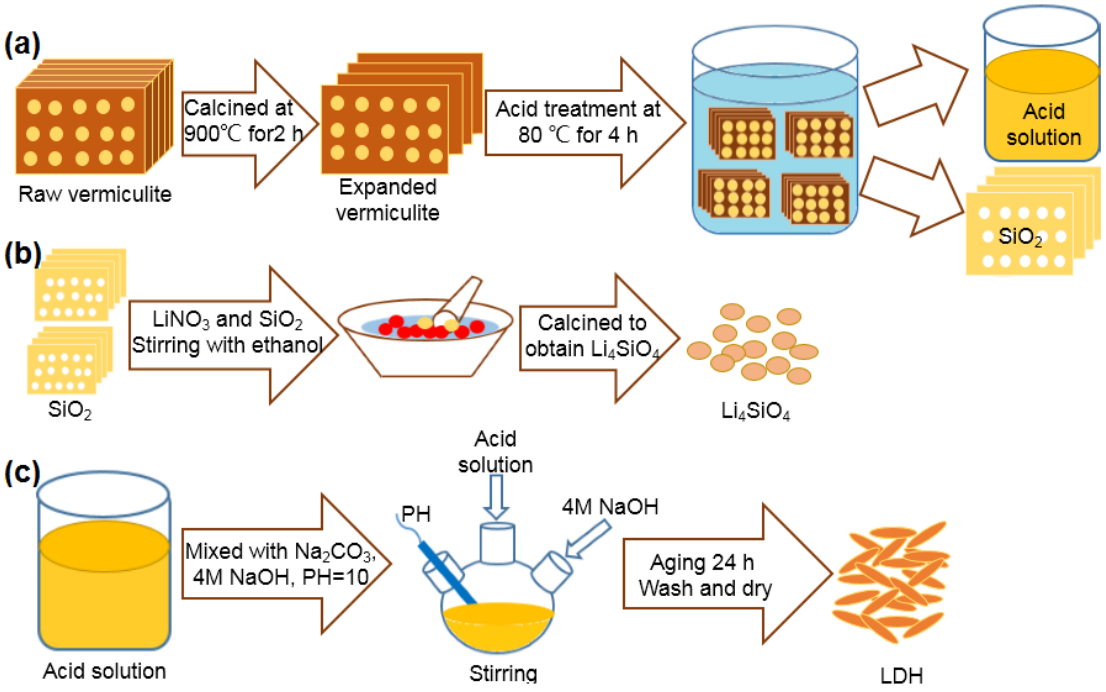


Figure 16. Schematic synthesis procedures for Li_4SiO_4 and LDH from vermiculite, (a) pretreatment of vermiculite in acid solution to obtain SiO_2 and an acid solution, (b) synthesis procedure for Li_4SiO_4 from the SiO_2 obtained in step (a), and (c) synthesis

procedure for LDH from the acid solution obtained in step (a).[121] Reprinted with permission from ref 121. Copyright 2017 MDPI.

However, it should be noted that in most cases, the use of solid wastes or minerals as Si resources require a complex and expensive acid pretreatment. Such acid pretreatment process will not only lead to equipment corrosion and additional cost, but also result in secondary environmental pollution. In a very recent work, Zhang et al.[124] reported the direct fabrication of Li_4SiO_4 sorbent from EXVMT without the acid pretreatment step for the first time. Thanks for the direct use of EXVMT mineral, this synthesis scheme was believed to be more environmentally friendly and economical. In addition to SiO_2, VMT also contains some impurity phases including MgO, Al_2O_3, K_2O, Fe_2O_3, CaO, Na_2O, and TiO_2. These impurity phases can work as supporting or separating materials, thus preventing sintering and increasing cycling stability of the formed Li_4SiO_4, as illustrated in Figure 17. The impurity elements Al^{3+}, Fe^{3+}, and Ti^{4+} could react with Li^+ and form Li_5AlO_4, Li_5FeO_4, and Li_4TiO_4, respectively, and may contribute to CO_2 capture as well.[124]

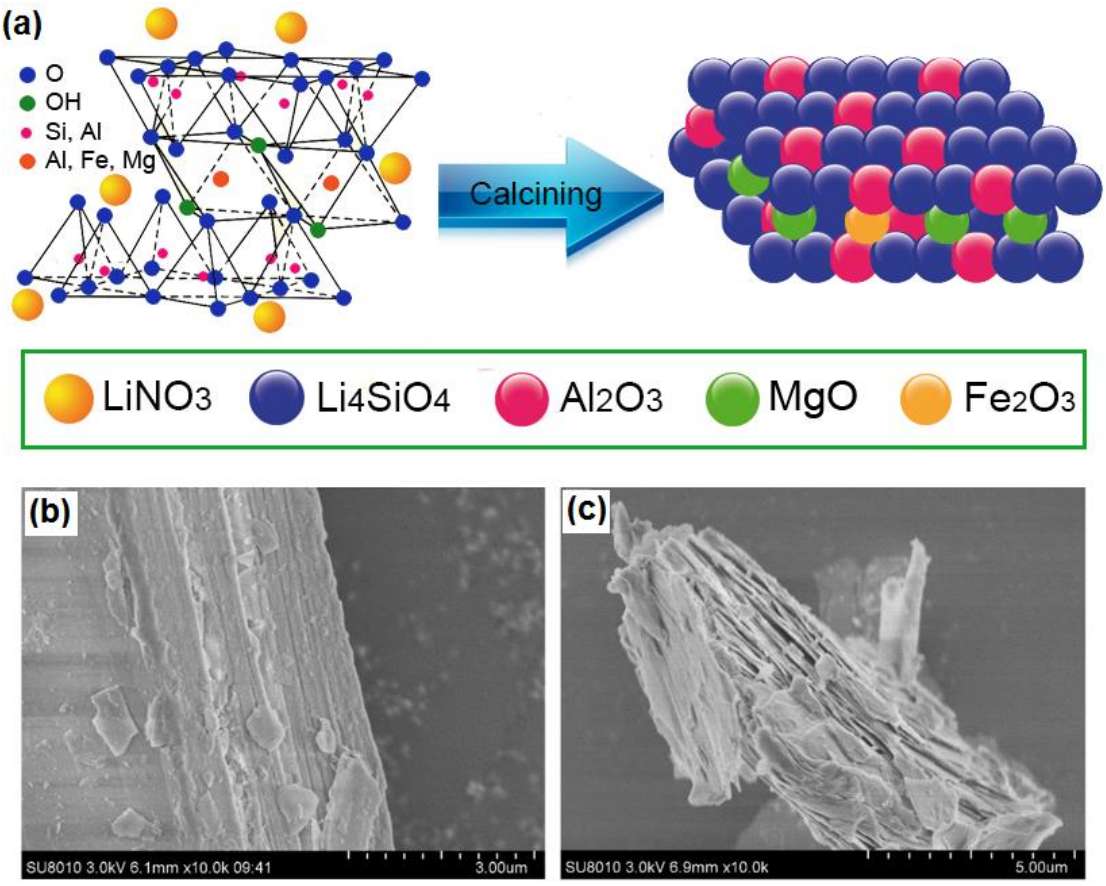


Figure 17. (a) Schematic illustration of the synthesis of Li_4SiO_4 based CO_2 sorbent from vermiculite precursor, and SEM images of (b) raw VMT and (c) EXVMT.[124] Reprinted with permission from ref 124. Copyright 2018 Elsevier B.V.

Thanks for the separating effect by the impurity phases, such newly synthesized CO_2 sorbent Li_4SiO_4-(EXVMT)-4 exhibited much enhanced stability during multi-cycles. This sorbent also showed higher CO_2 uptake and faster sorption rate at relatively lower sorption temperature (550 °C). It was also revealed that this sorbent was less affected by CO_2 concentration because it possessed lower activation energies for both the CO_2 sorption and the diffusion processes. At 550 °C, by decreasing the CO_2 concentration from 100 to 20 vol%, the CO_2 capture capacity only slightly declined from 19.4 to 18.5 wt%. However, under the same condition, the CO_2 uptake of the control sample

Li_4SiO_4-(SiO_2)-4 was significantly decreased from 22.0 to 11.3 wt%, as shown in Figure 18(a).[124] The Li_4SiO_4-(EXVMT)-4 sorbent also showed good cycling stability, with a CO_2 uptake of 18.8 and 18.3 wt% at the 3rd and 20th cycle, respectively. However, under the same condition, the CO_2 uptake of the control sorbent Li_4SiO_4-(SiO_2)-4 was only about 8.2 wt%. Because of the high CO_2 uptake, good cycling stability, fast sorption rate, and relatively low cost, the VMT derived Li_4SiO_4 sorbent was believed to be highly potential for practical applications.[124]

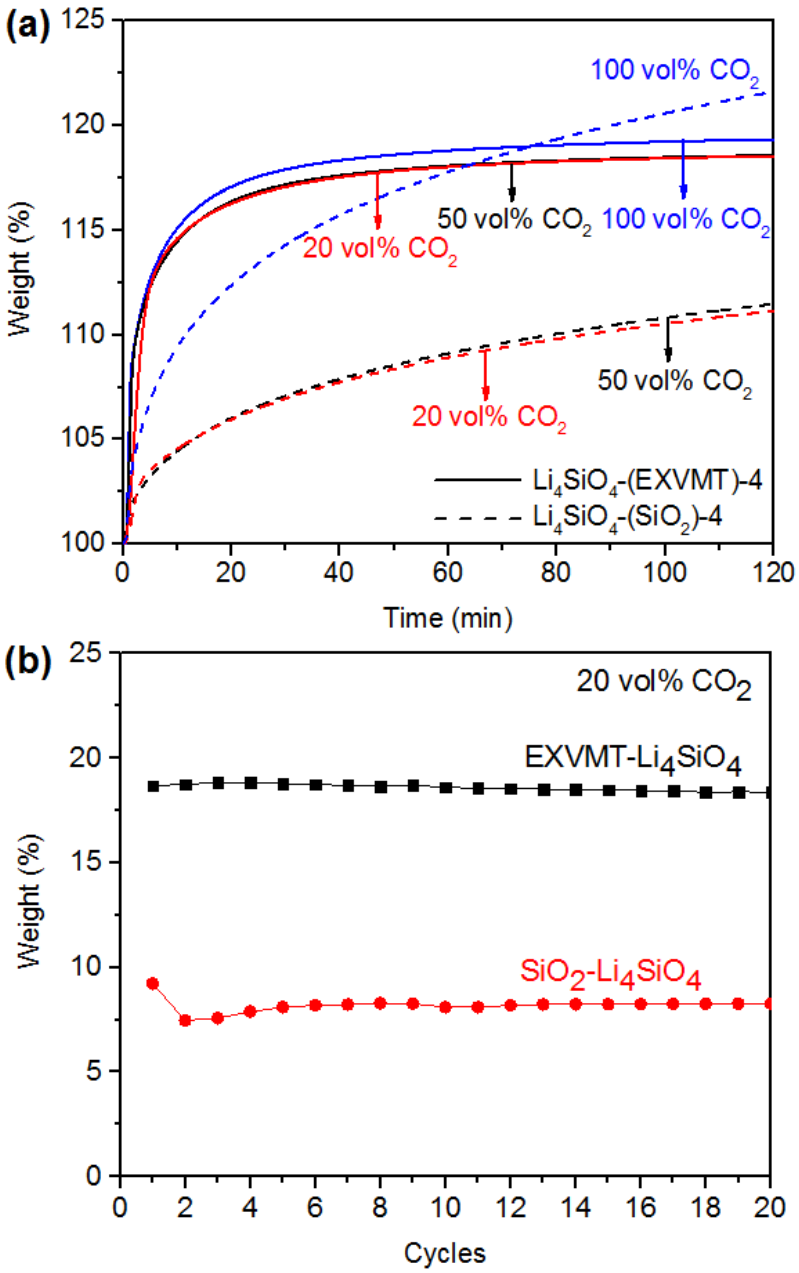


Figure 18. (a) Isothermal CO_2 sorption of Li-(EXVMT)-4 and Li-(SiO_2)-4 sorbents under 100, 50, and 20 vol% CO_2 at 550 °C, and (b) CO_2 sorption/desorption cycling performance of optimized Li-(EXVMT)-4 and Li-(SiO_2)-4 sorbents, the sorption process was performed under 20 vol% CO_2 at 550 °C for 30 min and the desorption process was performed under 100 vol% N_2 at 650 °C for 30 min.[124] Reprinted with permission from ref 124. Copyright 2018 Elsevier B.V.

2.6. High lithium content silicate (Li_8SiO_6)

Except for Li_4SiO_4, Li_8SiO_6 was also studied as a high temperature CO_2 sorbent.[41] Pfeiffer et al.[125] proved that Li_8SiO_6 has excellent CO_2 sorption performance, with a CO_2 uptake as high as 51 wt% at 700 °C. The CO_2 capture process on Li_8SiO_6 can be described by reactions (3-8), which indicate that Li_8SiO_6 would be able to react with different quantities of CO_2, producing Li_2CO_3, SiO_2 and different secondary lithium phases such as Li_2O, Li_4SiO_4, and Li_2SiO_3. The produced Li_2O and Li_4SiO_4 would further react with CO_2 according to the second and consecutive carbonation reactions (7) and (8). These CO_2 capture processes explain why Li_8SiO_6 has a very high CO_2 capture capacity, even much higher than Li_4SiO_4. Then, Pfeiffer et al.[126] further doped potassium carbonate, sodium carbonate, or a mixture of both into Li_8SiO_6 to tune its CO_2 sorption performance in a wide temperature range. The results showed that after doping with Na_2CO_3, K_2CO_3, or both Na_2CO_3 and K_2CO_3, the performance of Li_8SiO_6 samples can be greatly improved at the low-temperature range (350–650 °C), as shown in Figure 19(a). However, Figure 19(b) shows that the CO_2 sorption performance decreased significantly after repeated use. The performance decline can be associated to the high temperature (800 °C) applied for desorption, which could induce the particles sintering, inhibiting the CO_2 sorption in the subsequent cycles.

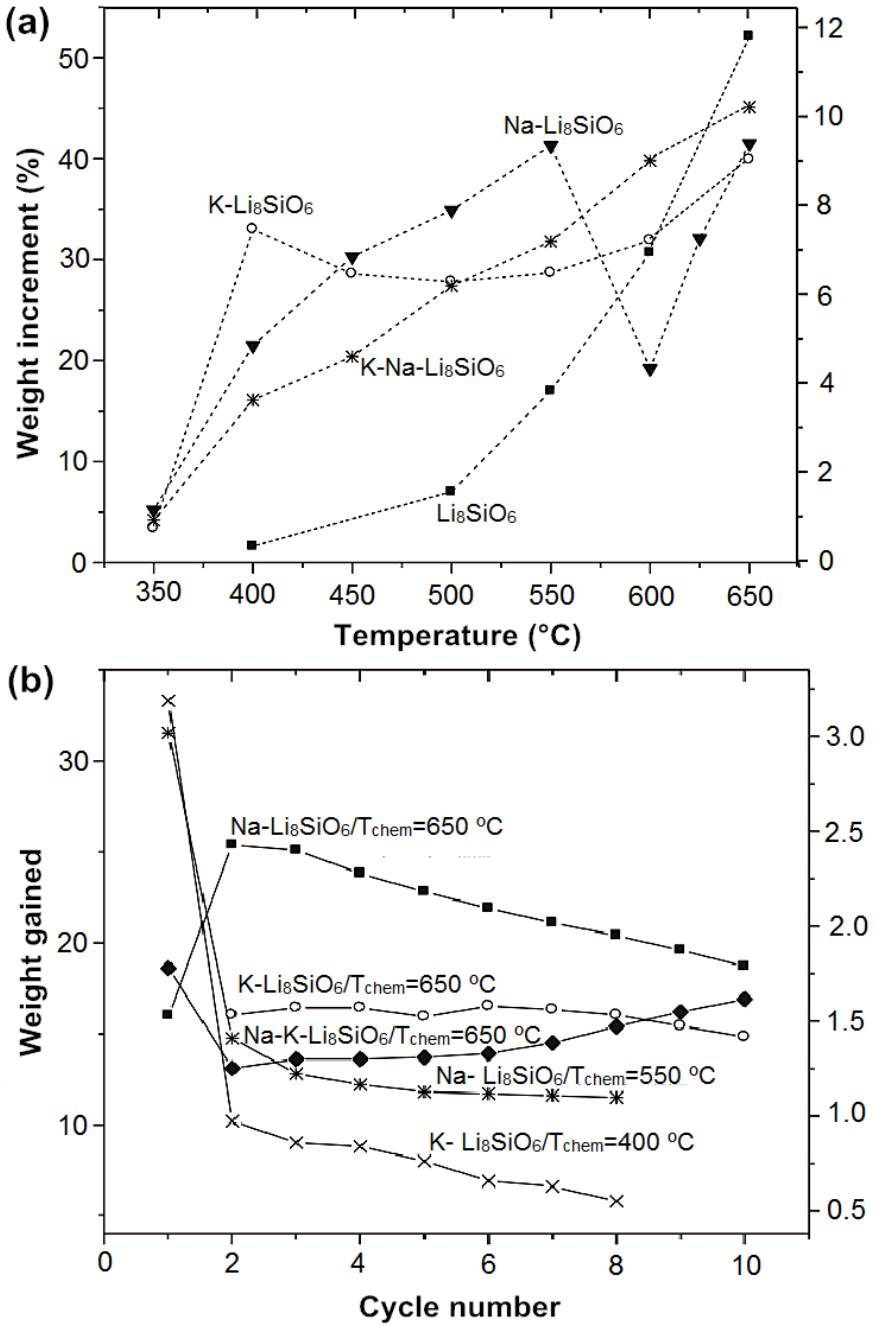


Figure 19. (a) Comparative graph of K-, Na-, K-Na-Li_8SiO_6 and pure Li_8SiO_6 as function of CO_2 weight gained and millimoles chemisorbed on Li_8SiO_6, between 350 and 650 °C, (b) Cycling performance of Li_8SiO_6, K-Li_8SiO_6, Na-Li_8SiO_6 and K-Na-Li_8SiO_6 samples (desorption process was performed into a N_2 flow at 800 °C).[126] Reprinted with permission from ref 126. Copyright 2014 Society of Chemical Industry and John Wiley & Sons, Ltd.

A similar result was also observed by Wang et al.[78] that the Li_8SiO_6 sorbent synthesized from SBA-15 precursor achieved a very high CO_2 capture capacity of 62 wt% at 650 ^oC with 100 vol% CO_2. However, the CO_2 uptake decreased sharply from 62.0 to 37.8 wt% as the CO_2 concentration diminished from 100 to 50 vol%. In contrast, the CO_2 uptake did not further decrease significantly under 20 vol% CO_2. This is because the CO_2 desorption process will be accelerated at lower CO_2 concentrations (Figure 20(a)). However, its regeneration capacity was poor, with only 10.5 wt% of reversible CO_2 uptake from the second cycle, as shown in Figure 20(b). Poor multi-cycle performance weakened its potential application, and more studies will be required for enhancing its performance.

$$Li_8SiO_6 + CO_2 \rightarrow Li_2CO_3 + Li_2O + Li_4SiO_4 \quad (3)$$

$$Li_8SiO_6 + 2CO_2 \rightarrow 2Li_2CO_3 + Li_4SiO_4 \quad (4)$$

$$Li_8SiO_6 + 3CO_2 \rightarrow 3Li_2CO_3 + Li_2SiO_3 \quad (5)$$

$$Li_8SiO_6 + 4CO_2 \rightarrow 4Li_2CO_3 + SiO_2 \quad (6)$$

$$Li_2O + CO_2 \rightarrow Li_2CO_3 \quad (7)$$

$$Li_4SiO_4 + CO_2 \rightarrow Li_2CO_3 + Li_2SiO_3 \quad (8)$$

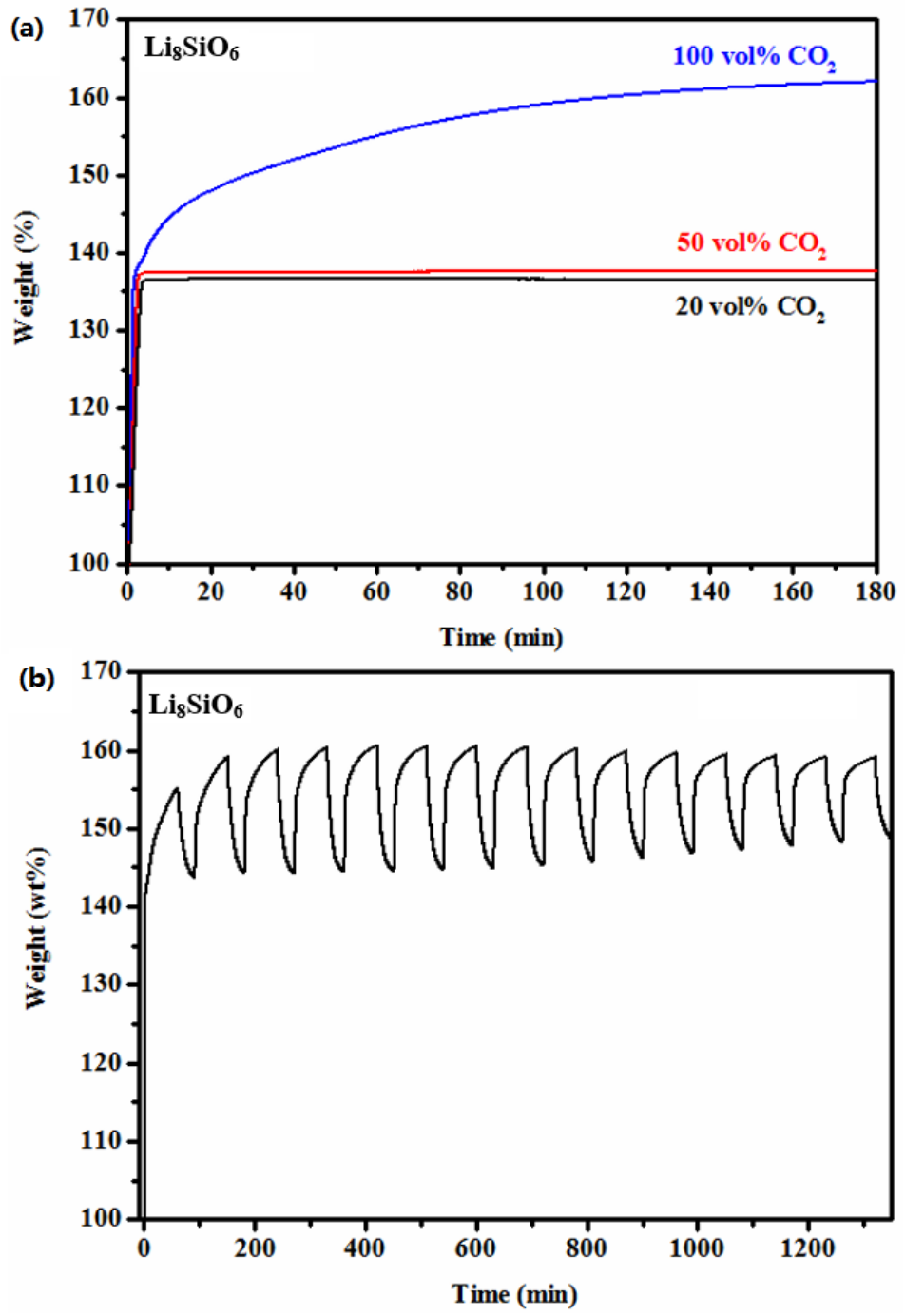


Figure 20. (a) CO_2 sorption isotherms of Li_8SiO_6 synthesized from SBA15 under different CO_2 concentrations (20 vol%, 50 vol%, and 100 vol%), (b) CO_2 sorption/desorption cycling performance of Li_8SiO_6 (both sorption and desorption were performed at 650 ^oC).[78] Reprinted with permission from ref 78. Copyright 2017 American Chemical Society.

2.7. Low lithium content silicate (Li_2SiO_3)

Although lithium metasilicate (Li_2SiO_3) has not been largely studied as possible CO_2 captor material, it is capable of trapping CO_2 at moderate and low temperature conditions. According to different thermodynamic data, this lithium ceramic is able to capture CO_2 at temperatures below 235 °C.[43] Based on that, different works have shown the feasibility to fabricate Li_2SiO_3 through different synthetic routs for CO_2 capture applications, as solid state samples present very low surface areas limiting the capture process.[127-129] Among these synthesis routes, Li_2SiO_3 nanoparticles, presenting large enough surface areas have been obtained coupling sol–gel method in reverse microemulsion or using organic templates with microwaves. The obtained powders showed the ability to trap CO_2 under certain conditions, in comparison to solid state samples. Then, it has been assumed that these specific microstructural features increased the Li_2SiO_3 reactivity.

Moreover, some of these works have shown that Li_2SiO_3 presents a higher CO_2 capture efficiency when it is reacted in the presence of water vapor. It seems that water vapor acts as a catalytic intermediate specie during CO_2 capture. Initially, water vapor reacts with the Li_2SiO_3 particle surface, producing Li-OH species that are more reactive to CO_2 than Li_2SiO_3, and favoring its carbonation process. For instance, Ortiz-Landeros et al.[127] prepared a series of Li_2SiO_3 powder materials by the microwave-assisted hydrothermal route using lithium hydroxide and tetraethyl-orthosilicate-derived sol precursors. Figure 21 shows the CO_2–H_2O (v) sorption isotherms of the different Li_2SiO_3 samples as a function of relative humidity (RH) at 50 ^oC. For the SSR sample, the weight increment was very small (0.49 wt%). In contrast, the MH, MH-Stirring, and MH-Surfactant samples exhibited significantly higher weight increments

of 7.8, 13.9, and 20.6 wt%, respectively. It is also clearly that weight increment increased with the increase in RH%.

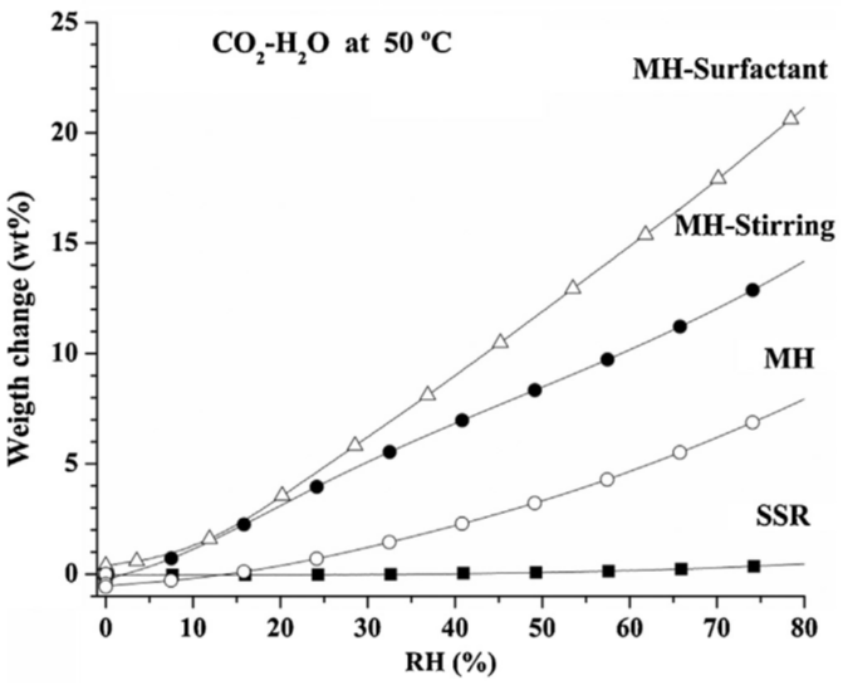


Figure 21. Isothermal carbonation of Li_2SiO_3 synthesized by different methods in the presence of water vapor at 50 °C. (Li_2SiO_3 synthesized via solid-state reaction, via microwave-assisted hydrothermal synthesis, microwave-assisted hydrothermal synthesis with mechanical stirring, or via the addition of surfactant, were labeled as SSR, MH, MH-Stirring, MH-Surfactant, respectively).[127] Reprinted with permission from ref 127. Copyright 2015 Elsevier B.V.

3. Lithium zirconates

3.1. Mechanism of CO_2 capture on Li_2ZrO_3

Li_2ZrO_3 was first reported as a promising high-temperature CO_2 sorbent (450–650 °C) by Nakagawa and Ohashi as early as in 1998.[130] This material possesses great potential due to its excellent CO_2 sorption capacity (28 wt%) and small volume change during the CO_2 sorption/desorption cycles.[131] The CO_2 sorption and desorption processes on

Li_2ZrO_3 can be described by reaction (9) and Figure 22. During CO_2 sorption process, CO_2 molecules react with lithium zirconate to form solid lithium carbonate shell on the outer surface and a dense zirconium oxide shell in the middle covering the unreacted lithium zirconate core. After the Li_2CO_3 and ZrO_2 shells are formed, the carbonation process continues with transporting CO_2 through the Li_2CO_3 shell, and diffusing Li^+ and O^{2-} through the ZrO_2 shell. For pure Li_2ZrO_3, the diffusion of CO_2 in the Li_2CO_3 shell was believed to be the rate-limiting step because CO_2 transfers much slower than Li^+ and O^{2-} due to its much bigger molecular size.

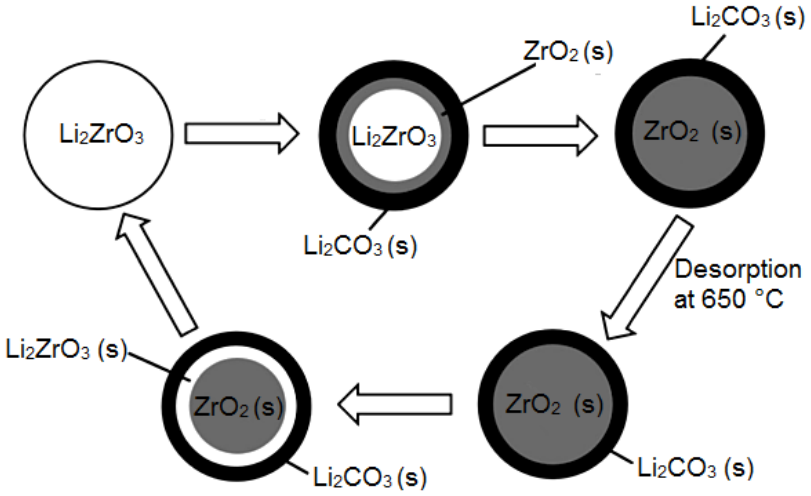


Figure 22. The CO_2 sorption and desorption processes on Li_2ZrO_3.[87] Reprinted with permission from ref 87. Copyright 2016 Springer Science + Business Media New York.

The main issues for the practical applications of Li_2ZrO_3 include relatively low CO_2 uptake capacity, slow sorption/desorption rates, severe sintering and poor cycling stability. During the past decade, in order to improve the performance of Li_2ZrO_3 for CO_2 capture, great efforts have been devoted, which includes (1) synthesis of Li_2ZrO_3 using different synthetic methods, (2) formation of solid solutions, and (3) incorporation of molten salt components. In addition to Li_2ZrO_3, some other lithium

zirconates with higher lithium content such as $Li_6Zr_2O_7$ and Li_8ZrO_6 have also been studied for high-temperature CO_2 capture. In the following sections, all the above mentioned works will be described.

$$Li_2ZrO_3 + CO_2 \rightarrow Li_2CO_3 + ZrO_2,\ \Delta H_{298\ K} = -160\ kJ\ mol^{-1} \quad (9)$$

3.2. Influence of synthesis methods for pure Li_2ZrO_3

It is well accepted that the bottleneck for CO_2 capture on lithium zirconates is mostly related to the formation of solid carbonate and zirconia layer surrounding the unreacted core of lithium zirconate, which consequently limits the chemisorption and diffusion rates.[32] Therefore, synthesis of Li_2ZiO_3 samples with reduced particle/crystallite sizes and increased specific surface area and porosity by different synthetic routes has been commonly proposed.[132, 133] So far, several synthesis methods including solid state,[32, 130] sol–gel method,[87, 132, 134, 135] soft-chemistry route,[136-139] and hydrothermal method[140, 141] have been investigated for the synthesis of Li_2ZrO_3. Herein, the performance of Li_2ZrO_3 sorbents synthesized by different methods will be comprehensively discussed and compared.

Solid-state method is a traditional synthesis route with the advantages of high yield and simple operation process. Similar to lithium silicates, solid-state method is also the most traditional synthesis method for Li_2ZrO_3. However, such synthesis method needs heating at high temperatures for a long time, consequently forms Li_2ZrO_3 crystals in large size. For instance, by heating zirconia and lithium carbonate at high temperatures, Nakagawat et al.[130] obtained Li_2ZrO_3 powder with a particle size of 0.5 to 1 μm. The sorbents were tested in four different conditions (gas A: CO_2 0%; gas B: CO_2 20%; gas C: CO_2 70%, balanced by air; and gas D: CO_2 20%, by H_2). In gas B and

C, the sorbents had obvious weight increases at 450 to 550 °C. However, no weight change was observed in gas A. In addition, considering the Li_2ZrO_3 based CO_2 sorbent is used in fuel reforming process, the CO_2/H_2 mixture gas (gas D) was used to simulate the real gas. In gas D, a weight increase of 21.9 wt% was achieved at 500 °C, which corresponds to 76.3% of the theoretical capacity. The highest CO_2 sorption rate was 290 cm^2/h for 1 cm^3 of Li_2ZrO_3. The result indicated that although Li_2ZrO_3 can be successfully synthesized via the solid-state method, both the CO_2 sorption capacity and rate remain relatively low, which can be attributed to the severe sintering of Li_2ZrO_3 samples. Thus, in order to further improve the CO_2 sorption performance, several other synthetic routes have been explored.

Sol–gel method has been a mature technique for decades for the synthesis of materials with fine particles. Comparing to the solid state method, it generally requires a much lower calcination temperature for the formation of desired products. Therefore, sol–gel method is believed to be promising for the synthesis of fine Li_2ZrO_3 particles for CO_2 capture. In 2004, Nakagawa et al.[132] compared three kinds of Li_2ZrO_3 samples that were synthesized by solid-state method (heated at 700 °C, 900 °C and 1300 °C, named SOS-temperature), sol-gel method (heated at 500 °C, 700 °C, and 900 °C, named SOL-temperature) and commercial-grade Li_2ZrO_3 powder (heated at 900 °C, named COM-900). All Li_2ZrO_3 samples were doped with K_2CO_3, and the Zr:Li:K ratio was 1:1.1:0.2. Among all samples, SOL-700, SOS-900, and SOS-U700 (treated with ball milling before used) had better CO_2 sorption capacity than other samples at 450 ^oC, which was 22.52, 26.28, and 20.04 wt%, respectively. The sorption rate at 450 °C of these three samples was 2.8, 3.1 and 5.8 mg^{-1} g min, respectively. However, for SOS-1300, COM, COM-900, and SOL-900 samples, the CO_2 sorption capacity was only 3.8,

14.21, 21.93, and 15.06 wt%, respectively. The sorption rate was also very low, which was only 0.04, 0.16, 0.68, and 0.4 mg g^{-1} min^{-1}, respectively. The morphological and structural studies of the powders suggested that the difference in CO_2 capture performance might be due to both the particle size and major phase presence of Li_2ZrO_3. Tetragonal Li_2ZrO_3 powders clearly showed a larger sorption rate than the monoclinic counterparts. And the particle size of the metastable tetragonal phase was also smaller than the monoclinic powder. This study demonstrated that sol-gel method can result in higher CO_2 capture capacity and faster sorption rate than solid state method for Li_2ZrO_3.

After that, some modified sol-gel routes including citrate sol-gel,[134, 135] starch-assisted sol-gel,[142] and epoxide-mediated sol-gel method[87] have been studied for the synthesis of Li_2ZrO_3 for high-temperature CO_2 capture. Zhu et al.[134, 135] synthesized Li_2ZrO_3 sorbent via a citrate sol-gel method (LZ-sg) and compared its performance with the samples obtained by co-precipitation (LZ-co) and liquid-phase (LZ-lp) methods. Different from the other two methods, the soluble Li and Zr salts were dissolved together in the citrate sol-gel method, followed by evaporation of the solvent to form a solid mixture containing Li and Zr species. Such a "bottom-up" synthesis method can lead to an intimate mixing down to the atomic level, the Li and Zr species interacted with citrate were confined within the citrate gel network (Figure 23). So, the LZ-sg sample showed excellent CO_2 sorption performance at 550 °C and CO_2 partial pressures above 0.5 bar, with a high capacity of 26 wt% within 20 min. Furthermore, the sorbent also demonstrated a good sorption/desorption stability. However, The Li_2ZrO_3 sample prepared by the liquid-phase method displayed the lowest CO_2 uptake rate under the investigated conditions. LZ-co, although showed some improved CO_2

capture properties in comparison with LZ-lp, its CO_2 uptake rate is still slower than LZ-sg. The excellent performance of the citrate sol-gel method prepared Li_2ZrO_3 can be attributed to its smaller particle size (17 nm) than LZ-co (26 nm) and LZ-lp (34 nm), and the existence of a tetragonal phase.

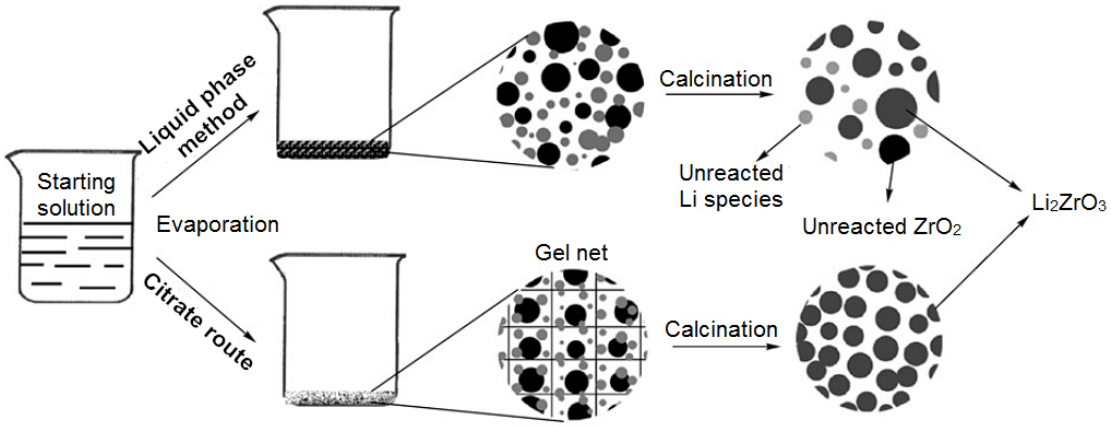


Figure 23. Block diagrams of the citrate route and the liquid-phase method for the synthesis of Li_2ZrO_3 sorbents.[135] Reprinted with permission from ref 135. Copyright 2013 Higher Education Press and Springer-Verlag Berlin Heidelberg.

Zhu et al.[142] further synthesized K-doped Li_2ZrO_3 (the molar ratio of K:Li:Zr is 0.2:1.6:1) by utilizing a starch-assisted sol-gel method combined with freeze-drying. The starch served as gelator agent and the K, Li, and Zr species were confined and well dispersed within the cross-linked gel network. The application of freeze-drying can remove the solvent efficiently and in the meantime avoid the migration of K, Li and Zr species in the gel network caused by capillarity, resulting in a K-doped Li_2ZrO_3 nanocrystalline sorbent with uniform distribution of K, Li, and Zr species. For comparison purpose, the sample synthesized without starch was also tested. At 550 °C and a CO_2 partial pressure of 0.25 bar, the uptake of CO_2 reached 22 wt% within 20 min and the maximum sorption rate can reach 19 mg g^{-1} min^{-1}. However, other two

samples (heating-drying and without using starch) showed clearly lower sorption capacity and slower capture rate (less than 8 mg g^{-1} min^{-1}). In addition, K-doped Li_2ZrO_3 sorbent prepared using the starch-assisted sol-gel method also showed excellent stability during five CO_2 capture-regeneration cycles. These results suggested that both starch-assistance and freeze-drying technique are favorable for obtaining K-doped Li_2ZrO_3 with improved CO_2 capture properties.

Recently, Guo et al.[87] synthesized nanocrystalline Li_2ZrO_3 with a particle size of 50–200 nm via an epoxide-mediated sol–gel process. The introduction of propylene oxide as an acid scavenger can increase the pH value of the system and mediate the sol–gel transition. By calcining the as-dried amorphous xerogel at different temperatures, Li_2ZrO_3 samples with different crystal phases were obtained, tetragonal-Li_2ZrO_3 (t-Li_2ZrO_3) at 650 °C and monoclinic-Li_2ZrO_3 (m-Li_2ZrO_3) at 900 °C. The t-Li_2ZrO_3 showed a CO_2 uptake of 21 wt% at 550 °C (pure CO_2 flow of 40 ml min^{-1}), which is 12 wt% more than that for m-Li_2ZrO_3, indicating a high CO_2 sorption performance for t-Li_2ZrO_3. The t-Li_2ZrO_3 sample also showed good stability, and no obvious decrease in CO_2 uptake was observed after three CO_2 capture-regeneration cycles.

Previous studies have revealed that tetragonal-Li_2ZrO_3 generally possesses better CO_2 sorption properties than monoclinic-Li_2ZrO_3. Recently, soft-chemistry route has been proved to be able to obtain pure tetragonal-Li_2ZrO_3 nanocrystals by using relatively low calcination temperatures.[136] Chen et al.[138] synthesized tetragonal nanocrystalline Li_2ZrO_3 by a soft chemistry route. The obtained sample showed good CO_2 sorption performance between 500 °C and 600 °C, with a maximum CO_2 uptake of 27 wt % at 575 °C and a very short saturation time of less than 5 min. The desorption temperature (650 °C) for the Li_2ZrO_3 prepared by soft-chemistry route is considerably

lower than that for Li_2ZrO_3 prepared by solid-state method (700–780 °C), which is more suitable for heat management in industrial applications such as sorption enhanced steam-methane reforming.[139]

Chen et al.[137] further studied the influence of Li_2O-ZrO_2 stoichiometry and the partial substitution of Li by K potassium as a promoter on the CO_2 sorption rate of pure Li_2ZrO_3. Three samples ($Li_{1.8}ZrO_{2.9}$, Li_2ZrO_3, $Li_{2.2}ZrO_{3.1}$) with Li/Zr molar ratios of 2, 1.8, and 2.2 were synthesized, and the samples with excess or deficient Li showed higher CO_2 capture capacity. Doping K was found to be able to increase the sorption kinetics but resulted in lower stability due to the formation of the molten carbonate that may favor crystal and particle growth the sorption/desorption process. Therefore, it was suggested that when doping K as a promoter, both the sorption kinetics and the cycling stability should be considered.

Gas diffusion in sorbents can be enhanced by creating porosity of solid materials.[143] In order to develop porous Li_2ZrO_3 sorbents, Iliuta et al.[144] synthesized Li_2ZrO_3 by ultrasound-assisted surfactant-template soft chemistry method, and investigated the effect of the amount of template and ultrasound on the performance of Li_2ZrO_3. The obtained porous nanopowders resulted in better sorption rate and capacity than the conventional sample. This performance is mainly because of a less aggregated structure and porous framework, which facilitates gas and ion diffusion to and from the particle layers. However, the sorbents synthesized without sonication were instable during multi-cycles, limiting its long-term application.

Hydrothermal method is well known for the controllable synthesis of high-purity materials at low temperatures.[145, 146] Wang et al.[140, 141] prepared high aspect-ratio Li_2ZrO_3 nanotubes (NTs) from ZrO_2 nanotube template by hydrothermal method.

Figure 24(a) shows the FE-SEM image of the highly ordered ZrO_2 templates anodically grown on Zr substrates, with the diameter of 150–200 nm. Figure 24(b-d) show the FE-SEM images of the NT arrays fabricated by hydrothermal treatment of ZrO_2 in different LiOH solutions. With 0.05 M LiOH solution, only minor difference in morphology of the layers was seen compared to as-prepared ZrO_2 NTs arrays (Figure 24(b)). The tubular wall became slightly thicker, with certain amount of particles attached on the surface. With 0.1 M LiOH solution, ordered porous structure still existed in the layer, but with evident distinctions. The wall of the NTs became thicker and the spacing between NTs became not obvious (Figure 24(c)). With 0.5 M LiOH, the NT arrays collapsed, with nanoparticles overlaid on the surface of the layer (Figure 24(d)).

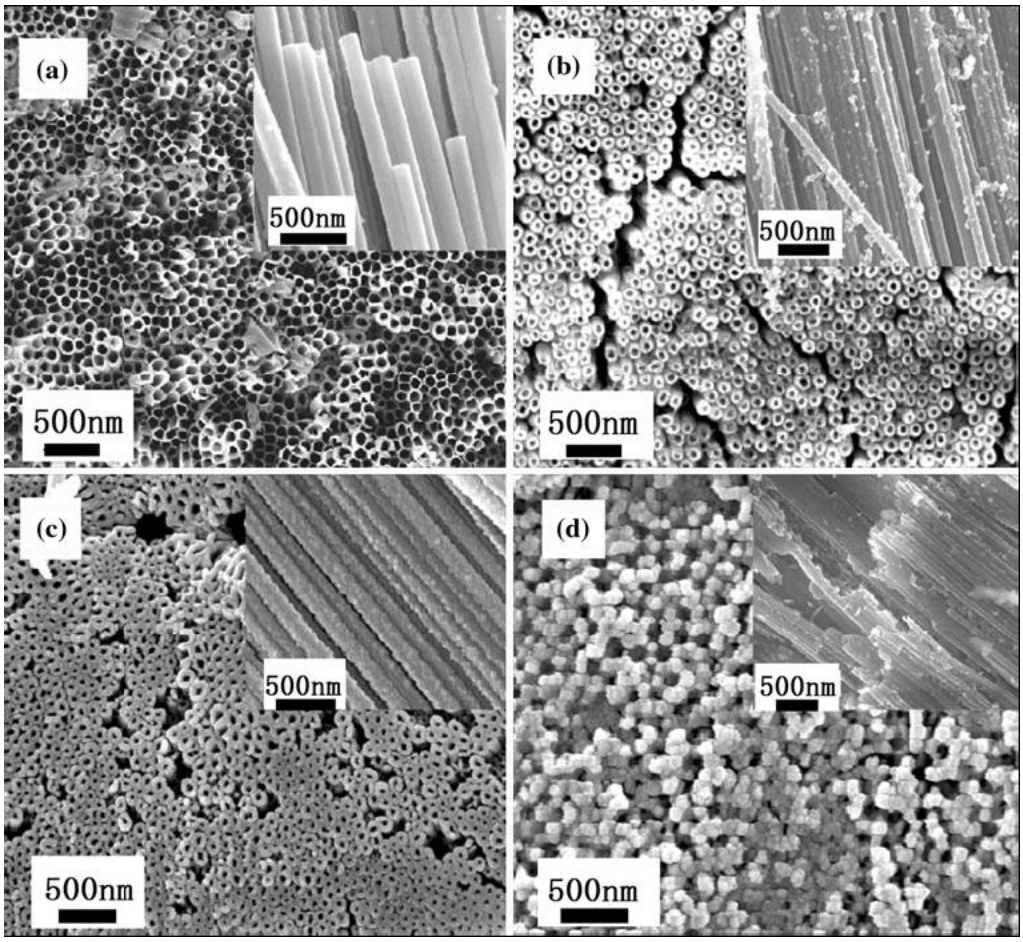


Figure 24. SEM images of (a) anodized ZrO_2 NTs, and ZrO_2 templates after hydrothermal reaction in (b) 0.05 M, (c) 0.1 M, and (d) 0.5 M LiOH solution at 200 ^oC for 4 h.[141] Reprinted with permission from ref 141. Copyright 2011 Springer Science+ Business Media, LLC.

Two mechanisms were proposed for the formation of Li_2ZrO_3 NTs: in situ mechanism and dissolution-precipitation process, as illustrated in Figure 25. First, dispersed Li^+ ions concentrate around ZrO_2 NTs arrays (Figure 25(a)). Partial supersaturated Li^+ ions then enter the crystal lattice of ZrO_2 under high pressure and form a tetragonal Li_2ZrO_3 NTs (Figure 25(b)). During this in situ growth process, the NTs walls become thicker and rougher due to the crystal cell expansion. However, for the blocking of the outer tubular walls, especially on the compact position (root of the NT or bottom barrier layer) of the layer, Li^+ ions are deficient and segmental ZrO_2 template remains (Figure 25(b, c)). Accompanying with the formation of Li_2ZrO_3 NTs, little portion of ZrO_2 is dissolved in the alkaline solution assisted by the high temperature and pressure. When ZrO^{2+} and Zr^{4+} are introduced into the solution, Li^+ are combined with the ZrO^{2+} or Zr^{4+} and agglomerate on the heterogeneous-nucleation sites provided by the NT arrays. Herein, the grainy Li_2ZrO_3 is formed on or in the already-formed Li_2ZrO_3 NTs (Figure 25(c)).[141]

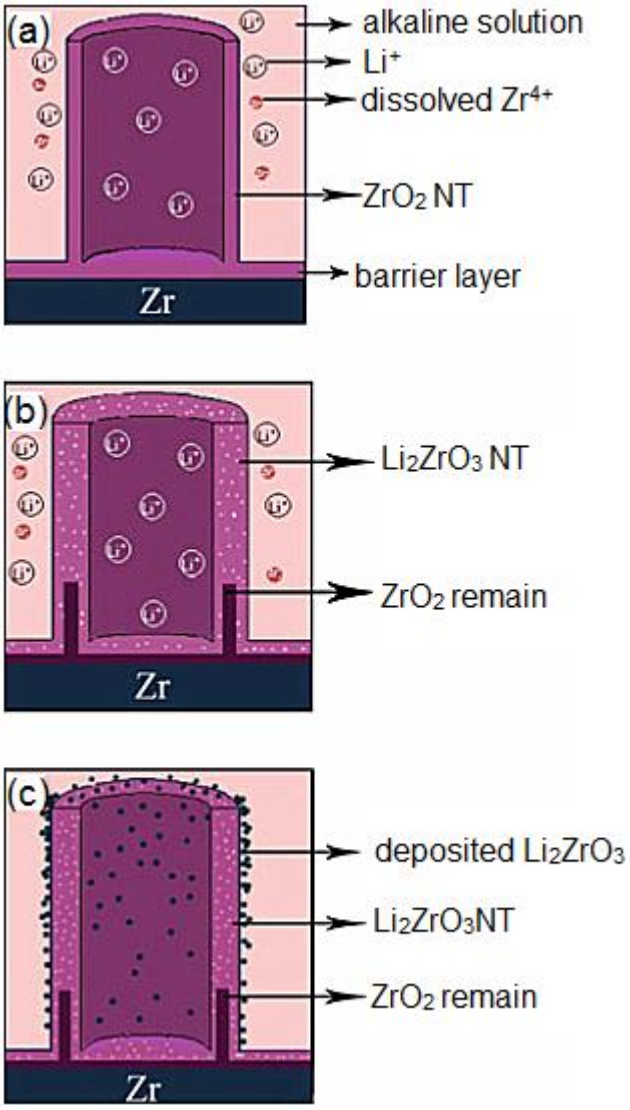


Figure 25. Growth mechanism of Li_2ZrO_3 NT by hydrothermal method in LiOH solution, (a) and (b) the supersaturated Li^+ ions enter the crystal lattice of ZrO_2 and form a tetragonal Li_2ZrO_3 structure, (c) partially dissolved Zr^{4+} ions react with the superfluous Li^+ ions and form tiny Li_2ZrO_3 particles on the top and wall of the already-formed NT.[141] Reprinted with permission from ref 141. Copyright 2011 Springer Science + Business Media, LLC.

The CO_2 capture performance of such prepared Li_2ZrO_3 NTs was tested at 550 °C under CO_2/N_2 (4:1, 0.5 bar), which reached a CO_2 uptake of 26 wt% in 60 min. For

contrast, Li_2ZrO_3 nanoparticles and bulk Li_2ZrO_3 only resulted in a capacity of ca. 15 wt%. Furthermore, the sorption rate of Li_2ZrO_3 NTs was also faster than that of bulk Li_2ZrO_3 and Li_2ZrO_3 nanoparticles in the initial 30 min. The enhancement of CO_2 sorption capacity for Li_2ZrO_3 NTs may be attributed to the nanotubular nature, large specific surface area, and the tetragonal crystalline structure. In addition, the excess ZrO_2 might acted as a dispersant and introduced more reactive boundaries in the Li_2ZrO_3 ceramics, which may induce a faster CO_2 capture rate.[140]

3.3. Formation of metazirconate solid solutions

3.3.1. $Li_{2-x}Na_xZrO_3$

The efficiency of Li_2ZrO_3 and Na_2ZrO_3 for CO_2 capture is highly related to the mobility of Li^+ or Na^+ in the ceramic skeleton made of $(ZrO_3)^{2-}$ chains. Thus, the diffusion of Li^+ or Na^+ is determined by their structure and morphology. Although these two zirconates possess the same elemental stoichiometry, their crystalline structure is not the same. The Li_2ZrO_3 structure turns out to be more packed than the Na_2ZrO_3 structure (Figure 26(a)). Na_2ZrO_3 has a lamellar structure, with the Na^+ located between the $(ZrO_3)^{2-}$ layers. However, the Li^+ in Li_2ZrO_3 locates in narrow channels. It was found that the insertion of Na^+ in those channels is harder than the intercalation of Li^+ among the Na_2ZrO_3 layers. Hence, if both Li_2ZrO_3 and Na_2ZrO_3 combine in a synergetic way, the mixed compounds will present original behaviors in CO_2 sorption.[147-149]

Pfeiffer et al.[86, 150] firstly prepared metazirconate solid solutions of $Li_{2-x}Na_xZrO_3$ ($0<x<2$) for CO_2 capture and revealed that the solubility limits of Na^+ into Li_2ZrO_3 and Li^+ into Na_2ZrO_3 are different. The maximum x for $Li_{2-x}Na_xZrO_3$ and $Na_{2-x}Li_xZrO_3$ is 0.2

and 0.6, respectively. The results also suggested that $Li_{2-x}Na_xZrO_3$ covers $Na_{2-x}Li_xZrO_3$, as in a cherry model. The size of the particle is around 1 μm, with a core of about 10–20 nm. The microscopic composition structure of $Li_{2-x}Na_xZrO_3$ solid solutions is shown in Figure 26(b).[150]

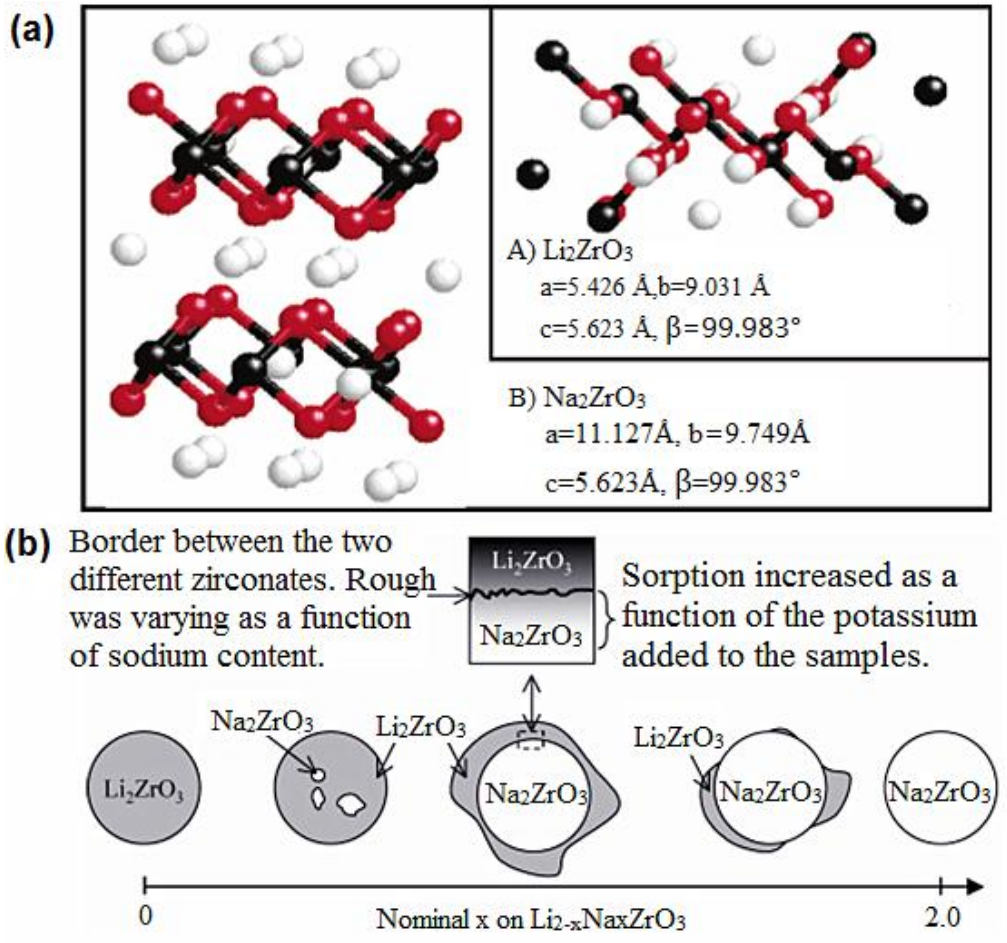


Figure 26. (a) Snapshots of Li_2ZrO_3 and Na_2ZrO_3 structures. The spheres represent, from the brightest to the darkest, the alkaline element (Li or Na), oxygen, and zirconium atoms, respectively, (b) model of the microscopic composition structure of $Li_{2-x}Na_xZrO_3$ solid solutions as a function of *x*. The porosity of ceramics is not represented in this model, but it is comparatively different, with Na_2ZrO_3 being more porous than Li_2ZrO_3.[150] Reprinted with permission from ref 150. Copyright 2006 American Chemical Society.

3.3.2. $Li_{2-x}K_xZrO_3$

Pfeiffer et al.[151] further revealed that doping very small quantities of potassium can also enhance the CO_2 capture capacity of Li_2ZrO_3. The mixed compounds Li_2ZrO_3-K_2ZrO_3 could present similar behaviors in CO_2 sorption to the $Li_{2-x}Na_xZrO_3$ solid solutions. Among a series of $Li_{2-x}K_xZrO_3$ (x = 0.0, 0.2, 0.3, 1.0, 1.4, and 1.8.) solid solutions, samples with x = 0 and 0.2 only showed the presence of Li_2ZrO_3. However, when the x value was increased to 0.3, a new second phase was found ($Li_{2.27}K_{1.19}Zr_{2.16}O_{6.05}$), whose crystal structure is shown in Figure 27(a). In this structure, the lithium atoms are located in different positions. Some lithium atoms are hexacoordinated, Li(1), while other lithium atoms are lonely pentacoordinated, Li(2) (Figure 27(b)). The LiO_6 polyhedra are distorted along the c-axis. On the other hand, the LiO_5 polyhedra do not present this kind of distortion. This effect may be attributed to Coulombic repulsion energies associated with the proximity of lithium and potassium atoms. For Li_2ZrO_3, $Li_{1.8}K_{0.2}ZrO_3$, and $Li_{1.4}K_{0.6}ZrO_3$, the CO_2 sorption capacity at 550 °C under a pure CO_2 atmosphere can reach 8.13, 17.7, and 18.6 wt%, respectively. Moreover, at short times (0–30 min), the slopes of the curves are 0.61, 2.04, and 3.06 mg g^{-1} min^{-1} for Li_2ZrO_3, $Li_{1.8}K_{0.2}ZrO_3$ and $Li_{1.4}K_{0.6}ZrO_3$, respectively. The $Li_{1.4}K_{0.6}ZrO_3$ sample captured CO_2 five times faster than Li_2ZrO_3. These results proved that the $Li_{2-x}K_xZr_2O_3$ solid solutions also present a better CO_2 sorption than pure Li_2ZrO_3.

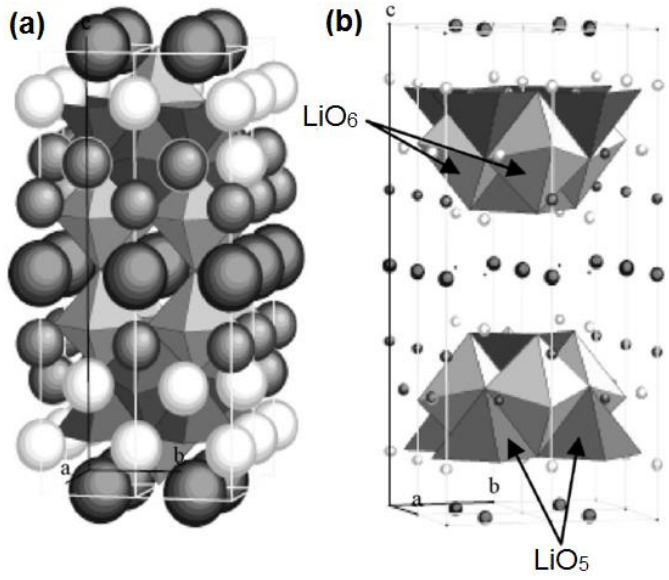


Figure 27. (a) Crystal structure of $Li_{2.27}K_{1.19}Zr_{2.16}O_{6.05}$, and (b) image showing only the lithium polyhedra: LiO_5 and LiO_6.[151] Reprinted with permission from ref 151. Copyright 2007 Elsevier Inc.

3.4. Incorporation of molten salt components in Li_2ZrO_3

3.4.1. Li_2CO_3/K_2CO_3

As in the lithium silicate case previously described, it has been reported that the incorporation of some molten salt components can further improve the CO_2 capture performance of Li_2ZrO_3.[32, 95, 133, 152, 153] Li_2CO_3-K_2CO_3 doped Li_2ZrO_3 revealed that the CO_2 sorption capacity can be dramatically improved. At 500 °C and under 50 vol% of CO_2 flow, the sorption capacity reached 20 wt% within 250 min, which was about 40 times faster than pure Li_2ZrO_3. Furthermore, even after one cycle of the CO_2 sorption/desorption process, the Li_2CO_3-K_2CO_3-doped Li_2ZrO_3 returned to its original state. Both Lin et al.[133] and Dou et al.[152] investigated the possible mechanism for CO_2 sorption on the Li_2CO_3-K_2CO_3 doped Li_2ZrO_3 sample, as show in Figure 28. The CO_2 sorption process by pure Li_2ZrO_3 and Li_2CO_3/K_2CO_3-doped Li_2ZrO_3 sorbents could be

divided into three phases by using a double-shell model. For pure Li_2ZrO_3 (Figure 28(a)), CO_2 molecules reacts with Li^+ and O^{2-} from Li_2ZrO_3 core, leading to the formation of ZrO_2 shell (first period). In the second period, Li^+ and O^{2-} from Li_2ZrO_3 core will penetrate the ZrO_2 shell and then reacts with CO_2, forming an additional Li_2CO_3 shell outside the ZrO_2 shell. In third period, the sorption reaction becomes weakened after the double-shell structure is stable, with a full formation of Li_2CO_3 shell. At this stage, the diffusion of Li^+ and O^{2-} onto the external surface of the dense Li_2CO_3 shell is very difficult. Only a small amount of CO_2 could react with. While the CO_2 sorption mechanism for Li_2CO_3/K_2CO_3-doped Li_2ZrO_3 is different (Figure 28(b)). Rather than the dense Li_2CO_3 shell, a molten carbonate phase will be formed, which can significantly reduce the resistance of CO_2 diffusion. The diffusivity of CO_2 in molten carbonate is ca. 10^{-5} cm^2 s^{-1} at 500–600 ^oC, much faster than that in solid carbonate.[154] Thus, the CO_2 sorption enhancement by Li_2CO_3-K_2CO_3 doping can be attributed to the CO_2 diffusion through the molten carbonate at a much faster rate.

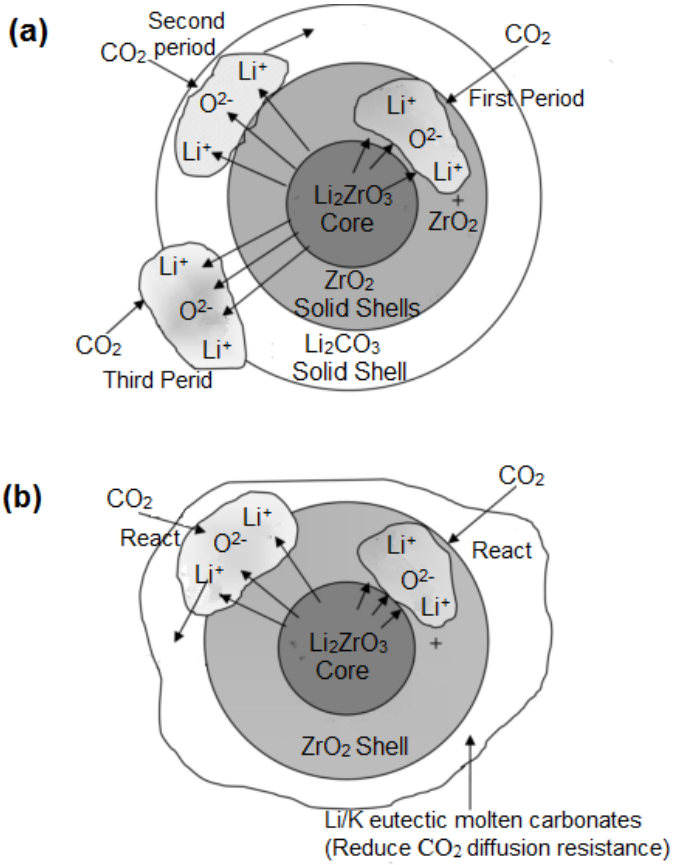


Figure 28. Illustration of the double-shell model for CO_2 sorption on (a) pure Li_2ZrO_3 and (b) Li_2CO_3/K_2CO_3-doped Li_2ZrO_3.[152] Reprinted with permission from ref 152. Copyright 2014 American Chemical Society.

Then, in order to identify the key microstructural parameters that control the sorption kinetics, Lin et al.[46] compared the CO_2 sorption rates of two K_2CO_3-doped Li_2ZrO_3 sorbents with different particle sizes. The K_2CO_3-doped Li_2ZrO_3 sample with average aggregate size of 5 μm can capture CO_2 up to 18 wt% of sample weight within 30 min at 650 °C. This sorption rate was more than four-fold faster than that of K_2CO_3-doped Li_2ZrO_3 with average aggregate size of 15 μm. The effect of temperature on sorption rate is complicated, depending on both thermodynamic and kinetic factors. A moderate temperature range from 550 to 590 °C is desirable for CO_2 sorption. They

also revealed that the oxygen ion diffusion in the ZrO_2 shell is the rate-limiting step of the sorption process. Pfeiffer et al.[155] studied the effect of O_2 addition on the thermokinetic properties of CO_2 sorption on K_2CO_3 doped Li_2ZrO_3. The results suggested that O_2 addition into the gas mixtures improved the CO_2 chemisorption when it was kinetically controlled by diffusion processes. The improvement of K_2CO_3 doping on Li_2ZrO_3 was also confirmed by monitoring the CO_2 sorption process on K-doped Li_2ZrO_3 using operando Raman spectroscopic spectroscopy analyses by Cornaglia et al.[156]

3.4.2. Multiple-eutectic salt

In addition, a number of binary and ternary eutectic salt-doped Li_2ZrO_3 sorbents have been investigated for high temperature CO_2 capture. Fauth et al.[157] found that the combination of binary alkaline carbonate, binary alkaline/alkaline earth carbonate, ternary alkaline carbonate, and ternary alkaline carbonate/halide eutectics to Li_2ZrO_3 can noticeably improve the CO_2 capture capacity and rate. Binary K_2CO_3/$MgCO_3$- and KF/Li_2CO_3-containing Li_2ZrO_3 powders revealed the fastest CO_2 capture rate at 500 ^oC. The formed eutectic molten carbonate layer on the surface of Li_2ZrO_3 was found to be able to facilitate CO_2 transfer. The ternary K_2CO_3/NaF/Na_2CO_3 eutectic led to highest CO_2 uptake and the fastest CO_2 sorption rate.

3.5. High lithium content zirconates ($Li_6Zr_2O_7$ and Li_8ZrO_6)

Besides Li_2ZrO_3, other high-lithium content zirconates, such as $Li_6Zr_2O_7$ and Li_8ZrO_6 were also found to be promising for high temperature CO_2 capture, due to the relatively higher lithium content in such zirconates. Therefore, these ceramics they were expected to capture more CO_2 than Li_2ZrO_3.

3.5.1. $Li_6Zr_2O_7$

The first study on $Li_6Zr_2O_7$ as high-temperature CO_2 sorbent was reported by Pfeiffer et al.[158] in 2005. They proposed that the reactions (10–12) may occur for CO_2 capture on $Li_6Zr_2O_7$. The CO_2 capture performance of $Li_6Zr_2O_7$ was compared with Li_2ZrO_3, as shown in Figure 29. At 500 °C, $Li_6Zr_2O_7$ captured almost 20 wt% CO_2 of the sorbent weight, much higher than that of Li_2ZrO_3 (only 6.3 wt %) during the same period of time. Particularly at the early stage (0–60 min), the CO_2 sorption rate of $Li_6Zr_2O_7$ (2.0 mg g^{-1} min^{-1}) was much faster than that of Li_2ZrO_3 (0.3 mg g^{-1} min^{-1}). While, due to the diffusion limit for Li^+ and CO_2 through the Li_2CO_3 layer, the sorption rate of both zirconates becomes similar after long-operation time.

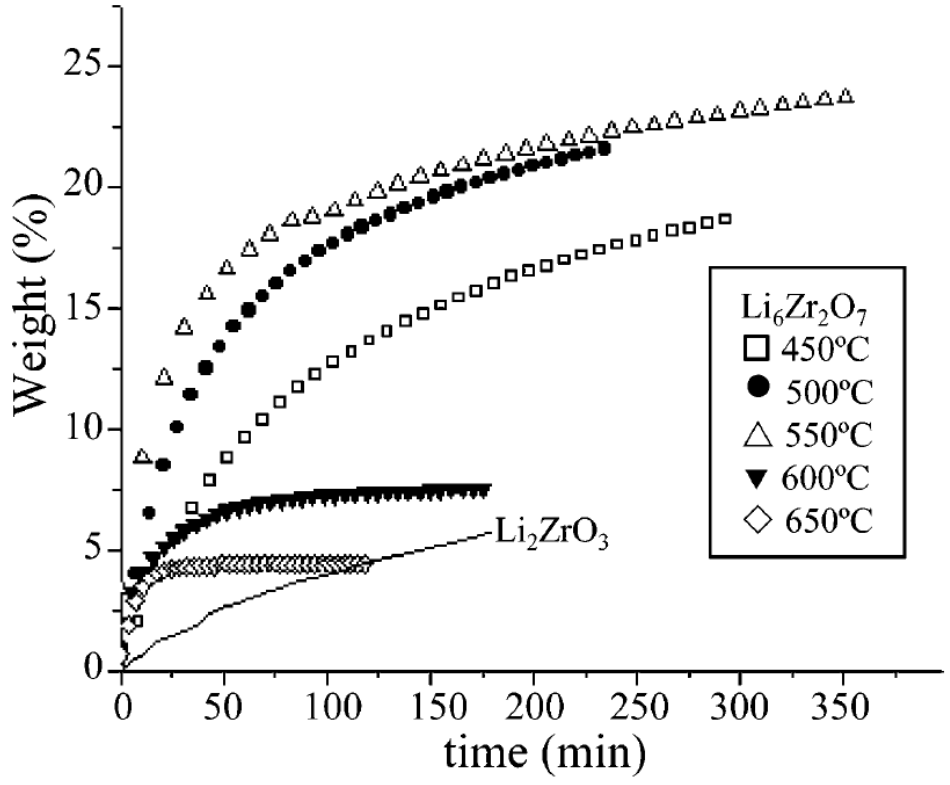


Figure 29. Isothermal sorption of CO_2 at 500 °C for Li_2ZrO_3 (line) and at different temperatures for $Li_6Zr_2O_7$ (marks).[158] Reprinted with permission from ref 158. Copyright 2005 American Chemical Society.

The CO_2 capture capacity of $Li_6Zr_2O_7$ is highly dependent on sorption temperatures. At 450 and 550 °C in 100 vol% CO_2, the CO_2 uptake of $Li_6Zr_2O_7$ was 19.2 and 23 wt%, respectively. However, when the sorption temperature was increased to 600 °C or higher, the CO_2 uptake of $Li_6Zr_2O_7$ decreased significantly to <7 wt%. These changes can be attributed to the decomposition of $Li_6Zr_2O_7$ into Li_2ZrO_3.[158]

$$Li_6Zr_2O_7\ (s) + 3CO_2\ (g) \rightarrow Li_2CO_3\ (s) + 2ZrO_2\ (s) \quad (10)$$

$$Li_6Zr_2O_7\ (s) + 2CO_2\ (g) \rightarrow Li_2CO_3\ (s) + ZrO_2\ (s) + Li_2ZrO_3 \quad (11)$$

$$Li_6Zr_2O_7\ (s) + CO_2\ (g) \rightarrow Li_2CO_3\ (s) + 2Li_2ZrO_3\ (s) \quad (12)$$

The CO_2 sorption mechanism on $Li_6Zr_2O_7$ was also proposed, as shown in Figure 30. They found that the optimal sorption temperature for $Li_6Zr_2O_7$ was 450–600 °C. First, the Li^+ reacts with CO_2 and forms a Li_2CO_3 layer on the surface of particles. Li^+ and CO_2 then have to diffuse in opposite ways to continue reaction, with the final product of ZrO_2, Li_2ZrO_3, and Li_2CO_3. However, when $Li_6Zr_2O_7$ was heated at temperatures >700 °C, then Li_2CO_3 started to decompose into CO_2 and Li^+. In this step, Li^+ reacts with ZrO_2 to produce Li_2ZrO_3, with certain part being sublimated to be Li_2O. Therefore, to efficiently use $Li_6Zr_2O_7$ as high-temperature CO_2 sorbent, too high operating temperatures should be avoid and prevent the occurrence of the its thermal decomposition.[158]

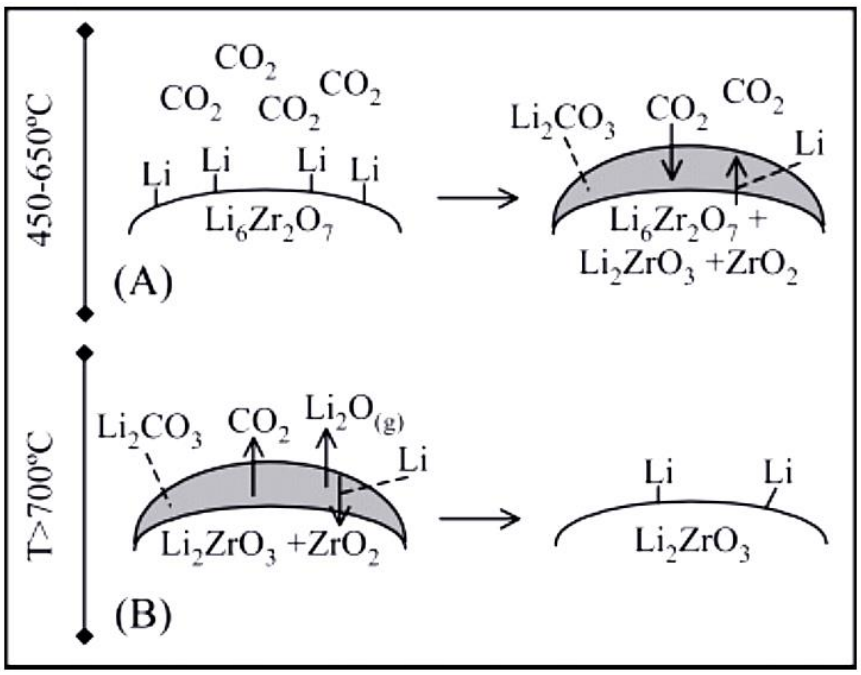


Figure 30. Schematic illustration of the carbonation and decarbonation mechanisms of $Li_6Zr_2O_7$ at high temperatures.[158] Reprinted with permission from ref 158. Copyright 2005 American Chemical Society.

$Li_6Zr_2O_7$ has two crystal phases (triclinic or monoclinic). Pfeiffer et al.[158] reported triclinic-phase $Li_6Zr_2O_7$ possesses higher CO_2 uptake than Li_2ZrO_3, while its regenerability needs to be improved. Then, Zhang et al.[159] studied the CO_2 sorption performance of monoclinic-phase $Li_6Zr_2O_7$ (m-$Li_6Zr_2O_7$) under low CO_2 concentration. The m-$Li_6Zr_2O_7$ showed the best sorption performance at 750 °C, at which temperature, a CO_2 uptake of about 11.2 wt% was obtained with the P_{CO2} in the range of 0.2–1 bar. At lower CO_2 partial pressure of 0.1 bar, the sorption capacity slightly decreased to 9.71 wt%. On the other hand, 575 °C was the best CO_2 capture temperature for Li_2ZrO_3. In pure CO_2, the CO_2 sorption capacity of Li_2ZrO_3 was 18.5 wt%. However, the capacity of Li_2ZrO_3 was reduced to 0.65 wt% at P_{CO2}=0.1. This result indicated that t-Li_2ZrO_3 is influenced by CO_2 concentration more than m-$Li_6Zr_2O_7$. It was believed that the higher

lithium content in t-Li_2ZrO_3 favors CO_2 sorption under low CO_2 concentration. During the CO_2 sorption-desorption cycles, m-$Li_6Zr_2O_7$ will be transformed into triclinicphase $Li_6Zr_2O_7$, retaining relatively good cycling performance.

3.5.2. Li_8ZrO_6

In 2010, Zhang et al.[160] noted that Li_8ZrO_6 also possesses high CO_2 capture capacity by first reacting with CO_2 to form $Li_6Zr_2O_7$ through reaction (13). Later, using a three-step calcination method, they synthesized high-purity Li_8ZrO_6 and characterized its CO_2 capture properties.[161] The results indicated that Li_8ZrO_6 can result in a CO_2 uptake of 53.98 wt% at temperatures higher than 725 ^oC. In addition, the CO_2 uptake almost did not change even in a wide range of CO_2 partial pressure of 0.1–1.0 bar. While, the major problem for Li_8ZrO_6 is its CO_2 uptake of gradually decreased during multicycles due to the reconstruction and sintering of sorbent at high temperature. The multiple CO_2 sorption-desorption process was illustrated in Figure 31. In step a, CO_2 can easily diffuse into the pores and react with Li_8ZrO_6, producing Li_2ZrO_3 and Li_2CO_3. In step b, due to the expandability of produced carbonate in pores, the large particles will be broken down to small particles. In the meantime, the molten Li_2CO_3 will cover the surface of large particles, leading to the loss of porosity. In step c, during the desorption process in N_2, the produced Li_2ZrO_3 will react with the surrounded Li_2CO_3 and transform back to Li_8ZrO_6. However, the specific surface area of regenerated Li_8ZrO_6 will be reduced due to the loss of porosity, with certain amount of Li_2O being sublimed. In the second cycle, the sorption rate will be slower due to the less specific surface area (steps d and e). In addition, the particles will be further sintered to larger particles during the regeneration process (step f). As a result, the reversible CO_2 sorption capacity will gradually decreased in the following cycles.

$$2Li_8ZrO_6 + 5CO_2 \leftrightarrow 5Li_2CO_3 + Li_6Zr_2O_7 \quad (13)$$

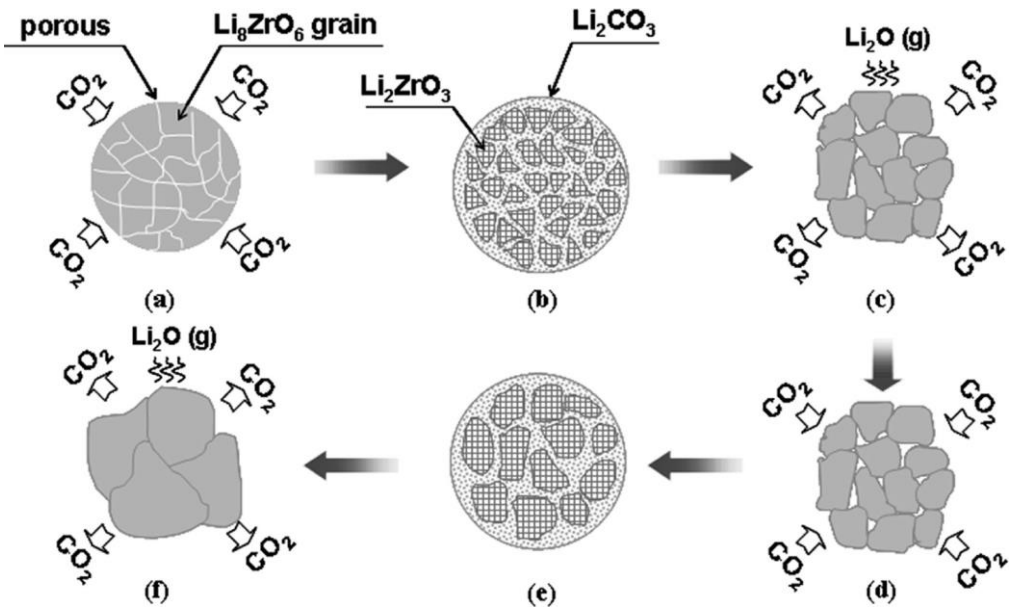


Figure 31. Schematic illustration for CO_2 sorption (at 750 ^oC) and desorption (at 900 ^oC) on Li_8ZrO_6. Steps a-c correspond to the first cycle of CO_2 sorption-desorption, steps d-f correspond to the second cycle of CO_2 sorption-desorption, and step g represents the possible Li_2O sublimation during regeneration.[161] Reprinted with permission from ref 161. Copyright 2011 American Chemical Society.

Another limitation relies on the difficult preparation of pure Li_8ZrO_6 phase.[6] Duan et al.[162] investigated the structural, electronic, and phonon properties of Li_8ZrO_6 using density functional theory and lattice phonon dynamics. The thermodynamics of CO_2 sorption-desorption for Li_8ZrO_6 was comparatively investigated with Li_2ZrO_3 and $Li_6Zr_2O_7$. They found that although Li_8ZrO_6 possesses much higher CO_2 uptake Li_2ZrO_3, its practical application is limited by the high regeneration energy, the capacity loss during multi-cycles, and the severe aggregation at high temperatures, etc.

4. Other lithium containing ceramics based CO_2 sorbents

In addition to lithium silicates and lithium zirconates, many other lithium containing compounds including lithium titanates (Li_4TiO_4, Li_2TiO_3), lithium aluminates (Li_5AlO_4), lithium ferrites (Li_5FeO_4, α-$LiFeO_2$), lithium cuprate (Li_2CuO_2), lithium bismuthates (Li_7BiO_6, Li_5BiO_5, Li_3BiO_4, $LiBiO_2$), and lithium borate (a-$LiBO_2$) have also been studied for capturing CO_2 at high temperatures. Therefore, in the following section, the CO_2 capture performance of all the above mentioned materials will be discussed in detail.

4.1. Lithium titanates

In 2007, Oh-ishi et al.[163] reported the CO_2 sorption property of Li_4TiO_4 at high temperature for the first time. They revealed that single phase Li_4TiO_4 can capture CO_2 in the temperature range of 300–856 °C, and the maximum sorption capacity was 42 wt% at 856 °C. The reaction between Li_4TiO_4 and CO_2 can be described by equation (14). However, it is worth to be noted that the regenerability of Li_4TiO_4 did not seem to be good, and the desorption of CO_2 is not complete even at 1000 °C.

$$Li_4TiO_4 + 1.5CO_2 \leftrightarrow LiTiO_x + 1.5Li_2CO_3 + (2.5–x)/2O_2 \qquad x=2–2.5 \qquad (14)$$

Then, Ariyama et al.[164] investigated the influence of particle size on CO_2 sorption capacity of Li_4TiO_4. Three different particle sizes (53, 100–200, and 200–250 μm) Li_4TiO_4 were prepared, which showed quite different sorption properties. The initial size of Li_4TiO_4 affected the reactivity below 700 °C. In addition, Li_4TiO_4 started to capture CO_2 at 250 °C and form Li_2TiO_3 and Li_2CO_3. The sorption rate was obviously improved at 710 °C due to the formation of the Li_2CO_3-based liquid phase. The maximum and minimum values of the weight change ratio in each cycle decrease gradually when the heat cycle is repeated. After the third CO_2 desorption, the sample weight decreased by approximately 5%. The decrease in the maximum value was thought to be caused by the decrease in the specific surface area and the crystal

growth of the oxide compound. The decrease in the minimum value might be caused by the sublimation of Li_2O from the Li_2CO_3-Li_2O-TiO_2 melt. Thus, to improve the repeatability of CO_2 sorption-desorption of Li_4TiO_4, lowering the operating temperature and the prevention of sintering are important.

Li_2TiO_3 is another type of lithium titanate that has been studied for high-temperature CO_2 capture. Liu et al.[165] investigated the CO_2 sorption properties of Li_2TiO_3 and Na-doped Li_2TiO_3. The result showed that Na-doped Li_2TiO_3 has higher CO_2 sorption capacity than Li_2TiO_3. The maximum capacity of 30 wt% can be obtained with the sample of $n(TiO_2):n(Li_2CO_3):n(Na_2CO_3)$ = 1:0.97:0.03 at 600 ^oC. The enhanced performance of Na-doped Li_2TiO_3 may be due to the created more crystal defects by sodium doping. In addition, sodium doping can improve the cycle stability of Li_2TiO_3. After 5 cycles, the CO_2 uptake decay for Na-doped Li_2TiO_3 was only 14.28 wt%, which was much lower than that for neat Li_2TiO_3.

4.2. Lithium aluminates

In 2009, Pfeiffer et al.[166] first reported the CO_2 sorption properties of lithium aluminates ($LiAlO_2$ and Li_5AlO_4), and the results showed that $LiAlO_2$ did not capture CO_2, while Li_5AlO_4 showed an excellent behavior as a possible CO_2 sorbent. At 700 °C, the CO_2 sorption quantity and rate on Li_5AlO_4 were very high and fast. In the first 3 min, the CO_2 uptake reached as high as 35.7 wt%. The sorption rate started to decrease between 3 and 30 min, getting a maximum CO_2 uptake of 47.8 wt%. Similar to other lithium containing compounds, the possible mechanism for CO_2 sorption on Li_5AlO_4 was also proposed, as described in reaction equation (15). The theoretical CO_2 sorption capacities for Li_5AlO_4 is 38.3 wt%, which is quite high in comparison with that

of other lithium containing ceramics (Figure 32). The effect of CO_2 partial pressure was also evaluated by using different partial pressures of CO_2 and O_2, which revealed using low P_{O2} (0.1) did not affect the kinetic and final CO_2 chemisorption process. Moreover, adding a small amount of oxygen (P_{O2} = 0.05) seemed to increase the CO_2 chemisorption on Li_5AlO_4. Doping an alkaline carbonate mixture can modify the diffusion conditions due to the carbonate melting process and decrease the CO_2 capture temperatures. Ionic conductivity and activation energy analyses confirmed the oxygen viability is very important for the carbonation process of Li_5AlO_4.[167]

$$2Li_5AlO_4 + 5CO_2 \rightarrow 5Li_2CO_3 + Al_2O_3 \quad (15)$$

Li_5AlO_4 has two different crystal polymorphs of α-Li_5AlO_4 and β-Li_5AlO_4, and both of which have an orthorhombic crystal structure. Thus, the effect of crystal phase on the CO_2 sorption property of Li_5AlO_4 was further studied.[168] The β-Li_5AlO_4 (59.4 wt%) sorbent showed higher CO_2 sorption capacity than α-Li_5AlO_4 (41.8 wt%) at 675 °C under 100 vol% CO_2, but both of them exhibited a gradually decrease in CO_2 capture capacity during multicycles. However, α-Li_5AlO_4 showed better cycling stability than β-Li_5AlO_4. After 20 cycles (CO_2 sorption was performed at 700 °C for 20 min, and CO_2 desorption process was performed at 750 °C for 20 min into a N_2 flux), the CO_2 capture capacity of α-Li_5AlO_4 decreased from 47.7 wt% to 22.1 wt%. For β-Li_5AlO_4, the CO_2 capture capacity decreased from 62.3 wt% to only 8.1 wt%. Next, α-Li_5AlO_4 was doped with 10 wt% Na_2CO_3 or K_2CO_3, and the obtained samples showed higher CO_2 capture capacity, 37–39 wt% at 660 °C and 50 wt% at 710 °C, respectively.[169] Cycling performance tests suggested that the doped samples showed similar stability to α-Li_5AlO_4 pure sample. In all, it can be concluded that these materials might be good candidates for multicycle CO_2 chemisorption processes.

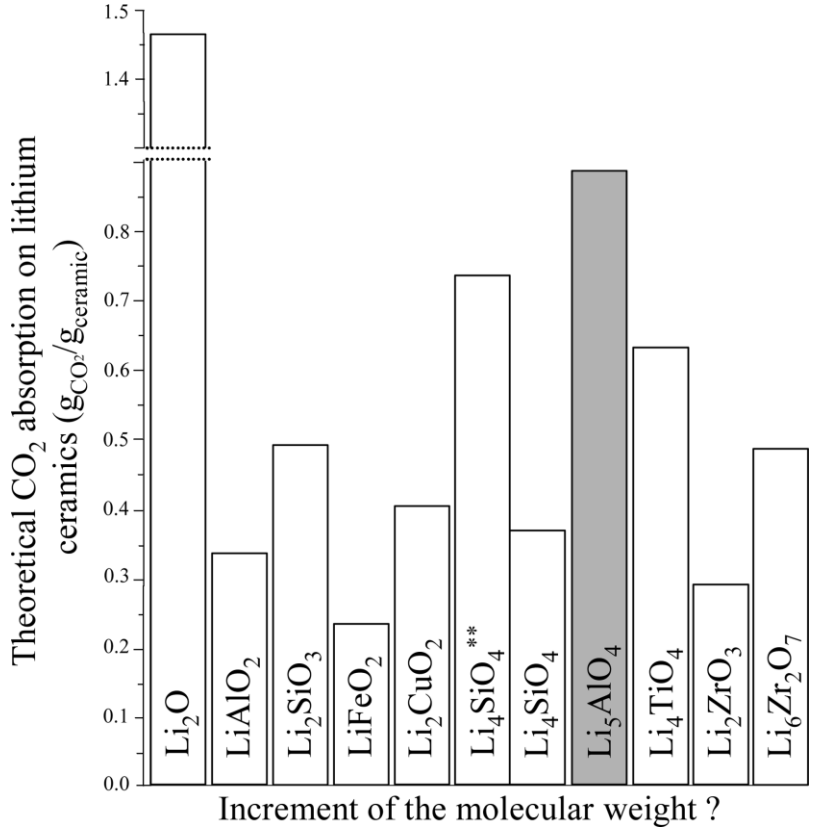


Figure 32. Comparison of the maximum theoretical CO_2 sorption capacities of different lithium containing ceramics. Li_4SiO_4** and Li_4SiO_4 represent the CO_2 sorption capacities, assuming a total and half lithium conversion to Li_2CO_3, respectively.[166] Reprinted with permission from ref 166. Copyright 2009 American Chemical Society.

4.3. Lithium ferrites and gallates

Different lithium ferrites ($LiFeO_2$ and Li_5FeO_4) have been studied for CO_2 capture under different CO_2 and O_2 concentrations. The results indicated that Li_5FeO_4[170] is able to capture CO_2 from 200 to 715 °C, and has the maximum CO_2 sorption capacity (50.3 wt%) at 800 °C in pure CO_2 atmosphere. Li_5FeO_4 also showed high sorption kinetics even at low CO_2 partial pressure of 0.2. In addition, the addition of oxygen was proved to enhance CO_2 capture on Li_5FeO_4 at temperatures below 700 °C, but favor CO_2

desorption at higher temperatures. In the same context, Li_5GaO_4[171] can uptake 39 wt% of CO_2 between 568 and 709 °C under pure CO_2 atmosphere, thus indicating that Li_5GaO_4 is also promising for CO_2 sorption.

Later on, $Li_5(Al_{1-x}Fe_x)O_4$ solid solutions with different compositions prepared and investigated for CO_2 capture.[172] Figure 33 indicates oxygen addition can improve CO_2 sorption during the first moment and at the end of the isotherms between 400 and 600 °C. The mechanism that how Fe enhances the CO_2 sorption can be explained in two different ways: (i) iron has the chemical ability to dissociate the oxygen molecules, facilitating the whole carbonation process, and (ii) iron can present different oxidation states, which may induce higher and faster oxygen affinity and diffusion.

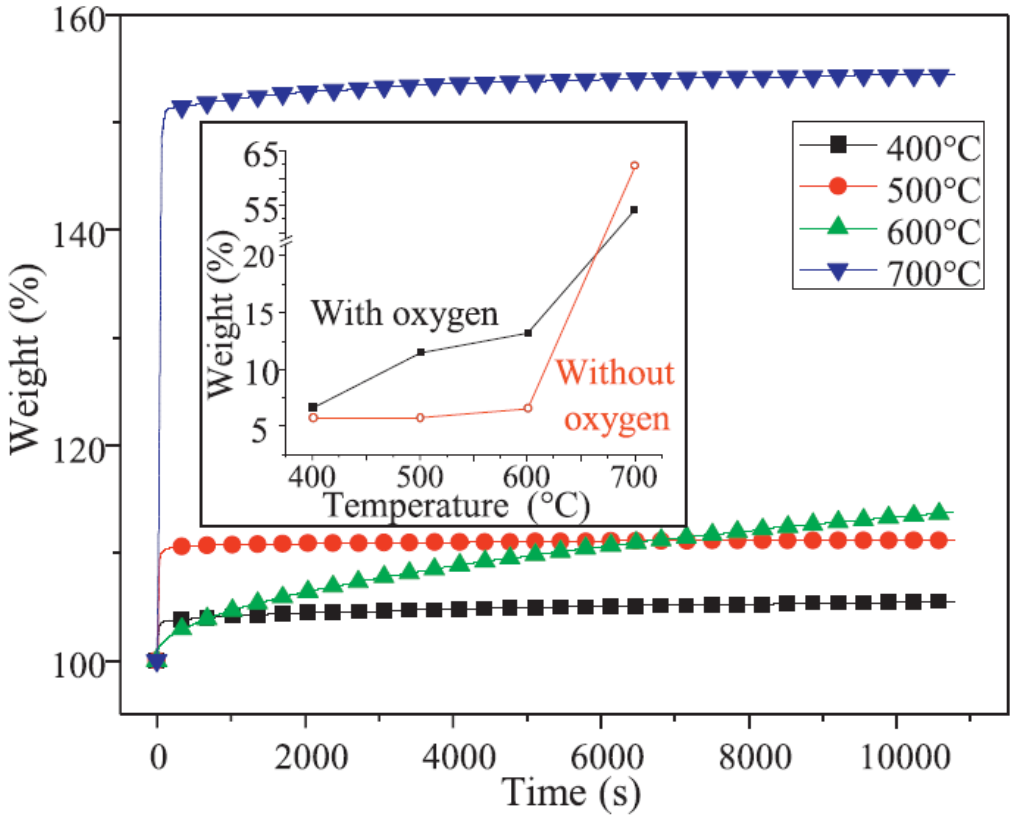


Figure 33. Isothermal TG experiments of the $Li_5(Al_{0.8}Fe_{0.2})O_4$ sample between 400 and 700 °C, using a P_{O2} = 0.05. The square inset shows a comparison of the total weight increments observed on the CO_2-$Li_5(Al_{0.8}Fe_{0.2})O_4$ isotherms in the absence or presence

of oxygen.[172] Reprinted with permission from ref 172. Copyright 2017 Elsevier B.V. and Science Press.

Gomez-Garcia et al.[170, 173] reported α-$LiFeO_2$ as a new high-temperature CO_2 sorbent and investigated the influence of excess lithium on CO_2 capture performance (Li/Fe molar ratios of 1, 1.1, 1.2 and 1.3). The α-$LiFeO_2$ phase was obtained by a novel method of nitrate pyrolysis involving two calcinations at 500 and 670 °C for 3 h. The behavior of the $Li_{1+x}FeO_2$ lattice parameter as a function of lithium content was studied. A linear behavior is observed at $x < 0.2$ values, indicating a solid solution system according to law of Vegard. The formation of solid solutions with the nominal formula $Li_{1+x}FeO_2$ at $0 \leq x \leq 0.3$, and the specific surface area of samples were 1–4 $m^2 g^{-1}$. The amount of captured CO_2 increased with the increase of lithium excess in the compound, and 4 wt% of CO_2 can be captured when the $x = 0.3$ at T > 600 °C. The CO_2 capture capacity was related to the excess lithium in each sample, which can be placed at the interstitial positions on the FCC lattice. However, one obvious drawback of α-$LiFeO_2$ is its low CO_2 uptake capacity. Yanese et al.[174] recently compared the CO_2 carbonation on three different $LiMO_2$ compounds, where M was Fe, Co or Ni, as all these samples have similar layered structures. Authors found that $LiCoO_2$ was chemically stable up to 600 °C, while $LiNiO_2$ reacted with CO_2 at around 500 °C. Moreover, these two phases did not present layered structure evolutions as $LiFeO_2$ did.

4.4. Lithium cuprates

The high lithium diffusion and structural characteristics of Li_2CuO_2 make it a potential CO_2 capture material with a similar mechanism to other lithium.[175] Comparing to other

sorbents, Li_2CuO_2 has some advantages. For instance, it begins to react with CO_2 at lower temperatures (120 °C), which may be used in different applications or under different thermal conditions. In addition, copper is cheaper and 31 wt% lighter than zirconium. Oh-ishi et al.[34] studied the synthesis and CO_2 capture performance of single-phase Li_2CuO_2. When the synthesis temperature was under 670 °C or over 700 °C in air, single-phase Li_2CuO_2 could not be obtained. Quench rate (°C s^{-1}) also impacted the synthesis of single-phase Li_2CuO_2, and revealed it started to capture CO_2 at 230 °C, then drastically capture CO_2 at temperatures higher than 600 °C, and emitted CO_2 from 900 °C. Li_2CuO_2 reached a CO_2 uptake of 40.2 wt%, which is higher than that of Li_4SiO_4 (36.7 wt%). Pfeiffer et al.[176] analyzed the structure of nonstoichiometric lithium cuprates ($Li_{2+x}CuO_{2+x/2}$) and evaluated their CO_2 capture performance. They revealed that the excess lithium may form lithium oxide and locate in the interlayers of Li_2CuO_2. As it can be expected, the CO_2 capture capacity increased with the increase of the total lithium.

Operating conditions also greatly affect the CO_2 sorption capacity of Li_2CuO_2 sorbent. Oh-ishi et al.[177, 178] and Pfeiffer et al.[177] found that using considerably low CO_2 partial pressures did not affect the CO_2 sorption significantly. Li_2CuO_2 seems to present much better CO_2 capture properties, using low partial pressures, than other lithium ceramics such as Li_4SiO_4. The results revealed that the CO_2 capture process can be enhanced by adding O_2 (P_{O2} = 0.03–0.2), as shown in Figure 34. Without the addition of O_2, O^{2-} can only be released from Li_2CuO_2 and such diffusion is so slow that it limits the overall carbonation process. However, after adding O_2, the copper in Li_2CuO_2 can facilitates O_2 dissociation, and thus the abundant O^{2-} can enhanced the CO_2 capture process. In addition, Li_2CuO_2 can be completely recovered after CO_2 desorption.

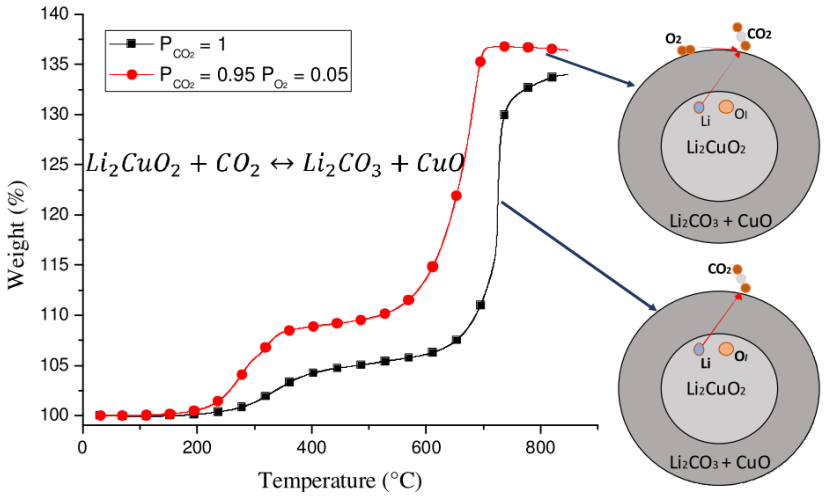


Figure 34. CO_2 capture process of Li_2CuO_3 with P_{CO2} = 1 and P_{CO2} = 0.95, P_{O2}=0.05.[177] Reprinted with permission from ref 177. Copyright 2016 Elsevier B.V.

Later on, Ham-Liu et al.[179] demonstrated that the CO_2 capture performance of Li_2CuO_2 can be enhanced by doping alkaline carbonates (K_2CO_3 and Na_2CO_3). Na-Li_2CuO_2 reached the highest CO_2 uptake of 30.6 wt% at 700 °C, while K-Li_2CuO_2 achieved the highest CO_2 uptake of 40.4 wt% at 650 °C, after 3 h. Such promoting effect was ascribed to the formation of eutectic phases between K_2CO_3 and Na_2CO_3 added mechanically and the formation of Li_2CO_3 due to CO_2 capture.

4.5. Lithium bismuthates and borates

Lithium bismuthates with different compositions including Li_7BiO_6, Li_5BiO_5, Li_3BiO_4 and $LiBiO_2$ phases were studied for CO_2 capture by Ortiz-Landeros et al.[180] The CO_2 capture capacity was enhanced with an increase of Li/Bi molar ratio, as shown in Figure 35. Among them, Li_7BiO_6 showed the highest CO_2 sorption capacity. At low temperatures (T<520 °C), the CO_2 uptake of Li_7BiO_6 was quite low, 5.17 wt%. When the sorption

temperature was higher than 520 °C, Li_7BiO_6 reached a maximum sorption rate at lower temperatures (590–600 °C), and exhibited a maximum weight increase of 32.9 wt% at 660 °C. The regeneration ability of the Li_7BiO_6 was studied through four carbonation–decarbonation cyclic tests (carbonation at 570 °C, and decarbonation at 640 °C). The results suggested an incomplete regeneration of the material during decarbonation under the studied experimental conditions. During the first carbonation cycle, the sample experienced a weight gain of 18.2 wt%. However, during the subsequent decarbonation, only 14.6 wt% CO_2 can be desorbed. Moreover, the CO_2 capture efficiency decayed gradually after each successive capture-regeneration cycle. Thus, future work must be focused on how to enhance the regenerability of Li_7BiO_6 based CO_2 sorbents.

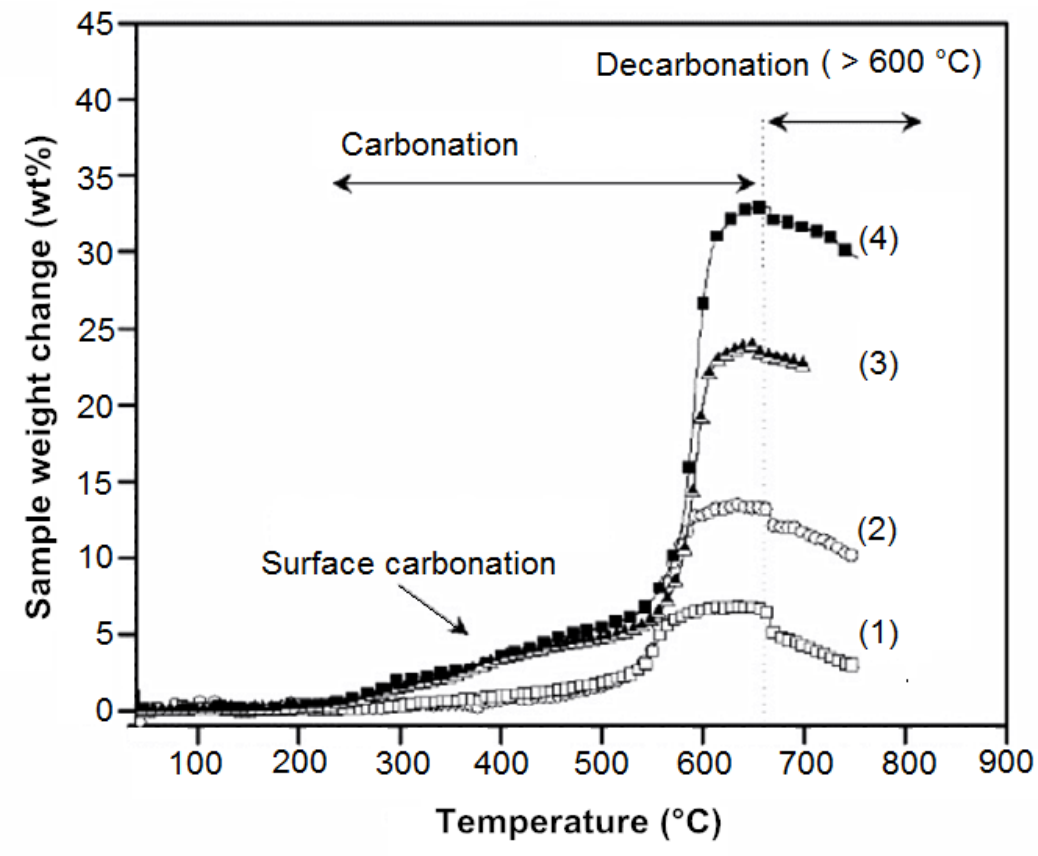


Figure 35. Dynamic TG analysis of the Li_2O–Bi_2O_3 samples in a 100 vol% CO_2 flow. (1)

$LiBiO_2$, (2) Li_3BiO_4, (3) Li_5BiO_5, (4) Li_7BiO_6.[180] Reprinted with permission from ref 180. Copyright 2016 Science Press and Dalian Institute of Chemical Physics.

$LiBO_2$ was also demonstrated to be able to capture CO_2 at high temperatures, during which a phase transformation from α-$LiBO_2$ to γ-$LiBO_2$ occurred[181] and the CO_2 sorption mainly occurs over the γ-$LiBO_2$ phase. They also revealed that the phase transformation may be the limiting step of the CO_2 capture process. However, the CO_2 sorption capacity was not considerably high. When the sorption temperature increased from 420 to 460 °C, the CO_2 sorption capacity increased from 1.9 wt% to 2.7 wt%, and the desorption process was achieved when the temperature was higher than 480 °C.

In order to have a better comparison of the CO_2 capture performance of the above discussed different lithium containing ceramic sorbents, the sorption temperature and the corresponding CO_2 sorption capacity were briefly summarized in Table 5. It can been seen that different sorbents have different optimal sorption temperatures, as well as different initial sorption capacities. Although some sorbents such as Li_8SiO_6, Li_8ZrO_6, Li_5AlO_4, and Li_5FeO_4 possess very high initial sorption capacity (50.3–62.0 wt%), their cycling performance is relatively poor and thus should be improved. Among all sorbents, Li_4SiO_4 still represents the best option so far for high-temperature CO_2 capture due to its better cycling stability.

Table 5. Summary of the sorption temperature and sorption capacity of different lithium-containing ceramic CO_2 sorbents.

Samples	Sorption temperature (°C)	CO_2 concentration (vol%)	Sorption capacity (wt%)	Reference
Li_4SiO_4	650	100	36.3	[78]
Li_8SiO_6	650	100	62.0	[126]
Li_2ZrO_3	575	100	27.0	[139]
$Li_6Zr_2O_7$	550	100	23.0	[158]
Li_8ZrO_6	725	100	54.0	[161]
Li_4TiO_4	856	100	42.0	[163]
Li_2TiO_3	600	100	30.0	[165]
Li_5AlO_4	700	100	59.4	[168]
Li_5FeO_4	800	100	50.3	[170]
$LiFeO_2$	550	100	1.5	[173]
Li_2CuO_2	875	100	40.5	[178]
Li_7BiO_6	660	100	32.9	[180]
Li_5GaO_4	709	100	39.0	[171]

5. Thermodynamic analysis

The CO_2 capture process on lithium-containing ceramics is controlled by several parameters. The first important parameter that influences CO_2 capture is the reactivity between CO_2 and lithium-containing sorbents. However, with the progress of CO_2 sorption, the whole process becomes diffusionally controlled. An ideal sorbent requires high reversible CO_2 uptakes during multiple sorption/desorption cycles as well as excellent stability at high temperatures. To address these issues, thermodynamic and kinetic analyses are important factors for determining the best CO_2 capture conditions, for instance, CO_2 sorption/desorption times and temperatures with regards to CO_2 concentrations, etc.

Chowdhury et al.[42] calculated the changes of Gibbs free energy of the carbonation and decarbonation processes for several alkaline ceramics, including Li_4SiO_4 and Li_2ZrO_3, among others. Negative Gibbs Energy values indicate although sorption can take place at room temperature (30 °C), it is not feasible due to very slow kinetics. Therefore, high temperature is needed to achieve adequate kinetics, and the

CO_2 capture process will be aided by the released heat from carbonation reaction.[83] In Figure 36, it can be seen that each ceramic has a specific temperature to get zero Gibbs Energy for carbonation, which is 325, 720, 750, and 900 ^oC for Na_2SiO_3, Li_4SiO_4, Li_2ZrO_3, and CaO, respectively. The temperatures that yield zero Gibbs energies are defined as "inversion point temperatures". It was pointed out that lower inversion temperatures allows CO_2 sorption with lower energy demands and helps in avoiding sorbent sintering. The equilibrium partial pressures for CO_2 sorption and desorption of Na_2SiO_3, Li_4SiO_4, Li_2ZrO_3, and CaO sorbents, as a function of temperature, were also examined, as shown in Figure 36(b). At P_{CO2} < 0.1 bar, CO_2 desorption from Li_4SiO_4 starts to occur at 560 °C, while if P_{CO2} > 0.1 bar, Li_4SiO_4 captures CO_2 at this temperature. These thermodynamic data also suggest that capturing CO_2 from hot flue gases (ca. 400–800 ^oC) using lithium-containing ceramics is thermodynamically viable. The effect of CO_2 concentration on the optimal CO_2 sorption and desorption temperatures has also been investigated by Wang et al.[78] They observed that the optimal sorption temperature shifted to lower values by decreasing CO_2 concentration.

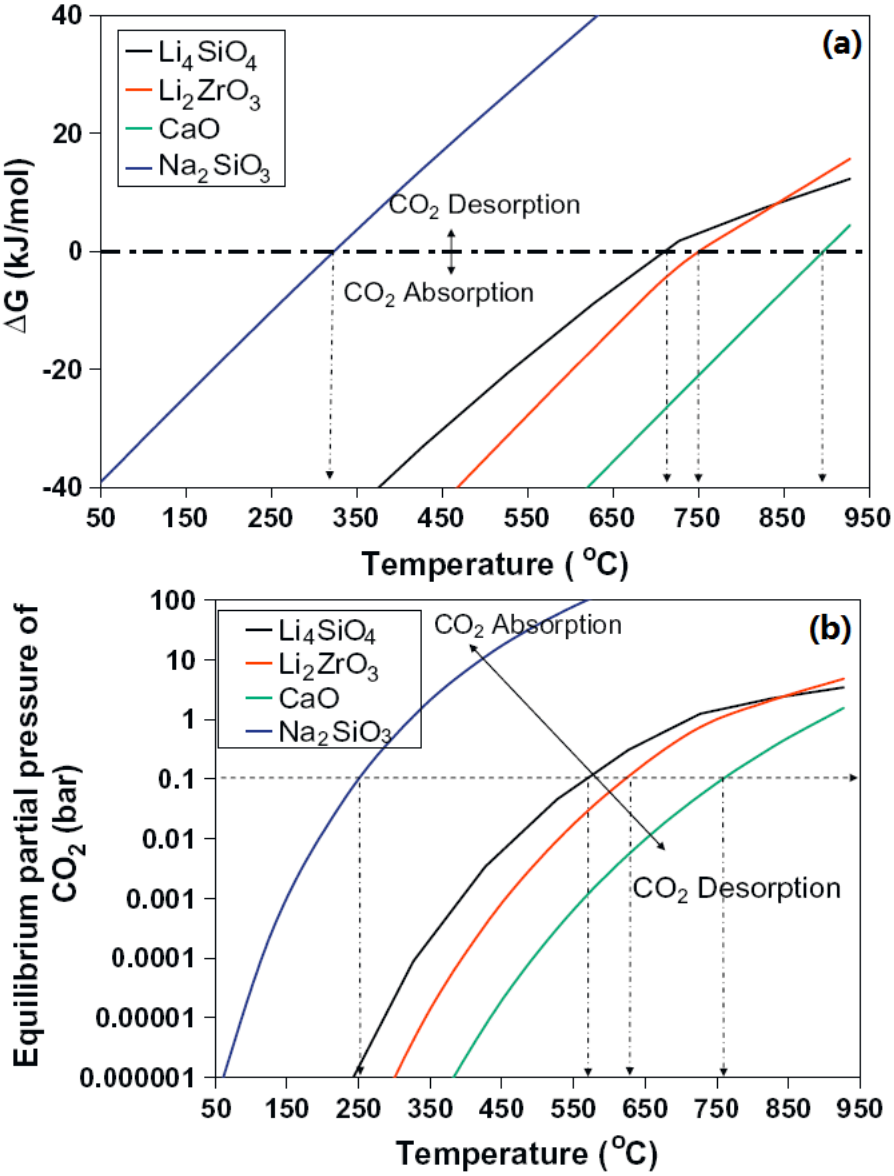


Figure 36. (a) Temperature dependence of Gibbs Energy of the carbonation and decarbonation reactions at P_{CO2} = 1 atm, over Li_4SiO_4 and Li_2ZrO_3, where CaO and Na_2SiO_3 are included for comparison purposes, (b) Equilibrium partial pressure dependence with temperature. Note: reported curves separate the CO_2 sorption conditions (carbonation) and CO_2 desorption (decarbonation) conditions. Broken horizontal line provides the inversion temperature for 0.1 bar equilibrium pressure.[42] Reprinted with permission from ref 42. Copyright 2013 Elsevier B.V.

In a different theoretical investigation, Duan et al.[41] analyzed the whole lithium silicate system, giving special attention to thermodynamics features. In that work, different lithium silicates including Li_8SiO_6, $Li_6Si_2O_7$, Li_4SiO_4, Li_2SiO_3, $Li_2Si_2O_5$, $Li_2Si_3O_7$, as well as Li_2O and SiO_2 for comparison purposes, were studied using first-principles DFT calculation. Based on theoretical energetic information, the CO_2 sorption performance was thermodynamically evaluated. Each lithium silicate that presented a higher CO_2 capture capacity at higher turnover temperatures and heats of reaction, required higher energy inputs for decarbonation processes. Moreover, from a kinetic point of view, this analysis corroborated that there are two different CO_2 sorption steps, which are the superficial reaction step and the diffusion step.

Similar theoretical analyses have been performed by the same research group for lithium zirconates (Li_8ZrO_6, $Li_6Zr_2O_7$, Li_2ZrO_3) and alkaline zirconate solid-solutions ($Na_{2-x}M_xZrO_3$ (M = Li, K)).[182] In the alkaline zirconate solid solution systems, it was found out that CO_2 sorption temperatures of $Na_{2-x}M_xZrO_3$, varied as a function of Li- or K-content, having lower turnover temperatures and higher CO_2 sorption capacities, in comparison to pristine Na_2ZrO_3. In fact, Li-containing samples presented the largest turnover temperatures. For lithium zirconates, it was determined from thermodynamic calculations that Li_8ZrO_6 has a carbonation-decarbonation turnover temperature at T > 830 °C, while other lithium zirconates (with lower Li/Zr molar ratios) have lower turnover temperatures. In addition, this analysis showed that Li_8ZrO_6 has importantly higher energy requirements than Li_2ZrO_3, decreasing its practical use, although Li_8ZrO_6 has 4 times more lithium. Based on these results obtained for different lithium-based zirconates, it was suggested that mixing or doping

these materials, it would be possible to produce new CO_2 ceramics for optimal performance at industrial levels.

As it was already mentioned, with the progress of CO_2 sorption on the surface of materials, the reaction becomes to be diffusion controlled due to the formation of an external shell. To improve the thermodynamic properties, Pfeiffer et al.[155] proposed to add certain amount of O_2 into the reaction system of Li_2ZrO_3. The results indicated adding certain amount of O_2 could facilitate CO_2 sorption if the whole process is kinetically diffusion controlled. Adding oxygen into gas flow may reduce the thermal dependency of CO_2 sorption on K-Li_2ZrO_3. Similar work has been performed with Li_5AlO_4, Li_2CuO_2 and Li_5FeO_4.[167, 170, 177]

Similar to the thermodynamic oxygen addition effect, different studies have shown that water vapor addition ($H_2O_{(v)}$) modified the CO_2 sorption process on lithium ceramics (Li_2SiO_3, Li_4SiO_4, Li_2CuO_2, Li_2ZrO_3 and Li_5AlO_4), mainly at low temperatures (T < 100 °C).[128, 183-186] All these studies show that $H_2O_{(v)}$ becomes an active intermediate specie during the CO_2 sorption, as it is represented in reaction (16), where Li_2CuO_2 is used as a lithium ceramic example. All those papers showed that hydroxylation (step 1 of reaction (16)) and subsequent carbonation (step 2 of reaction (16)) processes always have importantly lower formation enthalpy ($\Delta H^{\ddagger}$) values than direct carbonation process produced in H_2O absence. Thus, $H_2O_{(v)}$ reduces the energy requirements for the whole reaction process. Moreover, all these reaction have negative Gibbs free energy values, corroborating the thermodynamic stability of these reaction mechanisms.

$$Li_2CuO_2 \xrightarrow{H_2O} 2LiOH + CuO \xrightarrow{CO_2} Li_2CO_3 + H_2O \quad (16)$$

6. Applications of lithium containing ceramics based CO_2 sorbents

In recent years, post-combustion CO_2 capture at high temperatures based on regenerable sorbent materials has received great attention as an alternative to low-temperature CO_2 adsorption and conventional chemical absorption solvent systems. The use of high temperature solid looping systems involves the reversible reaction of the bulk of the solid material with CO_2 and they provide both high CO_2 sorption capacity and selectivity. Also, in contrast with other low-temperature capture options where the temperature needs to be low (< 100°C) to favor absorption and/or ensure material integrity, CO_2 capture at elevated temperature avoids the need to cool or quench combustion gases. As it was already described, lithium-based ceramics present interesting properties as CO_2 capture materials, as in many cases they have lower energy requirements for regeneration in comparison to other materials such as calcium looping process.[187]

On the other hand, the integration of solid CO_2 capturing materials into sorption-enhanced hydrogen production (SEHP) processes can increase methane/alcohol conversion and capture CO_2 simultaneously.[25-27, 29, 188-192] The desired sorbents should not only maintain large reversible CO_2 uptake and excellent stability, but also keep good mechanical properties.[191, 192] Lithium containing ceramics as one kind of high temperature CO_2 sorbents, possess many advantages such as high CO_2 sorption capacity and fast sorption kinetics.[191] Recently, many studies dealing with the combination of lithium containing ceramics based sorbents with some hydrogen production processes were reported, for example, sorption enhanced methane steam reforming and sorption enhanced alcohol reforming. In addition, the lithium containing ceramics have also been studied in the CO oxidation coupled with

subsequent CO_2 chemisorption process. Thus, in the following section, the applications of lithium containing ceramics in four processes will be reviewed, including (1) high-temperature post-combustion CO_2 capture from stationary flue gases, (2) sorption enhanced methane steam reforming, (3) sorption enhanced alcohol reforming, and (4) CO oxidation coupled with subsequent CO_2 chemisorption process.

6.1. High-temperature post-combustion CO_2 capture from stationary flue gases

For post-combustion CO_2 capture at high temperatures, in addition to the CO_2 capture capacity and cyclic stability, industrial processes also require sorbent materials maintain good performance when facing various impurities in flue gases. For instance, a typical gas composition of coal-fired power plant flue gas contains 10–15% CO_2, 3–4% O_2, 5–7% H_2O, 0.05–0.3 vol% SO_2, and 0.015–0.05 vol% of NO_x, and some trace amount of HCl, As, Hg, etc. These impurities may lead to significant impact on reversible CO_2 uptake.[193] Therefore, the effect of the major impurities such as SO_2, NO_x, H_2O, and CO_2 concentration on the performance of lithium-containing ceramics should be concerned.

Pacciani et al.[193] evaluated the influence of SO_2 on the capture performance of Li_4SiO_4 by cyclic exposure to gas mixtures containing different amount of SO_2, as shown in Figure 37. For the SO_2-free case (sorption/desorption at 550 ^oC, sorption in 15 vol.% CO_2 and 10 vol.% H_2O in N_2), the CO_2 uptake almost did not change and kept at 22.7 wt% during 10 cycles. However, after adding 0.002 vol% SO_2, the CO_2 uptake decreased from 22.8 to 21.4 wt% after 25 cycles. With higher SO_2 concentrations, more obvious declines in CO_2 uptake were seen. With 0.03 vol% and 0.95 vol% SO_2, the CO_2 uptake decreased to 16.2 and 1.4 wt%, respectively after several cycles. Such

influence was attributed to the irreversible reaction between Li_4SiO_4 and SO_2. Similar phenomenon was also observed by Puccini et al.[194] After being exposed to a gas containing 2000 ppm SO_2 for 2 h, the SO_2-loaded sorbent could not be regenerated even at 700 °C. This results further confirmed that the SO_2 poisoning effect is irreversible. Thus, for industrial applications, SO_2 has to be removed before performing CO_2 capture. In addition to Li_4SiO_4, it was found that other lithium-containing sorbents also suffers from SO_2 poisoning. In addition to SO_2, the influence of NO_x has also been studied. CO_2 sorption capacity (21 wt%) did not change with 0–1000 ppm NO concentration. Therefore, it was concluded that the Li_4SiO_4-based sorbent is inert with respect to NO.[194]

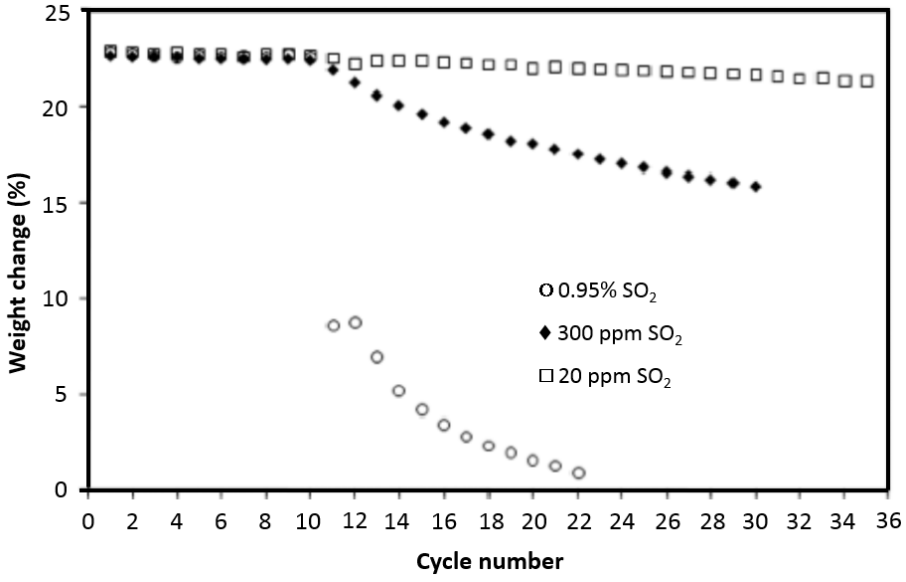


Figure 37. Sorbent weight change over cycles of sorption and desorption at 550 °C and 1 atm, sorption in 15 vol% CO_2 and 10 vol% H_2O in N_2 (1–10 cycles) or in 15 vol% CO_2, 10 vol% H_2O and 0.002 vol% SO_2 in N_2 (□), 0.03 vol% SO_2 in N_2 (♦) and 0.95 vol% SO_2 in N_2 (○), and desorption in 25 vol%H_2O in N_2.[193] Reprinted with permission from ref 193. Copyright 2011 American Chemical Society.

Since water vapor is always present in different flue gases, its influence on the capture and regeneration properties and stability of lithium-containing ceramics have also been investigated. Ochoa-Fernández et al.[195] demonstrated the presence of water steam can enhanced the CO_2 sorption and desorption rates over Li_4SiO_4. However, the CO_2 uptake decreased significantly comparing to value in dry condition. It was suggested that steam can improve the mobility of Li^+, which enhances the sorption ability of sorbents. The decrease in capacity was attributed to the sintering under high pressure of steam, vaporization of alkali metals, and/or phase segregation.

Similar results were also observed by Quinn et al.[196] Figure 38 compares the CO_2 capture capacity of Li_4SiO_4 sphere (5 mm in diameter) under dry and wet (10% water vapor) conditions at 550 °C. The breakthrough capacity in the presence of water (4.18 mmol/g) was about 4 times greater than that in its absence (0.90 mmol/g). Similarly, Li_4SiO_4 sphere (2 mm in diameter) also exhibited larger breakthrough capacity (6.77 mmol/g) under wet condition (10% water vapor) than that (4.45 mmol/g) under dry condition.

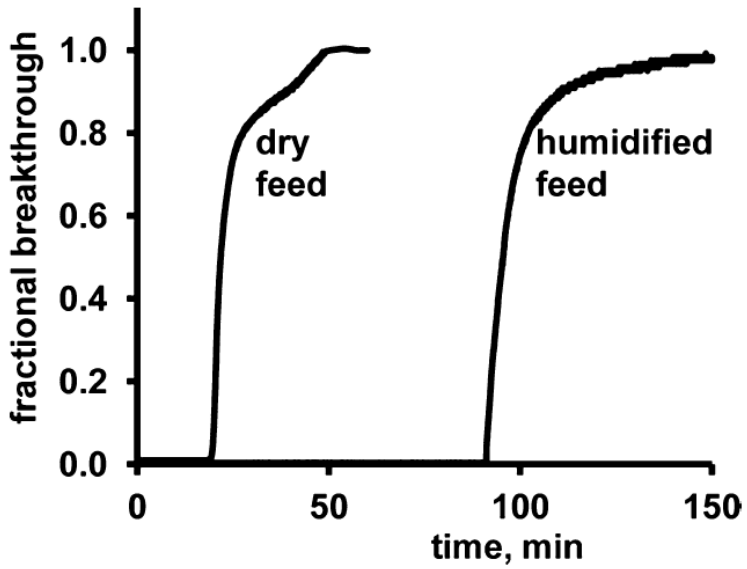


Figure 38. Breakthrough curves for Li_4SiO_4 sphere (5 mm in diameter) at 550 °C. Feed:

14.7% CO_2 dry or humidified to 10% H_2O as indicated.[196] Reprinted with permission from ref 196. Copyright 2012 American Chemical Society.

For the practical utilization of sorbents for the post-combustion CO_2 capture from stationary flue gases, several schemes have been proposed. For the fixed bed temperature swing process, the scale is so big that it is not practical for a 500 MW coal-fired power plant. Quinn et al.[196] proposed another three potential technologies, including sorbent wheel, moving bed, and rapid thermal swing chemisorption processes. For the sorbent wheel process, the wheel containing a CO_2 sorbent rotates between a sorption zone and a desorption zone alternatively, by which a shorter cycle time and a lower quantity of sorbent are required. For the moving bed process, the sorbent circulates between sorption and regeneration vessels, which is analogous to the liquid absorption process. For the rapid thermal swing chemisorption process, shell and tube type vessels were utilized to minimize heating and cooling times.

Up to now there is only one work describing thermodynamic assessments of these sorbents in power plants, which was published by Garcia et al.[187] Authors presented a simulation analysis of a thermal integration study of a post-combustion CO_2 capture plant using Li_4SiO_4 sorbents into a natural gas combined cycle (NGCC) plant, proposing a Li_4SiO_4/Li_2CO_3 looping cycle downstream of the gas turbine in a NGCC plant (829 MW base-load state-of-the-art). In fact, this possible technology was compared with two other well-known solvents, such as mono-ethanol amine (MEA) and a second generation solvent (CESAR-1). The integration of CO_2 post-combustion capture in the power plant resulted in a decrease of its net electric efficiency. However, capture with Li_4SiO_4 sorbents decreased the efficiency around 6.9 %, which is a lower

value than those presented by MEA (8.4 %) and CESAR-1 (7.5 %) solvents. Based on this initial result, the Li_4SiO_4/Li_2CO_3 looping system seems to be a promising alternative to amine solvents in the NGCC plants. Furthermore, additional improvements would be achieved through the use of different lithium-based ceramics, as all the previously materials proposed in this review.

6.2. Sorption enhanced methane steam reforming

Methane steam reforming consists of a steam-reforming reaction and a water gas shift reaction.[191] In order to reduce energy consumption, improve the hydrogen production rate and hydrogen purity, the concept of sorption enhanced methane steam reforming process was proposed. By utilizing a solid CO_2-sorbent, the normal thermodynamic limitation of steam methane reforming can be changed, which leads to the low operation temperatures (450 to 650 °C) and high H_2 yield of this technology.[25, 26] Figure 39 shows the schematic drawing of the sorption enhanced methane steam reforming process, and the overall reaction is shown in equation (16).

$$CH_4\,(g) + 2H_2O\,(g) + \text{sorbent}\,(s) \leftrightarrow \text{sorbent-}CO_2\,(s) + 4H_2\,(g) \qquad (16)$$

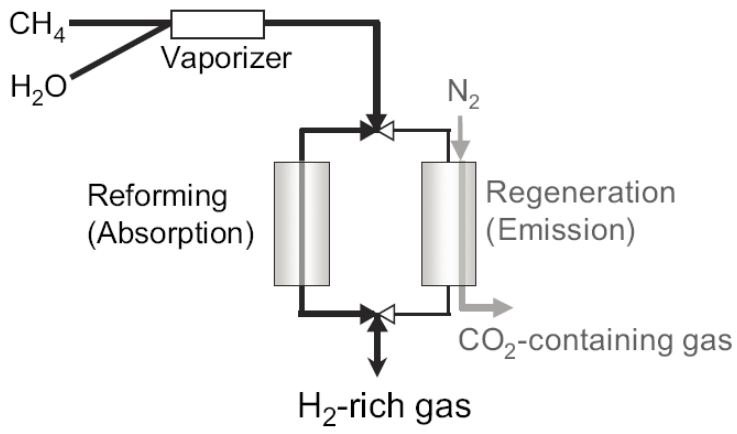


Figure 39. Schematic drawing of the sorption enhanced methane steam reforming process.[188] Reprinted with permission from ref 188. Copyright 2008 Elsevier Ltd.

In 2005, Hagiwara et al.[26] first proposed the pre-combustion CO_2 capture system by combining the methane steam reforming and Li_4SiO_4. The feasibility of the pre-combustion capture system was evaluated by measuring the CO_2 removal efficiency and methane conversion. At temperature lower than 650 ^oC, the methane conversion with both catalyst and sorbent was higher than that with catalyst alone. In addition, the CO_2 removal rate was close to 90%, demonstrating the high feasibility of this system. Essaki et al.[188] also investigated the relationship between CO_2 sorption and the equilibrium-shift effect in overall reactions. The results indicated temperature significantly affected the equilibrium-shift. The H_2 concentration was increased and reached 89.4 vol% at 500 °C, and 93.6 vol% at 550 °C, whereas by the conventional method, the H_2 concentration was only 65 vol% at both temperatures. The CH_4 conversion also greatly increased (around 30 %) at 550 °C due to the equilibrium-shift effect, with a very low CO concentration of below 0.2 vol%. In addition to neat Li_4SiO_4, the performance of K_2CO_3-doped Li_4SiO_4 in the sorption enhanced methane steaming reforming process had also been evaluated. Zhang et al.[191] demonstrated that K_2CO_3-doped Li_4SiO_4 sorbent can greatly promote the methane steaming reforming process, yielding high-purity H_2 at lower temperatures (500–550 ^oC).

The use of Li_2ZrO_3 as high temperature CO_2 sorbent in the sorption enhanced methane steam reforming process was also investigated.[197] Chen et al.[131] studied the kinetics of CO_2 sorption on Li_2ZrO_3 in an oscillating microbalance. The process is capable of directly producing H_2 with concentrations larger than 95 mol% with methane as the main side product with less than 0.2 mol% of CO. After sorbent saturation, the conversion of methane follows the thermodynamics and kinetics of a

conventional steam reforming process. Lithium zirconate has been demonstrated to be an appropriate CO_2 sorbent with high sorption capacity. However, in order to further improve the operating capacity of the process, the sorption properties of Li_2ZrO_3 at low CO_2 concentrations have to be improved.

Schouten et al.[198] compared the performance of Li_2ZrO_3 and K-promoted hydrotalcite for the low-temperature sorption enhanced methane steaming reforming system by a fundamental model-based analysis. With the hydrotalcite-based system, 98% CH_4 conversion with 99.8% H_2 and <250 ppm CO_2 contamination was achieved. While the Li_2ZrO_3-based system provided 99.9% CH_4 conversion and 99.9% H_2 purity under the identical condition. They also pointed out that the CO_2 sorption kinetics of Li_2ZrO_3 should be further improved, for instance, by modifying the structure of Li_2ZrO_3 to suppress any diffusional limitations.

Recently, there are quite a few studies on the comparison of Li_4SiO_4, Li_2ZrO_3 and some other high-temperature CO_2 sorbents for the sorption enhanced methane steam reforming.[192] Rusten et al.[25] compared the performance of sorption enhanced methane steam reforming with two CO_2 sorbents (Li_2ZrO_3 and Li_4SiO_4) using two reactor technologies (fluidized-bed reactor and fixed bed reactor). The results showed that Li_4SiO_4 possessed faster kinetics than Li_2ZrO_3, which led to higher production capacity. Furthermore, the fixed-bed technology led to achieve a higher conversion with respect to the fluidized-bed reactor. Zhang et al.[29] compared four kinds of CO_2 sorbents (CaO, HTC, Li_2ZrO_3 and Li_4SiO_4) performances in catalytic methane reforming process. At 550 °C and under 0.1 MPa, a 94% H_2 purity was obtained with Li_4SiO_4, CaO, and HTC as CO_2 sorbents. At 550 °C, increasing the working pressure could promote the CO_2 capture performance of Li_4SiO_4. Chen et al.[25] compared the performance of

Li_2ZrO_3, K-doped Li_2ZrO_3, Na_2ZrO_3, Li_4SiO_4, and CaO in terms of thermodynamics, kinetics and stability. They concluded that the sorbents that captures CO_2 well at low partial pressures can lead to higher H_2 yields and efficiencies. Under their tested conditions, CaO resulted the highest efficiency due to its more favourable thermodynamics and fast reaction rates. But the cycling stability of CaO during multiple cycles needs to be enhanced. On the other hand, Na_2ZrO_3 was demonstrated to be a potential sorbent thanks for its high sorption kinetics and excellent stability.

6.3. Sorption enhanced alcohol reforming

Ethanol is another biomass-derived fuel and raw material that is suitable for hydrogen production. Sorption enhanced ethanol steam reforming reaction systems have also been well studied. Essaki et al.[199] demonstrated that Li_4SiO_4 sorbent can greatly improve the efficiency and purity of hydrogen in the sorption enhanced ethanol steam reforming process. The results in the case of using a mixture of catalyst and absorbent were compared with the case of using a catalyst alone, from which the increase of H_2 yield by the equilibrium-shift effect caused by using Li_4SiO_4 was clearly observed. At 577 and 627 °C, a very high H_2 yield close to the stoichiometric limit was obtained and the value was kept for 0.5 h. Figure 40 shows the effect of equilibrium-shift on gas composition at around 0.5 h after the start of reforming reaction. The results in the case of using a mixture of catalyst and absorbent were compared with those in the case of using catalyst alone. At 577 and 627 °C, high H_2 concentrations were obtained in the case of using the mixture, which reached 99.3 dry vol% and 99.5 dry vol%, respectively. This is resulted from the equilibrium-shift effect by the existence of CO_2 sorbent. With Li_4SiO_4 sorbent, the CO_2 concentration (0.1 dry vol%) was much lower than that using a catalyst alone (0.22 dry vol%). Owing to the removal of CO_2, the CO

concentration in the case of using the mixture was also significantly reduced to a much lower value, 0.14 dry vol%, 0.11 dry vol%, and 0.19 dry vol% at 527, 577, and 627 ^{o}C, respectively. By considering both H_2 and CO concentrations, 577 ^{o}C was determined to be the most suitable temperature. At this temperature, H_2 concentration was 99.3 dry vol% and CO concentration was 0.11 dry vol% at 0.5 h after the start of reforming reaction. All those data clearly demonstrated that Li_4SiO_4 is also a very efficient high-temperature CO_2 sorbent for the sorption enhanced ethanol reforming reaction system.

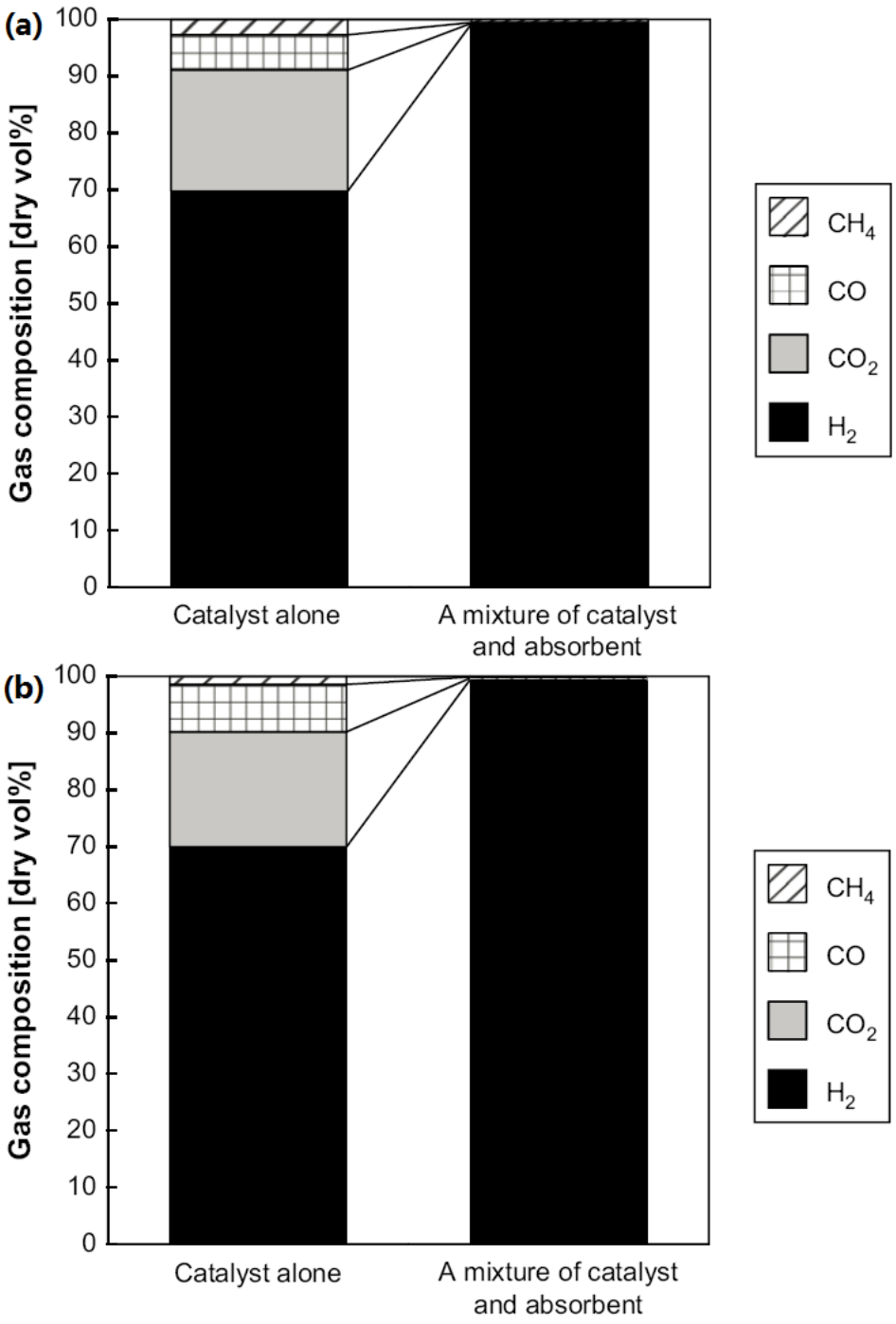


Figure 40. Effect of equilibrium-shift on gas composition (a) 577 °C, and (b) 627 °C.[199] Reprinted with permission from ref 199. Copyright 2008 International Association for Hydrogen Energy and Elsevier Ltd.

Lisbona et al.[192, 200] performed an energy assessment of sorption enhanced

ethanol steam reforming reaction by using Li_4SiO_4 sorbent. In their work, a fixed bed model was defined by Jander's equation compared with experimental data for the sorption enhanced ethanol steam reforming reaction system. The influences of the operating temperature, ethanol to water ratio, and gas inlet rate were analyzed and discussed. From the discussion above, temperature of 602 ^oC, axial velocity of 0.2 m/s, and ethanol to water ratio of 1:6 were determined as the optimal condition for H_2 production with the reformer studied, with highly pure H_2 and relatively lower energy consumption comparing to the conventional system without Li_4SiO_4 sorbent.

The "sorption-enhanced" principal can also be utilized in the glycerol steam reforming process to improve the thermodynamics. Wang et al.[201] investigated the sorption enhanced glycerol steam reforming for hydrogen production by adding K-doped Li_2ZrO_3 based CO_2 sorbent. For the first run, the CO_2 removal rate was very high and the process produced highly purified H_2 (99.59%). However, the performance of K−Li_2ZrO_3 sorbent deteriorated during multicycles due to sorbent deactivation, with a continuous decrease in H_2 purity and CO_2 removal rate. Therefore, it is very critical to improve the cycling stability of the lithium zirconate based CO_2 sorbent for the sorption enhanced reforming process of glycerol.

6.4. CO oxidation coupled with subsequent CO_2 chemisorption process

In order to increase the purity of H_2 and decrease the CO concentration of reformed fuels, catalytic oxidation coupled with subsequent CO_2 sorption has been proposed.[202, 203] Recently, lithium containing ceramics such as Li_2ZrO_3,[204] Li_2CuO_2,[205] Li_5FeO_4, and $LiFeO_2$[59] have been studied as bi-functional materials, catalysts for CO oxidation and sorbent for the subsequent produced CO_2. In the following section, the progress of the use of lithium containing ceramics in the CO oxidation coupled with subsequent CO_2

chemisorption process will be reviewed.

Alcántar-Vázquez et al.[204] compared Li_2ZrO_3 and Na_2ZrO_3 as bi-functional materials for the CO oxidation coupled with subsequent CO_2 sorption processes. The result indicated Na_2ZrO_3 possesses better CO oxidation performance conditions than Li_2ZrO_3. However, both Li_2ZrO_3 and Na_2ZrO_3 can only trap part of produced CO_2, which may due to the low CO_2 concentration. The results obtained in this work were also confirmed by different theoretical thermodynamic calculations.

Lara-García et al.[205] evaluated Li_2CuO_2 as a bi-functional material for the CO oxidation coupled with subsequent CO_2 chemisorption process. The results indicated that Li_2CuO_2 can catalyze CO oxidation in a wide temperature range with or without O_2. With O_2, Li_2CuO_2 transformed to Li_2CO_3 and CuO. While without O_2, metallic Cu rather than CuO was produced. The same research group[59] also studied Li_5FeO_4 and $LiFeO_2$ for the same process. They revealed that Li_5FeO_4 possesses better CO_2 sorption performance than $LiFeO_2$ under different conditions.[59] Among all studied sorbents, Li_5FeO_4 and Li_2CuO_2 were found to possess better performance as bifunctional materials than Li_2ZrO_3, Na_2ZrO_3 and $NaCoO_2$ for the CO oxidation coupled with subsequent CO_2 chemisorption process.[59, 205]

7. Current challenges and future prospects

So far, although great progresses have been made in the field of lithium-containing ceramic sorbents for CO_2 capture, there are still some challenges for their large-scale practical applications. In previous studies, researchers have mainly focused on how to improve the CO_2 sorption capacity. However, we believe that cycling stability and reversible CO_2 uptake are much more important than the initial CO_2 capture

capacity.[80] For this purpose, future work should either develop some new capturing materials or improving the capture-regeneration property of the existing materials. One solution might be the preparation of composite type sorbents with inert phases working as separating/supporting materials. Recently, Wang et al.[124] synthesized Li_4SiO_4-based CO_2 sorbent from vermiculite mineral with enhanced reversible capacity. The optimized sorbent Li_4SiO_4-(EXVMT)-4 resulted excellent cycling stability and enhanced CO_2 capture performance under low CO_2 concentrations and lower temperature. The improved performance was ascribed to the separating effect of impurity phases that may prevent Li_4SiO_4 sintering.

Comparing to CaO, the cost of lithium-containing ceramic sorbents is another concern. Therefore, we suggest that future work should try to use cheap raw materials such as cheap Si resource from industrial solid wastes or minerals, or Li resource from lithium battery wastes, etc. Future work should also focus on the structural modifications of pellets-type sorbents in order to guarantee strong mechanical property for anti-attrition, proper porosity for mass diffusion, and excellent thermal stability for anti-sintering.[206] The volume expansion/shrink of the pellets, and the heat absorption/release during the carbonation and de-carbonation processes should also be concerned, which may affect the mechanical and thermal stability of sorbents.

With good sorbents, another big issue is how to integrate these materials into a process. As we discussed above, for high-temperature post-combustion CO_2 capture from stationary flue gases, three schemes have been proposed, including sorbent wheel process, moving bed process, and rapid thermal swing chemisorption process. We believe that more studies are highly demanded as their operations in the required high-temperature range still remain a significant technical challenge. While for the

pre-combustion CO_2 capture processes, the sorbents can be either mixed with catalyst within the same catalytic reactor or placed in a separate sorption reactor downstream the catalytic reactor. After saturation, the saturated sorbents can be regenerated by either pressure swing adsorption or temperature swing adsorption processes. More studies are highly demanded on the optimization of operating parameters and techno-economic evaluations of all these different processes.[207] In addition, the influences of impurities such as SO_2, NO_x, and water vapor on the CO_2 sorption capacity and long-term stability should also be investigated in future.[194]

8. Conclusion

In this paper, the most recent research progresses of lithium containing ceramics based sorbents including lithium silicates, zirconates, titanates, aluminates, ferrites, cuprates, bismuthates, and borates for high-temperature CO_2 capture were thoroughly reviewed. For the mostly well-studied Li_4SiO_4 and Li_2ZrO_3, these two samples exhibit similar CO_2 sorption property, and both sorption processes follow the double shell model. Many different synthesis methods were utilized to further improve the CO_2 sorption capacity of neat Li_4SiO_4 and Li_2ZrO_3. Moreover, these two samples all have bad sorption capacity at low temperature and CO_2 concentrations. In order to solve this problem, similar schemes were utilized for enhanced performance, which include doping some molten salts into samples or formation of solid solutions by elemental substitution. Except for Li_4SiO_4 and Li_2ZrO_3, some other high lithium silicates and zirconates exhibited even much higher CO_2 uptakes, but with much worse cycling stability. Recently, many other lithium containing compounds including Li_4TiO_4, Li_2TiO_3, Li_5AlO_4, Li_5FeO_4, α-$LiFeO_2$, Li_2CuO_2, Li_7BiO_6, Li_5BiO_5, Li_3BiO_4, $LiBiO_2$, and α-$LiBO_2$ were

also studied for capturing CO_2 at high temperatures. Although these new sorbent also demonstrated good CO_2 capture capacity, their cycling stability under specific operational conditions such as the presence of oxygen, water vapor and other gaseous species in the operational atmosphere has to be improved for their practical applications. The lithium containing ceramics have also been demonstrated to be promising in four processes, including (1) high-temperature post-combustion CO_2 capture from stationary flue gases, (2) sorption enhanced methane steam reforming, (3) sorption enhanced alcohol reforming, and (4) CO oxidation coupled with subsequent CO_2 chemisorption process. Although the conversion of the catalytic reactions can be improved and produced CO_2 can be captured, the CO_2 capturing performance becomes worse with cycles for most of the sorbents. Thus, we believe that future research will mainly focus on improving the cycling stability of these lithium containing ceramics based CO_2 sorbents.

Acknowledgments

This work was supported by the National Natural Science Foundation of China (51572029, U1810209, 51622801), the Beijing Natural Science Foundation (2184114), and the Cai Yuanpei Grant.

References

1. K. L. Seip and Ø. Grøn, *Theor. Appl. Climatol.*, 2015, **127**, 923–938.
2. Y. Li, M. Su, X. Xie, S. Wu and C. Liu, *Appl. Energ.*, 2015, **145**, 60-68.
3. E. S. Sanz-Perez, C. R. Murdock, S. A. Didas and C. W. Jones, *Chem. Rev.*, 2016, **116**, 11840-11876.
4. A. Alvarez, A. Bansode, A. Urakawa, A. V. Bavykina, T. A. Wezendonk, M. Makkee, J. Gascon and F. Kapteijn, *Chem. Rev.*, 2017, **177**, 9804-9838.
5. S. T. Henriques and K. J. Borowiecki, *Energ. Policy*, 2017, **101**, 537-549.

6. H. Xu, W. Cheng, X. Jin, G. Wang, H. Lu, H. Wang, D. Chen, B. Fan, T. Hou and R. Zhang, *Ind. Eng. Chem. Res.*, 2013, **52**, 1886-1891.
7. X. Zhao, H. Zhou, V. S. Sikarwar, M. Zhao, A.-H. A. Park, P. S. Fennell, L. Shen and L.-S. Fan, *Energy Environ. Sci.*, 2017, **10**, 1885-1910.
8. D. J. Heldebrant, P. K. Koech, V. A. Glezakou, R. Rousseau, D. Malhotra and D. C. Cantu, *Chem. Rev.*, 2017, **117**, 9594-9624.
9. M. Pera-Titus, *Chem. Rev.*, 2014, **114**, 1413-1492.
10. S. Zeng, X. Zhang, L. Bai, X. Zhang, H. Wang, J. Wang, D. Bao, M. Li, X. Liu and S. Zhang, *Chem. Rev.*, 2017, **117**, 9625-9673.
11. X. Yang, R. J. Rees, W. Conway, G. Puxty, Q. Yang and D. A. Winkler, *Chem. Rev.*, 2017, **117**, 9524-9593.
12. A. Brunetti, F. Scura, G. Barbieri and E. Drioli, *Journal of Membrane Science*, 2010, **359**, 115-125.
13. C. A. Scholes, K. H. Smith, S. E. Kentish and G. W. Stevens, *International Journal of Greenhouse Gas Control*, 2010, **4**, 739-755.
14. Y. Huang, T. C. Merkel and R. W. Baker, *Journal of Membrane Science*, 2014, **463**, 33-40.
15. J. Y. Wang, L. Huang, R. Y. Yang, Z. Zhang, J. W. Wu, Y. S. Gao, Q. Wang, D. O'Hare and Z. Y. Zhong, *Energy. Environ. Sci.*, 2014, **7**, 3478-3518.
16. Q. Wang, J. Luo, Z. Zhong and A. Borgna, *Energy Environ. Sci.*, 2011, **4**, 42-55.
17. C. Chen, S. Zhang, K. H. Row and W. S. Ahn, *J. Energy Chem.*, 2017, **26**, 868-880.
18. Q. Wang, H. H. Tay, D. J. Ng, L. Chen, Y. Liu, J. Chang, Z. Zhong, J. Luo and A. Borgna, *ChemSusChem*, 2010, **3**, 965-973.
19. Y. Qiao, J. Wang, Y. Zhang, W. Gao, T. Harada, L. Huang, T. A. Hatton and Q. Wang, *Ind. End. Chem. Res.*, 2017, **56**, 1509-1517.
20. Q. W. Zheng, L. Huang, Y. Zhang, J. Y. Wang, C. Z. Zhao, Q. Zhang, W. J. Zheng, D. P. Cao, D. O'Hared and Q. Wang, *J Mater Chem A*, 2016, **4**, 12889-12896.
21. Q. Qin, J. Wang, T. Zhou, Q. Zheng, L. Huang, Y. Zhang, P. Lu, A. Umar, B. Louis and Q. Wang, *J. Energy Chem.*, 2017, **26**, 346-353.
22. J. Udomsirichakorn, P. Basu, P. A. Salam and B. Acharya, *Int. J. Hydrogen Energ.*, 2013, **38**, 14495-14504.
23. K. Wang, X. Guo, P. Zhao, F. Wang and C. Zheng, *J. Hazard. Mater.*, 2011, **189**, 301-307.
24. Q. Wang, H. H. Tay, L. Chen, Y. Liu, J. Chang, Z. Zhong, J. Luo and A. Borgna, *J. Nanoeng. Nanomanuf.*, 2011, **1**, 298-303.
25. H. K. Rusten, Ochoa-Fernandez E., Lindborg H., Chen D. and Jakobsen H. A., *Ind. Eng. Chem. Res.*, 2007, **46**, 8729-8737.
26. M. Kato, K. Nakagawa, K. Essaki, Y. Maezawa, S. Takeda, R. Kogo and Y. Hagiwara, *Int. J. Appl. Ceram. Technol.*, 2005, **2**, 467-475.
27. L. Barelli, G. Bidini, F. Gallorini and S. Servili, *Energy*, 2008, **33**, 554-570.
28. M. E. Bretado, M. D. D. Vigil, V. H. C. Martinez and A. L. Ortiz, *Int J Chem React Eng*, 2008, **6**, 77-90.
29. Y. Chen, Y. Zhao, J. Zhang and C. Zheng, *Sci. China Technol. Sc.*, 2011, **54**, 2999-3008.
30. K. Kim, D. Kim, Y. K. Park and K. S. Lee, *Int. J. Greenh. Gas Con.*, 2014, **26**, 135-146.
31. M. Kato, K. Nakagawa, K. Essaki, Y. Maezawa, S. Takeda, R. Kogo and Y. Hagiwara, *Int. J. Appl. Ceram. Technol.*, 2005, **2**, 467-475.

32. J. Ida, R. Xiong and Y. S. Lin, *Sep. Purif. Technol.*, 2004, **36**, 41-51.
33. J. Ortiz-Landeros, I. C. Romero-Ibarra, C. Gómez-Yáñez, E. Lima and H. Pfeiffer, *J. Phys. Chem. C*, 2013, **117**, 6303-6311.
34. Y. Matsukura, T. Okumura, R. Kobayashi and K. Oh-ishi, *Chem. Lett.*, 2010, **39**, 966-967.
35. H. Kim, H. D. Jang and M. Choi, *Chem. Eng. J.*, 2015, **280**, 132-137.
36. Q. Zhang, D. Han, Y. Liu, Q. Ye and Z. Zhu, *Aiche J.*, 2013, **59**, 901-911.
37. M. J. Venegas, E. Fregoso-Israel, R. Escamilla and H. Pfeiffer, *J. Ind. Eng. Chem.*, 2007, **46**, 2407-2412.
38. A. López Ortiz, M. A. Escobedo Bretado, V. Guzmán Velderrain, M. Meléndez Zaragoza, J. Salinas Gutiérrez, D. Lardizabal Gutiérrez and V. Collins-Martínez, *Int. J. Hydrogen Energ.*, 2014, **39**, 16656-16666.
39. Y. Duan and K. Parlinski, *Phys. Rev. B*, 2011, **84**, 3382-3391.
40. K. Oh-Ishi, R. Kobayashi and K. Oka, *J. Ceram. Soc. Jpn.*, 2017, **125**, 383-386.
41. Y. Duan, H. Pfeiffer, B. Li, I. C. Romero-Ibarra, D. C. Sorescu, D. R. Luebke and J. W. Halley, *Phys. Chem. Chem. Phys.*, 2013, **15**, 13538-13558.
42. M. R. Quddus, M. B. I. Chowdhury and H. I. de Lasasol, *Chem. Eng. J.*, 2013, **232**, 139-148.
43. Q. Wang, H. H. Tay, Z. Y. Zhong, J. Z. Luo and A. Borgna, *Energy. Environ. Sci.*, 2012, **5**, 7526-7530.
44. J. Ortiz-Landeros, T. L. Ávalos-Rendón, C. Gómez-Yáñez and H. Pfeiffer, *J. Therm. Anal. Calorim.*, 2011, **108**, 647-655.
45. M. R. Quddus, M. B. I. Chowdhury and H. I. de Lasasol, *Chem. Eng. J.*, 2015, **260**, 347-356.
46. R. Xiong, J. Ida and Y. S. Lin, *Chem. Eng. Sci.*, 2003, **58**, 4377-4385.
47. R. Rodríguez-Mosqueda and H. Pfeiffer, *J. Phys. Chem. A*, 2010, **114**, 4535–4541.
48. S. M. Amorima, M. D. Domenico, T. L. P. Dantas, H. J. José and R. F. P. M. Moreira, *Chem. Eng. J.*, 2016, **283**, 388-396.
49. S. Zhang, Q. Zhang, H. Wang, Y. Ni and Z. Zhu, *Int. J. Hydrogen Energ.*, 2014, **39**, 17913-17920.
50. H. Takasu, S. Funayama, N. Uchiyama, H. Hoshino, Y. Tamura and Y. Kato, *Ceram. Int.*, 2018, **44**, 11835-11839.
51. T. Tanaka, E. Tabata, T. Nakagaki, M. Mizunuma and Y. Y. Maruo, *J. Chem. Eng. Jpn.*, 2014, **47**, 561-568.
52. T. Tang, Z. Zhang, J. B. Meng and D. L. Luo, *Fusion Eng. Des.*, 2009, **84**, 2124-2130.
53. E. Carellan and M. T. Hernandez, *Ceram. Int.*, 2014, **40**, 9499-9508.
54. K. Wang, X. Wang, P. Zhao and X. Guo, *Chem. Eng. Technol.*, 2014, **37**, 1552-1558.
55. P. V. Subha, B. N. Nair, P. Hareesh, A. Peer Mohamed, T. Yamaguchi, K. G. K. Warriera and U. S. Hareesh, *J. Mater. Chem. A*, 2014, **2**, 12792–12798.
56. X. Yu, M. Yang, T. Lu, N. Wei, J. Wei, Y. Shi, Z. Huang, X. Xiang, Q. Zhang and W. Zhang, *J. Nucl. Mater.*, 2015, **456**, 455-460.
57. M. Escobedo Bretado, V. Guzmán Velderrain, D. Lardizábal Gutiérrez, V. Collins-Martínez and A. Lopez Ortiz, *Catal. Today*, 2005, **107-108**, 863-867.
58. H. Pfeiffer, P. Bosch and S. Bulbulian, *J. Nucl. Mater.*, 1998, **257**, 309-317.
59. H. A. Lara-García, E. Vera, J. A. Mendoza-Nieto, J. F. Gómez-García, Y. Duan and H. Pfeiffer, *Chem. Eng. J.*, 2017, **327**, 783-791.
60. T. Okumura, Y. Matsukura, K. Gotou and K. Oh-Ishi, *J. Ceram. Soc. Jpn.*, 2008, **116**, 1283-1288.
61. M. T. Izquierdo, A. Turan, S. García and M. M. Maroto-Valer, *J Mater Chem A*, 2018, **6**, 3249-

3257.
62. X. Wu, Z. Wen, X. Xu, X. Wang and J. Lin, *J. Nucl. Mater.*, 2009, **392**, 471-475.
63. Z. Yin, K. Wang, P. Zhao and X. Tang, *Ind. Eng. Chem. Res.*, 2016, **55**, 1142-1146.
64. K. Wang, W. Li, Z. Yin, Z. Zhou and P. Zhao, *Energ. Fuel*, 2017, **31**, 6257-6265.
65. I. C. Romero-Ibarra, J. Ortiz-Landeros and H. Pfeiffer, *Thermochim. Acta*, 2013, **567**, 118-124.
66. K. Wang, Z. Zhou, P. Zhao, Z. Yin, Z. Su and J. Sun, *Appl. Energ.*, 2016, **183**, 1418-1427.
67. Q. Zhang, D. Peng, S. Zhang, Q. Ye, Y. H. Wu and Y. Ni, *AIChE J.*, 2017, **63**, 2153-2164.
68. S. Kaniwa, M. Yoshino, E. Niwa, M. Yashima and T. Hashimoto, *Mater. Res. Bull.*, 2017, **94**, 134-139.
69. R. A. Varin, D. K. Mattar, A. S. Bidabadi and M. Polanski, *J. Energy Chem.*, 2017, **26**, 24-34.
70. K. Wang, Z. Yin and P. Zhao, *Ceram. Int.*, 2016, **42**, 2990-2999.
71. S. Shana, Q. Jiab, L. Jiang, Q. Li, Y. Wang and J. Peng, *Ceram. Int.*, 2013, **39**, 5437-5441.
72. X. Yang, W. Liu, J. Sun, Y. Hu, W. Wang, H. Chen, Y. Zhang, X. Li and M. Xu, *ChemSusChem*, 2016, **9**, 1607-1613.
73. S. Shan, S. Li, Q. Jia, L. Jiang, Y. Wang and J. Peng, *Ind. Eng. Chem. Res.*, 2013, **52**, 6941-6945.
74. A. Nambo, J. He, T. Q. Nguyen, V. Atla, T. L. Druffel and M. K. Sunkara, *Nano Lett.*, 2017, **17**, 3327-3333.
75. Y. Hu, W. Liu, Z. Zhou and Y. Yang, *Energ. Fuel*, 2017, **32**, 4521-4527.
76. G. J. Rao, R. Mazumder, S. Bhattacharyya and P. Chaudhuri, *J. Alloy. Compd.*, 2017, **725**, 461-471.
77. J. H. Lee, B. Moon, T. K. Kim, S. Jeoung and H. R. Moon, *Dalton T.*, 2015, **44**, 15130-15134.
78. Y. Pan, Y. Zhang, T. Zhou, B. Louis, D. O'Hare and Q. Wang, *Inorg. Chem.*, 2017, **56**, 7821–7834.
79. Y. Zhang, Y. Gao, B. Louis, Q. Wang and W. Lin, *Journal of Energy Chemistry*, 2018, DOI: 10.1016/j.jechem.2018.08.014.
80. M. Zhao, H. Fan, F. Yan, Y. Song, X. He, M. Z. Memon, S. K. Bhatia and G. Ji, *Dalton T.*, 2018, **47**, 9038-9050.
81. C. C. Chang, C. C. Wang and P. N. Kumta, *Mater. Design*, 2001, **22**, 617-623.
82. C. Gauer and W. Heschel, *J. Mater. Sci.*, 2006, **41**, 2405-2409.
83. V. L. Mejía-Trejo, E. Fregoso-Israel and H. Pfeiffer, *Chem. Mater.*, 2008, **20**, 7171-7176.
84. M. Xiang, Y. Zhang, H. Liu, C. Gu, M. Hong, S. Liu and Y. Zhang, *J. Mater. Sci.*, 2015, **50**, 4698-4706.
85. J. Ortiz-Landeros, C. Gómez-Yañez, L. M. Palacios-Romero, E. Lima and H. Pfeiffer, *J. Phys. Chem. A*, 2012, **116**, 3163-3171.
86. H. Pfeiffer, C. Vázquez, V. H. Lara and P. Bosch, *Chem. Mater.*, 2007, **19**, 922-926.
87. X. Guo, L. Ding, J. Ren and H. Yang, *J. Sol-Gel Sci. Techn.*, 2017, **81**, 844-849.
88. N. Gao, K. Ma, T. Ding, J. Cai, Y. Tian and X. Li, *Chinese Chem. Lett.*, 2017, **29**, 482-484.
89. J. Graetz, C. C. Ahn, R. Yazami and B. Fultz, *J. Electrochem. Soc.*, 2004, **151**, A698.
90. P. V. Subha, B. N. Nair, V. Visakh, C. R. Sreerenjini, A. P. Mohamed, K. G. K. Warrier, T. Yamaguchi and U. S. Hareesh, *J Mater Chem A*, 2018, **6**, 7913-7921.
91. M. Puccini, M. Seggiani and S. Vitolo, *Chem. Eng. Trans.*, 2013, **32**, 1279-1284.
92. M. Seggiani, M. Puccini and S. Vitolo, *Int J Greenh Gas Con*, 2013, **17**, 25-31.
93. M. Kato, K. Essaki, K. Nakagawa, Y. Suyama and K. Terasaka, *J. Ceram. Soc. Jpn.*, 2005, **113**, 252–254.
94. M. Seggiani, M. Puccini and S. Vitolo, *Int. J. Greenh. Gas. Con.*, 2011, **5**, 741-748.

95. G. Pannocchia, M. Puccini, M. Seggiani and S. Vitolo, *Ind. Eng. Chem. Res.*, 2007, **46**, 6696-6706.
96. T. Kodama, N. Gokon, S. Inuta, S. Yamashita and T. Seo, *J. Sol. Energy Eng.*, 2009, **131**, 041013.
97. X. Yang, W. Liu, J. Sun, Y. Hu, W. Wang, H. Chen, Y. Zhang, X. Li and M. Xu, *ChemSusChem*, 2016, **9**, 2480-2487.
98. M. Kato, S. Yoshikawa and K. Nakagawa, *J. Mater. Sci. Lett.*, 2002, **21**, 485-487.
99. S. Zhang, M. B. I. Chowdhury, Q. Zhang and H. I. de Lasa, *Ind. Eng. Chem. Res.*, 2016, **55**, 12524-12531.
100. S. Zhang, Q. Zhang, C. Shen, Y. H. Ni, Y. Q. Wu, Q. F. Wu and Z. B. Zhu, *Ind. Eng. Chem. Res.*, 2015, **54**, 7292-7300.
101. K. Wang, C. Wang, Z. Zhou, Z. Lin and P. Zhao, *Ind. Eng. Chem. Res.*, 2018, **57**, 8085-8092.
102. K. Wang, Z. Zhou, P. Zhao, Z. Yin, Z. Su and J. Sun, *Appl. Energ.*, 2017, **204**, 403-412.
103. P. V. Subha, N. N. Balagopal, P. Hareesh, A. P. Mohamed, T. Yamaguchi, K. G. K. Warrier and U. S. Hareesh, *J. Phys. Chem. C*, 2015, **119**, 5319-5326.
104. K. Wang, Z. Yin, P. Zhao, Z. Zhou, Z. Su and J. Sun, *Int. J. Hydrogen Energ.*, 2017, **42**, 4224-4232.
105. Z. Zhou, K. Wang, Z. Yin, P. Zhao, Z. Su and J. Sun, *Thermochim Acta*, 2017, **655**, 284-291.
106. L. Huang, Y. Zhang, W. Gao, T. Harada, Q. Zheng, A. Hatton and Q. Wang, *Energy Technol.*, 2017, **5**, 1-11.
107. X. Chen, Z. Xiong, Y. Qin, B. Gong, C. Tian, Y. Zhao, J. Zhang and C. Zheng, *Int. J. Hydrogen Energ.*, 2016, **41**, 13077-13085.
108. M. Wagemaker, A. P. M. Kentgens and F. M. Mulder, *Nature*, 2002, **418**, 397-399.
109. S. Weon and W. Choi, *Environ. Sci. Technol.*, 2016, **50**, 2556-2563.
110. Y. Tang, Y. Zhang, J. Deng, J. Wei, H. Le Tam, B. K. Chandran, Z. Dong, Z. Chen and X. Chen, *Adv. Mater.*, 2014, **26**, 6111-6118.
111. J. S. Lee and C. T. Yavuz, *Int. J. Hydrogen Energ.*, 2017, **56**, 3413-3417.
112. S. Jeoung, J. H. Lee, H. Y. Kim and H. R. Moon, *Thermochim Acta*, 2016, **637**, 31-37.
113. P. Puthiaraj and W. Ahn, *J. Energy Chem.*, 2017, **26**, 965-971.
114. M. Olivares-Marín, T. C. Drage and M. M. Maroto-Valer, *Int. J. Greenh. Gas Con.*, 2010, **4**, 623-629.
115. A. Sanna, I. Ramli and M. M. Maroto-Valer, *Appl. Energ.*, 2015, **156**, 197-206.
116. A. Choudhary, B. S. Sahu, R. Mazumder, S. Bhattacharyya and P. Chaudhuri, *J. Alloy. Compd.*, 2014, **590**, 440-445.
117. A. Choidhary, R. Mazumder, S. Bhattaryya and P. Chaudhuri, *Fusion. Sci. Technol.*, 2014, **65**, 273-281.
118. K. Wang, P. Zhao, X. Guo, D. Han and Y. Chao, *Environ. Prog. Sustain.*, 2015, **34**, 526-532.
119. M. Y. Niu, X. Y. Li, J. Ouyang and H. M. Yang, *Rsc Adv*, 2016, **6**, 44106-44112.
120. S. Shan, Q. Jia, L. Jiang, Q. Li, Y. Wang and J. Peng, *Chinese Sci. Bull.*, 2012, **57**, 2475-2479.
121. Y. Zhang, T. Zhou, B. Louis, F. Yu, J. Dan and Q. Wang, *Catalysts*, 2017, **7**, 105.
122. M. T. Izquierdo, V. Gasquet, E. Sansom, M. Ojeda, S. Garcia and M. M. Maroto-Valer, *Fuel*, 2018, **230**, 45-51.
123. K. Wang, X. Guo, P. Zhao, F. Wang and C. Zheng, *J. Hazard. Mater.*, 2011, **189**, 301-307.
124. Y. Zhang, F. Yu, B. Louis and Q. Wang, *Chem. Eng. J.*, 2018, **349**, 562-573.
125. F. Durán-Muñoz, I. C. Romero-Ibarra and H. Pfeiffer, *J. Mater. Chem. A*, 2013, **1**, 3919.
126. I. C. Romero-Ibarra, F. Duran-Muñoz and H. Pfeiffer, *Greenh. Gases*, 2014, **4**, 145-154.
127. J. Ortiz-Landeros, R. López-Juárez, I. C. Romero-Ibarra, H. Pfeiffer, H. Balmori-Ramírez and C.

Gómez-Yáñez, *Particuology*, 2016, **24**, 129-137.
128. J. Ortiz-Landeros, C. Gómez-Yáñez and H. Pfeiffer, *J. Solid State Chem.*, 2011, **184**, 2257-2262.
129. R. B. Khomane, B. K. Sharma, S. Saha and B. D. Kulkarni, *Chem. Eng. Sci.*, 2006, **61**, 3415-3418.
130. K. Nakagawat and T. Ohashi, *J. Electrochem. Soc.*, 1998, **145**, 1344-1346.
131. E. Ochoa-Fernández, H. K. Rusten, H. A. Jakobsen, M. Rønning, A. Holmen and D. Chen, *Catal. Today*, 2005, **106**, 41-46.
132. B. N. Nair, T. Yamaguchi, H. Kawamura, S. I. Nakao and K. Nakagawa, *J. Am. Ceram. Soc.*, 2004, **87**, 68-74.
133. J. Ida and Y. S. Lin, *Environ. Sci. Technol.*, 2003, **37**, 1999-2004.
134. Q. Xiao, Y. Liu, Y. Zhong and W. Zhu, *J. Mater. Chem.* , 2011, **21**, 3838.
135. Q. Xiao, X. Tang, Y. Liu, Y. Zhong and W. Zhu, *Front. Chem. Sci. Eng.*, 2013, **7**, 297-302.
136. A. Iwan, H. Stephenson, W. C. Ketchie and A. A. Lapkin, *Chem. Eng. J.*, 2009, **146**, 249-258.
137. E. Ochoa-Fernández, M. Rønning, X. Yu, T. Grande and D. Chen, *Ind. Eng. Chem. Res.*, 2008, **47**, 434-442.
138. E. Ochoa-Fernández, M. R. Rønning, T. Grande and D. Chen, *Chem. Mater.*, 2006, **18** 6037-6046.
139. E. Ochoa-Fernández, M. Rønning, T. Grande and D. Chen, *Chem. Mater.*, 2006, **18**, 1383-1385.
140. L. Guo, X. Wang, C. Zhong and L. Li, *Appl. Surf. Sci.*, 2011, **257**, 8106-8109.
141. L. Guo, X. Wang, S. Zhang, C. Zhong and L. Li, *J. Mater. Sci.*, 2011, **46**, 6960-6963.
142. Q. Xiao, X. Tang, Y. Zhong, W. Zhu and T. Gur, *J. Am. Ceram. Soc.*, 2012, **95**, 1544-1548.
143. Y. Wang, L. Yin, O. Palchik, Y. Rosenfeld Hacohen, Y. Koltypin and A. Gedanken, *Chem. Mater.*, 2001, **13**, 1248-1251.
144. H. R. Radfarnia and M. C. Iliuta, *Ind. Eng. Chem. Res.*, 2011, **50**, 9295-9305.
145. X. Chen, H. Fan and L. Liu, *J. Cryst. Growth*, 2005, **284**, 434-439.
146. R. I. Walton, *Chem. Soc. Rev.*, 2002, **31**, 230-238.
147. G. Ji, M. Z. Memon, H. Zhuo and M. Zhao, *Chem. Eng. J.*, 2017, **313**, 646-654.
148. M. Z. Memon, G. Ji, J. Li and M. Zhao, *Ind. Eng. Chem. Res.*, 2017, **56**, 3223-3230.
149. F. Bamiduro, G. Ji, A. P. Brown, V. A. Dupont, M. Zhao and S. J. Milne, *ChemSusChem*, 2017, **10**, 2059-2067.
150. H. Pfeiffer, E. Lima and P. Bosch, *Chem. Mater.*, 2006, **37**, 2642-2647.
151. M. Y. Veliz-Enriquez, G. Gonzalez and H. Pfeiffer, *J. Solid State Chem.*, 2007, **180**, 2485-2492.
152. C. Wang, B. Dou, Y. Song, H. Chen, Y. Xu and B. Xie, *Ind. Eng. Chem. Res.*, 2014, **53**, 12744-12752.
153. M. Olivares-Marín, M. Castro-Díaz, T. C. Drage and M. Mercedes Maroto-Valer, *Sep. Purif. Technol.*, 2010, **73**, 415-420.
154. P. L. Spedding and R. Mills, *J. Electrochem. Soc.*, 1965, **112**, 594-599.
155. L. Martínez-dlCruz and H. Pfeiffer, *Ind. Eng. Chem. Res.*, 2010, **49**, 9038-9042.
156. D. Peltzer, J. Múnera and L. Cornaglia, *RSC Adv.*, 2016, **6**, 8222-8231.
157. D. J. Fauth, E. A. Frommell, J. S. Hoffman, R. P. Reasbeck and H. W. Pennline, *Fuel Process. Technol.*, 2005, **86**, 1503-1521.
158. H. Pfeiffer and P. Bosch, *Chem. Mater.*, 2005, **17**, 1704-1710.
159. X. S. Yin, M. Song, Q. H. Zhang and J. G. Yu, *Ind. Eng. Chem. Res.*, 2010, **49**, 6593-6598.
160. X. S. Yin, S. P. Li, Q. H. Zhang and J. G. Yu, *J. Am. Ceram. Soc.*, 2010, **93**, 2837-2842.
161. X. S. Yin, Q. H. Zhang and J. G. Yu, *Inorg. Chem.*, 2011, **50**, 2844-2850.
162. Y. Duan, *Phys. Chem. Chem. Phys.*, 2013, **15**, 9752-9760.
163. N. Togashi, T. Okumura and K. OH-Ishi, *J. Ceram. Soc. Jpn.*, 2007, **115**, 324-328.

164. S. Ueda, R. Inoue, K. Sasaki, K. Wakuta and T. Ariyama, *Isij. Int.*, 2011, **51**, 530–537.
165. L. Zhirong, Z. Huan, W. Yun and Z. Xinxing, *J. Nanomater.*, 2014, **2014**, 1-5.
166. T. Ávalos-Rendon, J. Casa-Madrid and H. Pfeiffer, *J. Phys. Chem. A*, 2009, **113**, 6919–6923.
167. P. Sánchez-Camacho, J. F. Gómez-García and H. Pfeiffer, *J. Energy Chem.*, 2017, **26**, 919-926.
168. T. Ávalos-Rendón, V. H. Lara and H. Pfeiffer, *Ind. Eng. Chem. Res.*, 2012, **51**, 2622-2630.
169. Flores-Martínez, M. T. and H. Pfeiffer, *Biofuel. Bioprod. Bior.*, 2010, **4**, 296-309.
170. H. A. Lara-García, P. Sanchez-Camacho, Y. Duan, J. Ortiz-Landeros and H. Pfeiffer, *J. Phys. Chem. C*, 2017, **121**, 3455-3462.
171. T. Ávalos-Rendón and H. Pfeiffer, *Phytochem. Lett.*, 2011, **40**, 504-505.
172. P. Olavarría, E. Vera, E. Lima and H. Pfeiffer, *J. Energy Chem.*, 2017, **26**, 948-955.
173. J. F. Gomez-García and H. Pfeiffer, *RSC Adv.*, 2016, **6**, 112040-112049.
174. I. Yanase, J. Miura and H. Kobayashi, *Mater. Chem. Phys.*, 2017, **199**, 18-22.
175. L. M. Palacios-Romero and H. Pfeiffer, *Chem. Lett.*, 2008, **37**, 862-863.
176. L. M. Palacios-Romero, E. Lima and H. Pfeiffer, *J. Phys. Chem. A*, 2009, **113**, 193–198.
177. H. A. Lara-García and H. Pfeiffer, *Chem. Eng. J.*, 2017, **313**, 1288-1294.
178. K. Oh-ishi, Y. Matsukura, T. Okumura, Y. Matsunaga and R. Kobayashi, *J. Solid State Chem.*, 2014, **211**, 162-169.
179. I. Ham-Liu, J. A. Mendoza-Nieto and H. Pfeiffer, *J. CO_2 Util.*, 2018, **23**, 143-151.
180. E. M. Briz-López, M. J. Ramírez-Moreno, I. C. Romero-Ibarra, C. Gómez-Yáñez, H. Pfeiffer and J. Ortiz-Landeros, *J. Energy Chem.* , 2016, **25**, 754-760.
181. A. Román-Tejeda and H. Pfeiffer, *J. Therm. Anal. Calorim.*, 2011, **110**, 807-811.
182. Y. Duan, J. Lekse, X. Wang, B. Li, B. Alcántar-Vázquez, H. Pfeiffer and J. W. Halley, *Phys. Rev. Appl.*, 2015, **3**.
183. B. Alcántar-Vázquez, P. R. Díaz Herrera, A. Barrera González, Y. Duan and H. Pfeiffer, *Ind. Eng. Chem. Res.*, 2015, **54**, 6884-6892.
184. H. A. Lara-García, B. Alcántar-Vázquez, Y. Duan and H. Pfeiffer, *RSC Adv.*, 2015, **5**, 34157-34165.
185. T. L. Ávalos-Rendón and H. Pfeiffer, *Energ, Fuel.*, 2012, **26**, 3110-3114.
186. L. Martínez-dlCruz and P. H., *J. Phys. Chem. A*, 2010, **114**, 9453-9458.
187. S. Garcia, E. S. Fernandez, A. J. Stewart and M. M. Maroto-Valer, *Energy Procedia*, 2017, **114**, 2611-2617.
188. K. Essaki, T. Muramatsu and M. Kato, *Int. J. Hydrogen Energ.*, 2008, **33**, 4555-4559.
189. B. Dou, C. Wang, Y. Song, H. Chen, B. Jiang, M. Yang and Y. Xu, *Renew. Sust. Energ. Rev.*, 2016, **53**, 536-546.
190. F. Micheli, M. Sciarra, C. Courson and K. Gallucci, *J. Energy Chem.*, 2017, **26**, 1014-1025.
191. Q. Zhang, C. Shen, S. Zhang and Y. Q. Wu, *Int. J. Hydrogen Energ.*, 2016, **41**, 4831-4842.
192. M.Z. Memon, X. Zhao, V.S. Sikarwar, A.K. Vuppaladadiyam, S.J. Milne, A.P. Brown, J. Li and M. Zhao, *Environ. Sci. Technol.*, 2017, **51**, 12-27.
193. J. T. R. Pacciani, P. Solsona, C. Coe, R. Quinn, J. Hufton, T. Golden, L. F. Vega, *Environ. Sci. Technol.*, 2011, **45**, 7083-7088.
194. Monica Puccini, Eleonora Stefanelli, Maurizia Seggiani and S. Vitolo, 2015, **43**.
195. Esther Ochoa-Fernández, T. Zhao, Ph.D, Magnus Rønning and D. Chen, *J. Environ. Eng.-ASCE*, 2009, **135**, 397-403.
196. Robert Quinn, Ronald J. Kitzhoffer, Jeffrey R. Hufton and T. C. Golden, *Ind. Eng. Chem. Res.*, 2012, **51**, 9320-9327.

197. H. Kristian Rusten, E. Ochoa-Ferna´ndez, D. Chen and H. Jakobsen, *Ind. Eng. Chem. Res.*, 2007, **46** 4435-4443.
198. M. H. Halabi, M. H. J. M. de Croon, J. van der Schaaf, P. D. Cobden and J. C. Schouten, *Fuel*, 2012, **99**, 154-164.
199. K. Essaki, T. Muramatsu and M. Kato, *Int. J. Hydrogen Energ.*, 2008, **33**, 6612-6618.
200. Qiao X., Lisbona P., Guo X., Lara Y. and Romeo L. M., *Energ. Fuel*, 2016, **30**, 1879-1886.
201. C. Wang, Y. Chen, Z. Cheng, X. Luo, L. Jia, M. Song, B. Jiang and B. Dou, *Energ. Fuel*, 2015, **29**, 7408-7418.
202. A. Alihoseinzadeh, A. A. Khodadadi and Y. Mortazavi, *Int. J. Hydrogen Energ.*, 2014, **39**, 2056-2066.
203. X. Zhu, Y. Shi and N. Cai, *J. Energy Chem.*, 2017, **26**, 956-964.
204. B. Alcántar-Vázquez, Y. Duan and H. Pfeiffer, *Ind. Eng. Chem. Res.*, 2016, **55**, 9880-9886.
205. H. Lara-Garcia, B. Alcántar-Vázquez, Y. Duan and H. Pfeiffer, *J. Phys. Chem. C*, 2016, **120**, 3798-3806.
206. M. Seggiani, E. Stefanelli, M. Puccini and S. Vitolo, *Chem. Eng. J.*, 2018, **339**, 51-60.
207. M. Z. Memon, X. Zhao, V. S. Sikarwar, A. K. Vuppaladadiyam, S. J. Milne, A. P. Brown, J. Li and M. Zhao, *Environ. Sci. Technol.*, 2017, **51**, 12-27.